



THE UNIVERSITY *of* EDINBURGH

Edinburgh Research Explorer

Leaf-level photosynthetic capacity in lowland Amazonian and high-1 elevation, Andean tropical moist forests of Peru

Citation for published version:

Meir, P 2016, 'Leaf-level photosynthetic capacity in lowland Amazonian and high-1 elevation, Andean tropical moist forests of Peru', *New Phytologist*. <https://doi.org/10.1111/nph.14079>

Digital Object Identifier (DOI):

[10.1111/nph.14079](https://doi.org/10.1111/nph.14079)

Link:

[Link to publication record in Edinburgh Research Explorer](#)

Document Version:

Peer reviewed version

Published In:

New Phytologist

Publisher Rights Statement:

© 2016 The Authors. New Phytologist © 2016 New Phytologist Trust

General rights

Copyright for the publications made accessible via the Edinburgh Research Explorer is retained by the author(s) and / or other copyright owners and it is a condition of accessing these publications that users recognise and abide by the legal requirements associated with these rights.

Take down policy

The University of Edinburgh has made every reasonable effort to ensure that Edinburgh Research Explorer content complies with UK legislation. If you believe that the public display of this file breaches copyright please contact openaccess@ed.ac.uk providing details, and we will remove access to the work immediately and investigate your claim.



Leaf-level photosynthetic capacity in lowland Amazonian and high-elevation, Andean tropical moist forests of Peru

Nur H.A. Bahar¹, F. Yoko Ishida², Lasantha K. Weerasinghe^{1,5}, Rossella Guerrieri^{3,4}, Odhran S. O'Sullivan¹, Keith J. Bloomfield¹, Gregory P. Asner⁸, Roberta E. Martin⁸, Jon Lloyd^{2,6}, Yadvinder Malhi⁷, Oliver L. Phillips⁹, Patrick Meir^{1,3}, Norma Salinas^{7,10}, Eric G. Cosio¹⁰, Tomas Domingues¹¹, Carlos A. Quesada¹², Felipe Sinca⁸, Alberto Escudero Vega¹⁰, Paola P. Zuloaga Ccorimanya¹³, Jhon del Aguila-Pasquel^{14,15}, Katherine Quispe Huaypar¹⁰, Israel Cuba Torres¹⁰, Rosalbina Butrón Loayza¹⁶, Yulina Pelaez Tapia¹⁰, Judit Huaman Ovalle¹⁰, Benedict M. Long^{1, 17}, John R. Evans^{1,17} and Owen K. Atkin^{1,18,*}

¹Div Plant Sciences, Research School of Biology, The Australian National University, Canberra, ACT, 2601, Australia; ²College of Marine and Environmental Sciences and Centre for Tropical Environmental and Sustainability Science, James Cook University, Cairns, Queensland, Australia; ³School of Geosciences, University of Edinburgh, Edinburgh EH9 3JN, UK; ⁴Earth Systems Research Center, University of New Hampshire, Morse Hall, 8 College Rd, Durham, NH 03824, USA; ⁵Faculty of Agriculture, University of Peradeniya, Peradeniya 20400, Sri Lanka; ⁶Dept Life Sciences, Imperial College London, Silwood Park Campus, SL5 7PY, UK; ⁷Environmental Change Institute, School of Geography and the Environment, University of Oxford, South Parks Road, Oxford OX1 3QY, UK; ⁸Dept of Global Ecology, Carnegie Institution for Science, Stanford, CA 94305; ⁹School of Geography, University of Leeds, Woodhouse Lane, Leeds LS9 2JT, UK; ¹⁰Pontificia Universidad Católica del Perú, Seccion Quimica, Av Universitaria 1801, San Miguel, Lima, Perú; ¹¹Universidade de São Paulo, Faculdade de Filosofia Ciências e Letras de Ribeirão Preto, Brazil; ¹²Instituto Nacional de Pesquisas da Amazonia (INPA), Manaus, Brazil; ¹³Seccion Biología, Universidad Nacional de San Antonio Abad del Cusco, Av de la Cultura, No. 733, Cusco, Perú; ¹⁴Instituto de Investigaciones de la Amazonia Peruana (IIAP), Av. José A. Quiñones km. 2.5, Apartado Postal 784, Iquitos, Perú; ¹⁵School of Forest Resources and Environmental Science, Michigan Technological University, 1400 Townsend Drive, Houghton, Michigan, 49931, USA; ¹⁶Museo de Historia Natural, Universidad Nacional de San Antonio Abad del Cusco, Av de la Cultura, No. 733, Cusco, Perú; ¹⁷ARC Centre of Excellence in Translational Photosynthesis, Research School of Biology, Building 134, The Australian National University, Canberra, ACT 2601, Australia; ¹⁸ARC Centre of Excellence in Plant Energy Biology, Research School of Biology, Building 134, The Australian National University, Canberra, ACT 2601, Australia.

* Author for correspondence: Owen Atkin, tel +61 (0)2 6125 5046, email: Owen.Atkin@anu.edu.au

41 Number of Figures: 9 (plus 6 in Supporting Information and 5 in SM3)
42 Number of Tables: 3 (plus 7 in Supporting Information)
43 Number of References: 90
44 Number of Pages (text plus references): 30
45
46 Total Word count: 7658 (excluding Abstract, References, Figures and Tables)
47 Abstract: 200 words
48 Introduction: 1279 words
49 Materials and Methods: 1826 words
50 Results: 2319 words
51 Discussion: 2228 words
52
53
54

Summary

- We examined whether variations in photosynthetic capacity are linked to variations in the environment and/or associated leaf traits for tropical moist forest (TMFs) in the Andes/western-Amazon regions of Peru.
- We compared photosynthetic capacity (V_{cmax} and J_{max}), leaf mass, nitrogen and phosphorus per unit leaf area (M_a , N_a and P_a respectively), and chlorophyll from 210 species at 18 field sites along a 3,300-m elevation gradient. Western-blotting was used to quantify abundance of the CO_2 -fixing enzyme, Rubisco.
- Area- and N-based rates of photosynthetic capacity at 25°C were higher in upland- than lowland-TMFs, underpinned by greater investment of N in photosynthesis in high-elevation trees. Soil [P] and leaf P_a were key explanatory factors for models of area-based V_{cmax} and J_{max} but did not account for variations in photosynthetic N-use efficiency. At any given N_a and P_a , the fraction of N allocated to photosynthesis was higher in upland than lowland species. For a small subset of lowland TMF trees examined, a substantial fraction of Rubisco was inactive.
- These results highlight the importance of soil- and leaf-phosphorus in defining photosynthetic capacity of TMFs, with variations in N allocation and Rubisco activation state further influencing photosynthetic rates and N-use efficiency of these critically important forests.

Keywords: Elevation, carboxylation capacity, leaf traits, nitrogen, phosphorus, ribulose biphosphate regeneration, temperature, tropical forests

Introduction

Tropical moist forests (TMFs) play a significant role in the terrestrial carbon cycle, contributing one-third to global gross primary productivity (Beer *et al.*, 2010; Malhi, 2010). Understanding the factors that regulate leaf photosynthesis (A) in TMFs is a prerequisite for modelling carbon storage in tropical ecosystems, with A being influenced *inter alia* by nutrient supply [particularly nitrogen (N) and phosphorus (P)], elevation and growth temperature.

Early studies in lowland TMFs implicated low foliar P concentrations as a major influence on light-saturated net photosynthesis (A_{sat}) (Reich & Walters, 1994; Raaimakers *et al.*, 1995), with soil P being a major factor limiting Amazon productivity (Quesada *et al.*, 2012). Foliar P is crucial to the fine-tuning A_{sat} (Fredeen *et al.*, 1989; Jacob & Lawlor, 1993) via regulation of key intermediates in carbon metabolism (e.g. ATP, NADPH and sugar phosphates including ribulose 1,5-bisphosphate - RuBP). While the direct effect of P-limitation is primarily on RuBP regeneration, reductions in Rubisco activity also occur (Brooks, 1986; Jacobs & Lawlor, 1992; Loustau *et al.*, 1999). Although Meir *et al.* (2002; 2007) and Reich *et al.* (2009) showed that A_{sat} at a given leaf N concentration ($[N]$) was less in lowland tropical trees than their temperate counterparts, the extent to which P limitations *per se* alter $A_{\text{sat}} \leftrightarrow [N]$ relations within TMFs is uncertain (Bloomfield *et al.*, 2014a; Domingues *et al.*, 2015). A further unknown is the extent to which large elevation gradients affect $A_{\text{sat}} \leftrightarrow [N]$ relations in the tropics. Upland TMFs are more likely to be limited by N than their lowland counterparts (Tanner *et al.*, 1998). Upland TMFs also experience lower temperatures and atmospheric CO_2 partial pressures, more frequent cloud cover and experience greater leaf wetness (Grubb, 1977; Vitousek, 1984; Girardin *et al.*, 2010; Bruijnzeel *et al.*, 2011). Such factors can limit A_{sat} (Terashima *et al.*, 1995; Bruijnzeel & Veneklaas, 1998; Letts & Mulligan, 2005), leading to declines in productivity (Girardin *et al.*, 2010). A_{sat} in upland TMFs have been documented (e.g. Quilici & Medina, 1998; Cordell *et al.*, 1999; Hikosaka *et al.*, 2002; Letts & Mulligan, 2005; Rada *et al.*, 2009), showing A_{sat}

114 being constant with increasing elevation (Cordell *et al.*, 1999), or declining with
115 increasing elevation (Hikosaka *et al.*, 2002; Wittich *et al.*, 2012).

116 Rates of A_{sat} are subject to variations in stomatal conductance (g_s) and the
117 partial pressure of internal leaf CO_2 (C_i) (Santiago & Mulkey, 2003). Since
118 variations in C_i alter both CO_2 uptake and photorespiratory CO_2 release, it could
119 potentially confound our understanding of how environmental gradients alter N
120 investment in A. By contrast, variations in g_s have less impact on the fundamental,
121 biochemical parameter of photosynthetic capacity – that being the maximum rate
122 of carboxylation by Rubisco (i.e. V_{cmax}). Positive correlations between V_{cmax} and
123 leaf [N] have been reported for some tropical species (Carswell *et al.*, 2000; Meir
124 *et al.*, 2002; Domingues *et al.*, 2005; Kumagai *et al.*, 2006; Meir *et al.*, 2007;
125 Vårhammar *et al.*, 2015) – whereas in others no strong $V_{\text{cmax}} \leftrightarrow [\text{N}]$ relationship was
126 observed (Coste *et al.*, 2005; van de Weg *et al.*, 2012; Dusenge *et al.*, 2015).
127 Although reports on V_{cmax} are less widespread in the tropics than A_{sat} , the
128 available data suggest that V_{cmax} values, as well as V_{cmax} per unit N (herein termed
129 ' $V_{\text{cmax},\text{N}}$ '), are lower in lowland TMFs than their non-tropical counterparts (Carswell
130 *et al.*, 2000; Meir *et al.*, 2002; Domingues *et al.*, 2007; Meir *et al.*, 2007; Domingues
131 *et al.*, 2010; Walker *et al.*, 2014; Vårhammar *et al.*, 2015). Kattge *et al.* (2009) re-
132 analysed data to show that V_{cmax} per unit N in TMFs growing on young, relatively
133 high nutrient status soils was higher compared to their older, Ferralsol and Acrisol
134 soil counterparts that are characterised by very low soil P availability (Quesada *et al.*
135 *et al.*, 2010). These observations are consistent with laboratory studies showing
136 reduced V_{cmax} (Lauer *et al.*, 1989; Loustau *et al.*, 1999) and reduced N allocation
137 to Rubisco (Warren & Adams, 2002) under P-limited conditions. Increased
138 allocation of N to non-photosynthetic components may also play a role
139 (Domingues *et al.*, 2010; Lloyd *et al.*, 2013), as might inactivation of Rubisco (Stitt
140 & Schulze, 1994). Yet, doubt remains regarding the general $V_{\text{cmax}} \leftrightarrow [\text{N}]$
141 relationship in TMFs due to the scarcity of data, both in lowland and upland TMFs.
142 Comprehensive surveys of V_{cmax} (and J_{max} - maximum rate of electron transport)
143 across lowland and upland TMFs are required to establish whether there are

144 generalized patterns of photosynthetic capacity in relation to environmental
145 conditions and/or other leaf traits.

146 TMF species with higher leaf nutrient concentrations and lower leaf mass
147 per unit leaf area (M_a) values are often found in more fertile soils (Fyllas *et al.*,
148 2009), and M_a tends to increase with increasing elevation (Hikosaka *et al.*, 2002;
149 van de Weg *et al.*, 2009; Almeida *et al.*, 2012; Asner *et al.*, 2014b); leaf chemistry
150 also systematically shifts along elevation gradients in the tropics (Asner *et al.*,
151 2014b). Large variations in leaf traits also observed among co-occurring species,
152 reflecting the importance of phylogenetic relationships in determining trait values
153 in TMFs (Townsend *et al.*, 2007; Kraft *et al.*, 2008; Fyllas *et al.*, 2009). Whether
154 similar patterns hold for estimates of V_{cmax} in lowland and upland TMFs (and
155 $V_{\text{cmax,N}}$), is, however, not known.

156 Variations in $V_{\text{cmax,N}}$ underlie variations in photosynthetic N use efficiency.
157 Further insights can be gained by quantifying the proportion of N allocated to
158 the pigment-protein complexes (n_P), electron transport (n_E) and Rubisco (n_R)
159 (Evans & Seemann, 1989; Pons *et al.*, 1994; Hikosaka, 2004). Quantification of
160 V_{cmax} , J_{max} , leaf chlorophyll and [N] can be used to estimate n_P , n_E and n_R (Evans &
161 Seemann, 1989; Niinemets & Tenhunen, 1997). In non-tropical plants, lower A_{sat}
162 at a given N (A_N) are associated with reduced allocation of N to photosynthesis
163 and increased allocation to non-photosynthetic components (Poorter & Evans,
164 1998; Westbeek *et al.*, 1999; Warren & Adams, 2001; Takashima *et al.*, 2004;
165 Hikosaka & Shigeno, 2009). Similarly, variations in A_N were associated with
166 differences in N allocation to and within the photosynthetic apparatus in
167 greenhouse-grown tropical tree seedlings (Coste *et al.*, 2005) and in high
168 elevation TMFs of Rwanda (Dusenge *et al.*, 2015). To our knowledge, no study has
169 quantified N allocation patterns in field-grown tropical trees, and not with respect
170 to field sites in upland and lowland TMFs.

171 We examined variations in photosynthetic capacity and leaf traits across
172 TMF canopies located at 18 sites along a 3,300-m elevation gradient stretching
173 from lowland western Amazonia to the Andean tree line in Peru. The study

174 included 11 lowland sites in northern and southern Peru (elevation 117-223 m
175 a.s.l.), and seven upland sites at elevations of 1527-3379 m a.s.l. in southern Peru.
176 Our site selection enabled an assessment of the potential role of P-availability on
177 photosynthetic performance across Amazonian-Andean TMF sites differing >40-
178 fold in total soil P. The upland sites were characterised by a floristically distinct
179 assemblage of montane forest species, with the transition from lowland moist
180 forests to upland montane forests coinciding with an increase in cloud formation
181 (van de Weg *et al.*, 2009; Bruijnzeel *et al.*, 2011). In conjunction with the recent
182 findings of the key role of P in modulating carbon investment (Quesada *et al.*,
183 2012) and photosynthesis (Bloomfield *et al.*, 2014b) of tropical trees, and that leaf
184 P varies predictably along soil P and elevation gradients (Asner *et al.*, 2014b), we
185 addressed the following questions:

- 186 (1) Do tropical TMF species growing on low-P soils exhibit lower photosynthetic
187 capacity and photosynthetic N use efficiency than TMF trees growing on
188 sites with higher P availability?
- 189 (2) Are there marked differences in V_{cmax} , J_{max} and $V_{\text{cmax,N}}$ between lowland
190 Amazonian and upland Andean TMFs?
- 191 (3) Are differences in V_{cmax} , J_{max} and $V_{\text{cmax,N}}$ linked to concomitant variations in
192 other leaf traits and/or environmental variables?

193

194 **Materials and Methods**

195

196 *Study sites*

197 Field work was carried out in 18 one-hectare long-term monitoring plots in Peru
198 which contribute to the ABERG and RAINFOR networks of permanent sample
199 plots. The plots are arrayed along gradients of elevation (117 to 3379 m above
200 sea level) and soil nutrient status (Table 1). For each site, climate data were
201 obtained from Asner *et al.* (2014a) and Malhi *et al.* (in prep). Marked changes in
202 species richness, canopy cover and tree height occur along the elevation gradient
203 (Asner *et al.*, 2014a; Girardin *et al.*, 2014b; Silman, 2014), reflecting local geological

204 substrates, as well as changes in growth temperature, cloud cover and light
205 environment. In addition to marked inter-site differences in total soil [N] (0.6 -
206 15.5 g N kg⁻¹), substantial variation in total soil [P] occurs across both the lowland
207 (38 - 727 mg P kg⁻¹) and upland sites (496 - 1631 mg P kg⁻¹) (Table 1). Soils at
208 three of the lowland sites in northern Peru (JEN-12, ALP-30 and ALP-40) are
209 notable for being low nutrient status arenosols/podzols ('white sands'). Among
210 the lowland and upland sites, mean annual precipitation (MAP) values range from
211 1560 to 5300 mm a⁻¹. Mean annual temperature ranged from 8.0 to 18.8 °C
212 across the upland sites, and 24.4 to 26.6 °C among the lowland sites.

213 At each site, tree climbers collected from dominant tree species upper
214 canopy branches supporting leaves considered to typically be exposed to full
215 sunlight for much of the day, but with little replication of individual species
216 possible at any site. Each tree was initially identified to the genus-level and,
217 whenever possible, to the species-level. A total of 353 individual trees drawn from
218 210 species were sampled across the 18 sites. See SM1 in Supporting Information
219 for further details.

220

221 *Leaf gas exchange measurements*

222 Measurements of leaf gas exchange were made during July to September 2011,
223 using portable photosynthesis systems (Licor 6400XT infrared gas analyser, Li-Cor
224 BioSciences, Lincoln, NE, USA). Measurements were made on the most recently
225 fully expanded leaves attached to the cut branches (which had been re-cut under
226 water immediately after harvesting to ensure xylem water continuity).

227 CO₂ response curves of light-saturated photosynthesis ($A \leftrightarrow C_i$ curves) (at
228 1800 $\mu\text{mol photons m}^{-2} \text{ s}^{-1}$) were performed within 30–60 minutes after branch
229 detachment. CO₂ concentrations inside the reference chamber ranged in a
230 stepped sequence from 35 to 2000 $\mu\text{mol mol}^{-1}$ (see SM2 in Supporting
231 Information for details). Block temperatures within the chamber were set to the
232 prevailing day-time air temperature at each site (from 25–28 °C). The resultant
233 $A \leftrightarrow C_i$ curves (examples shown in Fig. 1) were fitted following the model described
234 by Farquhar *et al.* (1980) in order to calculate V_{cmax} and J_{max} on a leaf area basis –

235 see SM2 in Supporting Information for details. For every $A \leftrightarrow C_i$ curve, recorded air
236 pressure was used to correct for altitudinal changes in O_2 partial pressure, and to
237 calculate intercellular CO_2 (C_i) values on a partial pressure basis.

238 Rates of CO_2 exchange were corrected for diffusion through the gasket of
239 the LI-6400 leaf chamber (Bruhn *et al.*, 2002) prior to calculation of V_{cmax} and J_{max} .
240 Assuming infinite internal diffusion conductance (g_m), Michaelis constants of
241 Rubisco for CO_2 (K_c) and O_2 (K_o) at a reference temperature 25°C were assumed
242 to be 40.4 Pa and 24.8 kPa, respectively (von Caemmerer *et al.*, 1994); these values
243 were adjusted to actual leaf temperatures assuming activation energies of 59.4
244 and 36 kJ mol⁻¹ for K_c and K_o , respectively (Farquhar *et al.*, 1980). Fitted parameters
245 were then scaled to a reference temperature of 25°C using activation energies of
246 64.8 and 37.0 kJ mol⁻¹ for V_{cmax} and J_{max} , respectively (Farquhar *et al.*, 1980). Finally,
247 rates of A obtained at ambient CO_2 concentrations of 400 and 2000 $\mu\text{mol mol}^{-1}$
248 (A_{400} and A_{2000} , respectively) were extracted from the $A \leftrightarrow C_i$ curves and reported
249 separately.

250 As atmospheric CO_2 was not always saturating for measurements of
251 upland species (due to low atmospheric partial pressure, resulting in insufficient
252 CO_2 -saturated rates of A to enable calculate J_{max}), it was likely that J_{max} may have
253 been underestimated in some cases; where this was likely the case (i.e. where
254 there was no clear plateauing of A at high C_i values), we excluded the resultant
255 J_{max} values from the Andean data set. With the exception of a few cases (e.g.
256 *Schefflera* sp.; Fig. 1), $A \leftrightarrow C_i$ curves typically flattened out at high C_i values (> 90%
257 of curves), with A increasing slightly as C_i values increased further (see Fig. 1),
258 suggesting that feedback inhibition of A through limitations in triose-phosphate
259 utilization (TPU) was unlikely.

260

261 *Leaf structure and chemistry determination*

262 Leaves were collected immediately following the gas exchange measurements.
263 Initially, the leaf mid rib was removed; thereafter, a digital photograph was taken
264 using a high resolution scanner (CanoScan LiDE 210, Vietnam) and later analysed
265 for leaf area (Image J, version 1.38x, NIH, USA). Leaves were then placed in an
266 oven at 70 °C for at least two days, the dry mass measured and leaf mass per unit

267 leaf area (M_a) calculated for each sample. Total leaf N and P concentrations in
268 dried leaves were extracted using Kjeldahl acid digest method, as detailed in Ayub
269 *et al.* (2011).

270

271 *Chlorophyll and Rubisco measurements*

272 Leaf discs from the nearest mature leaves adjacent to the gas exchange leaf were
273 collected and transferred to -80 °C cryogenic field container for subsequent
274 chlorophyll and Rubisco assays in the laboratory.

275 Chlorophyll content of each set of leaf discs was determined using a dual-
276 beam scanning UV-VIS spectrometer (Lambda 25, Perkin-Elmer) after extraction
277 of chlorophyll pigments from two frozen leaf discs (0.77 cm² each) with 100%
278 acetone and MgCO₃, as outlined in Asner *et al.* (2014b). Chlorophyll a:b ratios
279 varied between 2.45 and 2.75, which is consistent with results of past studies on
280 tropical trees in the Peruvian Amazon (Asner & Martin, 2011).

281 Protein was extracted from frozen leaf discs following the method outlined
282 in Gaspar *et al.* (1997) with slight modifications (see SM3 in Supporting
283 Information for details on optimization of protein assays). Frozen samples of 0.50
284 cm² were ground in Eppendorf tubes and washed consecutively in 100%
285 methanol, hexane and acetone. Treated leaf powder was then resuspended in
286 protein extraction buffer (140 mM Tris base, 105 mM Tris-HCl, 0.5 mM
287 ethylenediaminetetraacetic acid, 2% lithium dodecyl sulfate (LDS), 10% glycerol)
288 containing 5 mM DTT and protease inhibitor cocktail (Sigma-Aldrich Co, Castle
289 Hill, NSW, Australia), heated for 10 min at 100 °C to completely dissolve extracted
290 protein, then clarified by centrifugation (14,000 x *g*; 10 min; room temperature).
291 The supernatant was used as the source of leaf protein.

292 Equivalent volumes of supernatant were diluted in 4 × SDS-PAGE sample
293 buffer (Invitrogen - Life Technologies, Carlsbad, CA, USA) then loaded onto gels.
294 Since we extracted protein from a known amount of leaf area, we were able to
295 analyse our samples on an equivalent leaf area basis. Rubisco purified from
296 tobacco with varying concentrations was also loaded onto gels, serving as a

297 calibration series. Proteins were run on 4-12% NuPAGE Bis-Tris gels (Invitrogen -
 298 Life Technologies, Carlsbad, CA, USA) according to the manufacturer's
 299 instructions and transferred to Immobilon-P PVDF membranes (Merck Millipore,
 300 Kilsyth, Vic., Australia) using an XCell II Blot module (Invitrogen). Membranes were
 301 blocked with 5% skim milk powder in Tris-buffered saline containing 0.5% Tween-
 302 20 (TBS-T) and an antibody raised in rabbits against tobacco Rubisco (used at
 303 1:5,000) prepared by Spencer Whitney (Research School of Biology, Australian
 304 National University, Canberra). Secondary antibody (goat-anti-rabbit-alkaline
 305 phosphatase conjugate, Agrisera) was diluted 1:5,000. Blots were visualized using
 306 Attophos AP fluorescent substrate system (Promega, Madison, WI, USA) and
 307 imaged using a Versa-Doc (Bio-Rad, Hercules, CA, USA) imaging system. Blots
 308 were analysed using Quantity One software (Bio-Rad) and relative band densities
 309 of each protein determined from duplicate samples, and data averaged. Rubisco
 310 concentration was calculated from the large subunit (molecular mass of 55 kD
 311 and 16% N by weight).

312

313 *Estimation of N allocation in photosynthetic metabolism*

314 N allocation in three major components (pigment-protein complexes, electron
 315 transport and Rubisco) for all leaves was estimated from chlorophyll
 316 concentration, V_{cmax} and J_{max} respectively. N allocation to pigment-protein
 317 complexes (n_P) was calculated by assuming 44 mol N per mol of chlorophyll
 318 (Evans, 1989). N allocation to Rubisco (n_R) was estimated from values of V_{cmax}
 319 according to Harrison *et al.* (2009), with slight modification [2.33 mol CO₂ (mol
 320 Rubisco sites)⁻¹ s⁻¹ for the catalytic turnover number of Rubisco at 25 °C (Harrison
 321 *et al.*, 2009)]. We assumed all Rubisco was fully activated and mesophyll
 322 conductance was infinite. The allocation of N to electron transport components
 323 (n_E) was calculated from J_{max} assuming 160 mol electrons (mol cytochrome f)⁻¹ s⁻¹
 324 ¹ and 8.85 mol N (mmol cytochrome f)⁻¹ (Evans & Seemann, 1989). The proportion
 325 of total leaf N allocated to each photosynthetic component was calculated by
 326 dividing the N investment in each component by the N content per unit leaf area.

327

328 *Data analysis*

329 Log₁₀ transformations were carried out on leaf traits when necessary to ensure
330 normality and minimize heterogeneity of residuals. Student *T*-tests (two-tailed)
331 were used to compare overall means of lowland and upland species. Standardized
332 major axis (SMA) estimation was used to describe the best-fit relationship
333 between pairs of variables and to assess whether relationships differed between
334 lowland vs upland elevation classes, using SMATR Version 2.0 software (Falster *et al.*, 2006; Warton *et al.*, 2006). The decision to compare upland and lowland trait
335 relationships reflects the strong elevation contrast in environments, phylogeny,
336 floristic composition and forest structure (Gentry, 1988; van de Weg *et al.*, 2009;
337 Asner *et al.*, 2014b). Significance of SMA regression was tested at $\alpha = 0.05$.

339 In addition to the above bivariate analyses, we also used a mixed-effects
340 linear model combining fixed and random components (Pinheiro & Bates, 2000)
341 to account for variability in area- and N-based rates of V_{cmax} , and area-based rates
342 of J_{max} , where the linear mixed-effects model combined fixed and random
343 components. This approach enabled the structured nature of the data set to be
344 recognized, and for interactions between multiple terms to be considered. The
345 fixed effect included continuous variables only: leaf traits (M_a , area-based leaf N
346 and P), and environment variables (soil P and N concentration, mean annual
347 temperature (MAT) and effective cation exchange capacity of soil (ECEC)). Model
348 specification and validation was based on the protocols outlined in Zuur *et al.*
349 (2009) and fitted using the *nlme* package (R package ver. 3.1–105, R Foundation
350 for Statistical Computing, Vienna, Austria, R Development Core Team 2011).
351 Details on the model selection process are provided in Table S6. Briefly,
352 phylogeny (family/genus/species) were treated as random effects, placing focus
353 on the variation contained within these terms, rather than mean values for each
354 level. For the mixed-effects linear model, site variation was captured by soil and
355 environmental factors considered in the fixed component; because of this, no site
356 term was included in the random component. Model comparisons and the

significance of fixed-effects terms were assessed using Akaike's information criterion (AIC). Unless otherwise stated, statistical analysis was performed using SPSS version 20 (IBM Corporation, NY, USA).

Results

Variations in leaf chemistry and structure

Among lowland sites, there was a six-fold variation in leaf N:P ratios (7.6 - 45.9) (Table S1, Supporting Information), but for upland sites, when ranked according to increasing elevation, mean values of leaf N:P were largely consistent across sites of similar elevation (Table 1). Across all sites (lowland and upland combined), variations in leaf N:P ratios were predominantly driven by variations in leaf [P] ($r^2=0.59$, $p<0.01$; Table S2) rather than leaf [N]. Variations in area-based leaf [P] (P_a) were positively correlated with soil [P] ($r^2=0.37$, $p<0.01$) and elevation ($r^2=0.48$, $p<0.01$). Weaker positive associations were observed for area-based leaf [N] (N_a) with total soil [N] ($r^2=0.10$, $p<0.01$) and elevation ($r^2=0.14$, $p<0.01$).

Leaf mass per unit leaf area (M_a) varied widely, both among and within lowland (54-230 g m⁻²) and upland (60-249 g m⁻²) sites (Table 1 and Table S1). Although variations in M_a were not correlated with variations in soil [P], there were significant (but weak) correlations between M_a and total soil [N] ($r^2=0.04$, $p<0.01$) and elevation ($r^2=0.03$, $p<0.01$) (Table S2). Overall means of M_a for the sampled upland species (143 ± 39 g m⁻²) were significantly higher than that of the lowland species (132 ± 35 g m⁻²; Table 2, $p<0.05$).

Across all 18 sites, leaf N_a was positively correlated with M_a ($p<0.01$, $r^2=0.12$; Table S2), with the $N_a\leftrightarrow M_a$ relationship being stronger among upland than lowland sites ($r^2=0.07$ for lowland sites and $r^2=0.20$ for upland; see Table S3 for p -values, slopes and intercepts of each SMA relationship). The slope and intercept of the relationship differed between the two elevation classes (Fig. 2A) - upland species exhibited higher N_a for a given M_a than lowland species, particularly in low M_a species. Across all sites, leaf P_a exhibited a weak, positive

387 correlation with M_a ($p < 0.01$, $r^2 = 0.04$; Table S2). Similarly, a weak positive $P_a \leftrightarrow M_a$
388 relationship ($p = 0.003$, $r^2 = 0.04$; Table S3) was found among upland species (Fig
389 2B). Although no significant $P_a \leftrightarrow M_a$ relationship was found among lowland
390 species (with leaf P_a varying 20-fold; Table S1), mean values of P_a at a given M_a
391 were lower than their upland counterparts.

392

393 *Variations in photosynthetic metabolism*

394 Light-saturated rates of photosynthesis per unit leaf area, measured at the
395 prevailing day-time air temperature (T) at each site and at an atmospheric CO_2
396 concentration of $400 \mu\text{mol mol}^{-1}$ ($A_{400,a}$), differed among co-occurring species
397 (Table S1). However, there was no significant difference between mean values of
398 $A_{400,a}$ from lowland and upland classes (Table 2). This uniformity of $A_{400,a}$ occurred
399 despite significantly lower measuring T_s at the high elevation sites [overall means:
400 lowland $29.4 \pm 0.9^\circ\text{C}$; upland $25.7 \pm 2.1^\circ\text{C}$, $p < 0.05$] and lower intercellular CO_2
401 partial pressure (C_i) (overall means: lowland $28.4 \pm 3.7 \text{ Pa}$; upland $18.8 \pm 3.0 \text{ Pa}$,
402 $p < 0.05$) (Table S4). Assessed on a per unit leaf N basis ($A_{400,N}$), average rates were
403 lower at the upland sites compared to their lowland counterparts (Tables 2 and
404 S4), reflecting higher leaf N_a for trees at high elevation (Table 1). Across sites,
405 mean $A_{400,N}$ decreased with decreasing mean annual temperature (MAT) (Figure
406 S1D). Area-based rates of photosynthesis at elevated CO_2 ($A_{2000,a}$) were higher in
407 upland ($17.1\text{--}26.5 \mu\text{mol m}^{-2} \text{ s}^{-1}$; Table S4) than lowland ($16.1\text{--}22.6 \mu\text{mol m}^{-2} \text{ s}^{-1}$)
408 species ($p < 0.05$). The higher values of $A_{2000,a}$ at the upland sites were achieved
409 despite the colder temperatures. On a per unit leaf N basis ($A_{2000,N}$), average rates
410 were similar for both elevation classifications (Table S4; Fig. S1E).

411 To explore differences in rates of the underlying components of net
412 photosynthesis, we compared maximal area-based rates of CO_2 fixation by
413 Rubisco ($V_{\text{cmax},a}$) and photosynthetic electron transport ($J_{\text{max},a}$), using values
414 normalized to a measuring temperature of 25°C (i.e. $V_{\text{cmax},a}^{25}$ and $J_{\text{max},a}^{25}$). Site
415 mean values of $V_{\text{cmax},a}^{25}$ and $J_{\text{max},a}^{25}$ were significantly higher in the upland class
416 ($V_{\text{cmax},a}^{25}$ and $J_{\text{max},a}^{25}$ were 36 and 45% higher, respectively, in the upland class;

Table 2; $p < 0.05$), reflecting the parameters' negative relationships with MAT (Fig. S1A, B). Similarly, the mean $V_{\text{cmax},\text{N}}$ at 25 °C ($V_{\text{cmax},\text{N}}^{25}$) of the upland group was greater than that of lowland counterparts (Table 2; $p < 0.05$). Thus, when assessed at a common T and when controlling for elevation differences in C_i (by adopting V_{cmax}), photosynthetic N use efficiency was, on average, greater at high elevations. Importantly, considerable within-site variability was observed for all three parameters ($V_{\text{cmax},\text{a}}^{25}$, $J_{\text{max},\text{a}}^{25}$, and $V_{\text{cmax},\text{N}}^{25}$) (Fig. 3; Table S1), highlighting the heterogeneity of these key photosynthetic traits among trees within each site. Within-site variability was particularly pronounced at the upland sites (Fig. 3; Table S1).

Variations in $J_{\text{max},\text{a}}^{25}$ were strongly correlated with $V_{\text{cmax},\text{a}}^{25}$, both for lowland ($r^2 = 0.59$) and upland classifications ($r^2 = 0.75$) (Fig. 4). Overall, the $J_{\text{max},\text{a}}^{25} \leftrightarrow V_{\text{cmax},\text{a}}^{25}$ relationship was similar in the two elevation groups, with mean $J_{\text{max},\text{a}}^{25} : V_{\text{cmax},\text{a}}^{25}$ ratios being statistically equivalent in lowland and upland classes (Table 2). Importantly, marked differences in $J_{\text{max},\text{a}}^{25} : V_{\text{cmax},\text{a}}^{25}$ ratios were observed among individuals (Figs 3 and 4), underpinned by fundamental differences in the CO_2 response of net photosynthesis (e.g. Fig. 1B). In most leaves, $J_{\text{max},\text{a}}^{25}$ and $V_{\text{cmax},\text{a}}^{25}$ co-varied, resulting in relatively constant $J_{\text{max},\text{a}}^{25} : V_{\text{cmax},\text{a}}^{25}$ ratios, as illustrated by data from individual plants of *Cecropia angustifolia* and *Glycydendron amazonicum* where the $J_{\text{max},\text{a}}^{25} : V_{\text{cmax},\text{a}}^{25}$ ratio was 1.8 (Fig. 1A and Fig. 4). However, some leaves exhibited high $V_{\text{cmax},\text{a}}^{25}$ but low $J_{\text{max},\text{a}}^{25}$ (Fig. 1B; individual of *Schefflera* sp., where $J_{\text{max},\text{a}}^{25} : V_{\text{cmax},\text{a}}^{25} = 1.1$) while other leaves with a similar $V_{\text{cmax},\text{a}}^{25}$ had markedly higher $J_{\text{max},\text{a}}^{25}$ (e.g. the *Citronella incarum* individual in Fig. 1B) leading to a higher $J_{\text{max},\text{a}}^{25} : V_{\text{cmax},\text{a}}^{25}$ value (2.4). Such variations in $J_{\text{max},\text{a}}^{25}$ and $V_{\text{cmax},\text{a}}^{25}$ likely reflect intra- and/or inter-specific variations in relative allocation of N allocation to Rubisco versus electron transport/bioenergetics.

Bivariate relationships

Across all 18 sites, $V_{\text{cmax},\text{a}}^{25}$ and $J_{\text{max},\text{a}}^{25}$ exhibited positive correlations with soil P, soil N and elevation, and negative correlations with MAT (Table S2); the strength

of these relationships was greater for $J_{\max,a}^{25}$ than $V_{\max,a}^{25}$. Relationships with MAP were either weak ($J_{\max,a}^{25}$) and not significant ($V_{\max,a}^{25}$) (Table S2). Across all sites, variations in $V_{\max,a}^{25}$ and $J_{\max,a}^{25}$ were also correlated with leaf chemical composition traits (Table S2), with bivariate relationships being stronger against P_a ($p < 0.01$, $r^2 = 0.11$ for $V_{\max,a}^{25}$, $r^2 = 0.13$ for $J_{\max,a}^{25}$) than N_a ($p < 0.01$, $r^2 = 0.05$ for both $V_{\max,a}^{25}$ and $J_{\max,a}^{25}$). Leaf N:P ratios exhibited weak, negative correlations with $V_{\max,a}^{25}$ and $J_{\max,a}^{25}$ ($p < 0.01$, $r^2 = 0.08$ for $V_{\max,a}^{25}$, $r^2 = 0.06$ for $J_{\max,a}^{25}$; Table S2). No significant relationship was found between $V_{\max,a}^{25}$ and M_a , whereas the $J_{\max,a}^{25} \leftrightarrow M_a$ relationship was significant ($p < 0.05$, $r^2 = 0.04$; Table S2).

When assessed among upland sites, no significant relationships were found between $V_{\max,a}^{25}$, M_a , N_a , P_a or N:P ratio (Fig. 5A-D). For lowland sites, $V_{\max,a}^{25}$ was positively related with P_a ($p = 0.013$, $r^2 = 0.04$; Table S3) and N_a ($p = 0.050$, $r^2 = 0.02$; Table S3), but not leaf N:P ratio or M_a (Fig 5A-D). The absence of a N:P effect for upland or lowland classes was consistent with SMA analyses comparing the slopes of $V_{\max,a}^{25} \leftrightarrow N_a$, $V_{\max,a}^{25} \leftrightarrow P_a$ and $V_{\max,a}^{25} \leftrightarrow M_a$ for the lowland class, split according to leaf N:P ratios below and above 20 - this ratio generally being thought to be roughly indicative of the N:P above which physiological processes are more likely to be limited by P as opposed to N (and vice versa) (Güsewell, 2004). No significant difference in slopes of the relationships were found ($p > 0.05$, data not shown). Similar patterns were observed for $J_{\max,a}^{25}$ (Fig. 5E-H), which was positively related with N_a ($p = 0.012$, $r^2 = 0.05$; Table S3) and P_a ($p = 0.002$, $r^2 = 0.08$; Table S3) for the lowland class only.

Investigating whether variations in photosynthetic N use efficiency were related to M_a , both across all sites (Table S2) and within each elevation class (Fig. 6A), there was no significant $V_{\max,N}^{25} \leftrightarrow M_a$ relationship across all 18 sites (Table S2) or within the upland elevation class (Table S3). Nevertheless, for the lowland class, a weak negative $V_{\max,N}^{25} \leftrightarrow M_a$ relationship was observed ($p = 0.01$; Table S3). On average, $V_{\max,N}^{25}$ at a given M_a was higher in upland species than their lowland counterparts. With respect to foliar phosphorus, there was no significant relationship between $V_{\max,N}^{25}$ and leaf P_a or with leaf N:P when considering the

477 elevation classes separately. This conclusion was held for $V_{\text{cmax},\text{N}}^{25} \leftrightarrow P_a$ when
478 combining upland and lowland data (Table S2). For $V_{\text{cmax},\text{N}}^{25} \leftrightarrow \text{N:P}$, combining
479 upland and lowland data resulted in a weak significant relationship ($p < 0.05$, $r^2 =$
480 0.02 ; Table S2); similarly, relationships between $V_{\text{cmax},\text{N}}^{25}$ and soil P, soil N and
481 elevation were relatively weak (Table S2). Collectively, these results show that the
482 proportion of the variance in $V_{\text{cmax},\text{N}}^{25}$ accounted for by the above soil and leaf
483 level parameters was negligible.

484

485 *Variation in N-allocation patterns*

486 To further explore what factors might contribute to variations in $V_{\text{cmax},\text{N}}^{25}$, we
487 calculated the fraction of leaf N allocated to photosynthesis (n_A); n_A is dependent
488 on the allocation of leaf N to Rubisco (n_R), electron transport (n_E) and pigment-
489 protein complexes (n_P). Figure 7 shows that mean values of n_A and its underlying
490 components exhibited relatively little variation across sites. Nevertheless, inter-
491 specific variations were evident at each site, with n_R varying up to seven-fold at
492 some sites (e.g. CUZ-03; 0.03-0.20; Table S1). A large proportion of N was inferred
493 to be allocated in pigment-protein complexes, with n_P being greater than n_R and
494 n_E combined. The overall mean of n_R for the upland class (0.105) was significantly
495 higher than that for the lowland class (0.090; Table 2, $p < 0.05$). Similarly, n_E was
496 higher for upland (0.034) than for lowland groups (0.028; Table 2, $p < 0.05$). There
497 was no difference between the elevation classes in n_P . Overall, n_A was similar in
498 the lowland and upland groupings (37-38%; Table 2).

499 There was considerable variability in n_A among lowland and upland species
500 (0.1 to 0.6), with significant negative correlations being found with M_a , N_a and P_a
501 for the lowland group (Fig. 8, Table S5). Similar significant correlations existed for
502 the upland class but with the important caveat that upland species consistently
503 exhibited higher n_A at a given N_a and P_a (Figs. 8 and S2; Table S5). Thus, while
504 mean values of n_A were similar in upland and lowland species, the fraction of leaf
505 N allocated to photosynthesis was greater in upland plants when comparisons
506 were made at common leaf N_a and P_a values.

507

508 *Validation of Rubisco estimates by in vitro assays*

509 We used *in vitro* Rubisco assays on 16 lowland species (Fig. 9A) to quantify n_R ,
510 thus allowing direct comparison of n_R obtained for these *in vitro* assays with that
511 of the *in vivo* estimates derived from $V_{\text{cmax},a}^{25}$. Figure 9B shows that there was
512 considerable discrepancy between *in vitro* and *in vivo* predicted n_R . If one
513 assumes that the *in vitro* values provide an estimate of potential Rubisco capacity,
514 and that the *in vivo* values are indicative of the realized maximum rate in intact
515 tissues, then it is possible that the *in vivo* approach underestimates the proportion
516 of N allocated in Rubisco. Reliance on the *in vitro* values resulted in marked
517 increases in n_R at a given M_a , albeit with the overall pattern of increasing n_R with
518 decreasing M_a still held (Fig. S3A). Considering the overall N investment pattern
519 in photosynthetic metabolism, adopting *in vitro* estimates of n_R resulted in
520 marked increases in the total fraction of N allocated to photosynthesis compared
521 to *in vivo* (Fig. S4). Indeed, in some cases *in vitro* estimates of N allocation to
522 Rubisco was similar to, or even higher than, N allocation to pigment protein
523 complexes (Fig. S4). Collectively, these results suggest that the answer to the
524 question '*how much leaf N is allocated to photosynthesis*' will depend on whether
525 *in vivo* or *in vitro* estimates of n_R are used in the underlying calculations.

526

527 *Modelling variations in $V_{\text{cmax},a}^{25}$, $J_{\text{max},a}^{25}$ and $V_{\text{cmax},N}^{25}$*

528 We used linear mixed-effects to model variations in $V_{\text{cmax},a}^{25}$, $J_{\text{max},a}^{25}$ and $V_{\text{cmax},N}^{25}$,
529 the starting model included only continuous terms for leaf traits and
530 environmental variables. Additional details of the model selection procedure are
531 provided in Table S6. When presented with information on soil and leaf P and N
532 as key nutrients driving maximum carboxylation capacity of Rubisco, the final
533 preferred model for $V_{\text{cmax},a}^{25}$ (model 6, Table S6) retained P only, suggesting an
534 increase of $V_{\text{cmax},a}^{25}$ as soil and foliar P increase (Table 3). A combination of site-
535 level soil P and individual-level foliar P as fixed effects, and family as a random
536 effect, explained 39% of the variation in $V_{\text{cmax},a}^{25}$ (Fig. S5). Inclusion of MAT, soil

537 N, leaf N_a , M_a and effective cation exchange capacity of soils as fixed effects did
538 not improve the criteria score (Table S6). The model's variance components, as
539 defined by the random term, indicated that family accounted for only 2.5% of the
540 unexplained variance (i.e. the response variance not accounted for by the fixed
541 terms) (Table 3). Finer phylogenetic detail (genera and species) did not improve
542 the model. A review of diagnostic plots from the final preferred model showed
543 that inclusion of elevation class did not improve model performance, when a
544 range of environmental variables that describe the elevation gradient (e.g. soil P,
545 soil N and MAT) were included. Hence, it was not necessary to include elevation
546 class in the fixed components of the mixed-effects model.

547 Similar to $V_{\text{cmax},a}^{25}$, variations in $J_{\text{max},a}^{25}$ were largely accounted for by a
548 combination of site-level soil P and individual-level foliar P, with $J_{\text{max},a}^{25}$ increasing
549 with increasing soil and foliar P (Table 3); the final model explained 44% of the
550 variation in $J_{\text{max},a}^{25}$ (Fig. S5). The preferred model (determined by assessing the
551 effect of dropping sequentially explanatory variables; Table S6) did not retain soil
552 N, leaf N_a , M_a or MAT (Table S6). For the random effects, family contributed 2.8%
553 to the unexplained variance (Table 3).

554 For $V_{\text{cmax},N}^{25}$ (i.e. photosynthetic N use efficiency), we attempted to
555 construct a model using combinations of soil and leaf P, soil and leaf N, soil ECEC,
556 and climate (MAT). However, in contrast to $V_{\text{cmax},a}^{25}$ and $J_{\text{max},a}^{25}$, $V_{\text{cmax},N}^{25}$ model
557 performance was not improved via sequential deletion of explanatory terms; thus,
558 the inputted soil, climate and leaf variables did not permit identification of the
559 key factors influencing variation in $V_{\text{cmax},N}^{25}$. This suggests that other factors, such
560 as how leaf N is allocated and/or whether Rubisco is fully active may have played
561 a role.

562

563 Discussion

564

565 *Regional and inter-biome context*

566 Past studies on tropical and non-tropical forests revealed variability in the slope

567 of $V_{\text{cmax},a}^{25} \leftrightarrow N_a$ relationships, with lower rates of V_{cmax} per unit N in nutrient-poor,
 568 lowland tropical forests compared to lowland forests on more fertile soils, upland
 569 tropical forests and temperate broadleaf forests (Carswell *et al.*, 2000; Domingues
 570 *et al.*, 2007; Meir *et al.*, 2007; Kattge *et al.*, 2009; Domingues *et al.*, 2010; Mercado
 571 *et al.*, 2011; van de Weg *et al.*, 2012). Moreover, Reich *et al.* (2009) concluded that
 572 the slope of mass-based $A \leftrightarrow N$ relationships is lower in the tropics than in colder
 573 arctic and temperate biomes. Our study supports such studies, with $V_{\text{cmax},N}^{25}$
 574 values for our upland and lowland TMFs (22.5 and 18.9 $\mu\text{mol CO}_2 \text{ g N}^{-1} \text{ s}^{-1}$,
 575 respectively) being markedly lower than reported for temperate broadleaved
 576 trees [34 $\mu\text{mol CO}_2 \text{ g N}^{-1} \text{ s}^{-1}$ (Kattge *et al.*, 2009)].

577 How do our results compare with other analyses of photosynthetic
 578 capacity in tropical ecosystems? The range of $V_{\text{cmax},a}^{25}$ (6–96 $\mu\text{mol m}^{-2} \text{ s}^{-1}$; Table
 579 S1) and $J_{\text{max},a}^{25}$ (21–176 $\mu\text{mol m}^{-2} \text{ s}^{-1}$; Table S1) values from our study were wider
 580 than those reported for drier tropical sites in West Africa (Domingues *et al.*, 2010),
 581 perhaps reflecting environmental differences, or differences in the number of
 582 species sampled (210 here versus 39 in the West African study). For our lowland
 583 TMFs (which included three low nutrient status white sand sites in Northern Peru),
 584 the overall mean $V_{\text{cmax},a}^{25}$ ($36 \pm 15 \mu\text{mol m}^{-2} \text{ s}^{-1}$) was lower than previously
 585 reported tropical values: Carswell *et al.* (2000): 43 $\mu\text{mol m}^{-2} \text{ s}^{-1}$; Domingues *et al.*
 586 (2007): 53 $\mu\text{mol m}^{-2} \text{ s}^{-1}$; Meir *et al.* (2007): 49–68 $\mu\text{mol m}^{-2} \text{ s}^{-1}$; Kattge *et al.* (2009):
 587 41 $\mu\text{mol m}^{-2} \text{ s}^{-1}$ (non-oxisol); Bloomfield *et al.* (2014a): 63 $\mu\text{mol m}^{-2} \text{ s}^{-1}$;
 588 Domingues *et al.* (2015): 39–46 $\mu\text{mol m}^{-2} \text{ s}^{-1}$. By contrast, our mean $V_{\text{cmax},a}^{25}$ values
 589 were higher than the values for lowland TMFs only growing on nutrient-poor,
 590 oxisol [29 $\mu\text{mol m}^{-2} \text{ s}^{-1}$ (Kattge *et al.*, 2009)]. Since $J_{\text{max},a}^{25}$ was tightly correlated
 591 with $V_{\text{cmax},a}^{25}$ (Fig. 4), our estimates of $J_{\text{max},a}^{25}$ for lowland TMFs were also lower
 592 than those reported in above-mentioned studies. Rates of $V_{\text{cmax},a}^{25}$ at our upland
 593 sites ($49 \pm 20 \mu\text{mol m}^{-2} \text{ s}^{-1}$) were similar to those reported by van de Weg *et al.*
 594 (2012): 56 $\mu\text{mol m}^{-2} \text{ s}^{-1}$ for the same Andean region, and fell mid-range of values
 595 reported in Dusenge *et al.* (2015) and Vårhammar *et al.* (2015) for high elevation
 596 tropical trees of Rwanda.

597 Taken together, our results support the hypothesis that both $V_{\text{cmax},a}^{25}$ and
598 photosynthetic N efficiency are lower in lowland TMFs than in temperate
599 broadleaved forests. In addition, each parameter is highly variable, both among
600 co-existing tropical species growing at individual sites and between
601 environmentally-contrasting sites.

602

603 *Phosphorus –does it modulate photosynthetic capacity and/or N-use efficiency?*

604 Our site selection aimed to assess the potential role of phosphorus-limitation on
605 photosynthetic performance across TMFs in western Amazonia and the Andes
606 where substantial variations in soil P occur (lowland sites: 38-727 mg P kg⁻¹;
607 upland sites: 496-1631 mg P kg⁻¹). Low P availability can limit rates of
608 photosynthesis via reduced maximal rates of RuBP regeneration (i.e. J_{max}), with
609 maximal Rubisco activity (i.e. V_{cmax}) also often being reduced (Brooks, 1986;
610 Jacobs & Lawlor, 1992; Loustau *et al.*, 1999). While the mechanisms responsible
611 for reduced V_{cmax} remain uncertain, possible factors include the need to maintain
612 co-limitation by RuBP regeneration and carboxylation, as well as feedback
613 inhibition on Rubisco resulting from inability to export triose phosphates to the
614 cytosol (Wullschlegel, 1993; Walker *et al.*, 2014).

615 The hypothesis that photosynthetic capacity would be positively correlated
616 with soil [P] and leaf P_a was supported by our results – a finding consistent with
617 earlier studies on tropical species in South America, West Africa and Australia
618 (Domingues *et al.*, 2007; Meir *et al.*, 2007; Kattge *et al.*, 2009; Domingues *et al.*,
619 2010; Bloomfield *et al.*, 2014b). Among lowland sites alone, and the combination
620 of lowland and upland sites together, significant positive relationships were
621 observed between photosynthetic capacity (expressed either as $V_{\text{cmax},a}^{25}$ or $J_{\text{max},a}^{25}$)
622 and foliar P_a , and against soil [P] (Tables S2, S3). Across all 18 TMF sites, $V_{\text{cmax},a}^{25}$
623 and $J_{\text{max},a}^{25}$ also exhibited significant negative relationships with leaf N:P (Table
624 S2). Moreover, foliar P_a and soil [P] emerged as significant explanatory variables
625 in linear mixed-effect models of variations in photosynthetic capacity (Table 3),
626 accounting for ~40% of the observed variations in $V_{\text{cmax},a}^{25}$ and $J_{\text{max},a}^{25}$. The

627 absence of mean annual temperature (MAT) in the preferred models suggest that,
628 while growth temperature can affect photosynthetic capacity (Hikosaka *et al.*,
629 2006; Sage & Kubien, 2007) and patterns of N investment, knowledge of growth
630 temperature along the western Amazon-Andes elevation gradient is not required
631 when data on leaf and soil P is available.

632 Past studies reported that P-deficiencies also reduce photosynthetic N use
633 efficiency (Reich *et al.*, 2009) and the fraction of leaf N allocated to photosynthesis
634 (Warren & Adams, 2002). While average values $V_{\text{cmax},\text{N}}$ and foliar [P] were highest
635 in our upland trees, no significant $V_{\text{cmax},\text{N}} \leftrightarrow \text{P}_a$ relationships were observed, either
636 across all sites or within each elevation class. Furthermore, we could not identify
637 key factors explaining variation in $V_{\text{cmax},\text{N}}$ using linear mixed-effects models; this
638 included models that contained data on soil and foliar [P]. While this does not
639 preclude a role for deficiencies in cytosolic [P] in regulating *in vivo* values of
640 $V_{\text{cmax},\text{N}}$, it seems unlikely that either soil or total leaf [P] can be used a predictor of
641 variations in *in vivo* Rubisco capacity per unit leaf N.

642

643 *Activation state of Rubisco*

644 *In vitro* quantification in several lowland TMF species revealed that Rubisco
645 content inferred from CO_2 response curves may have substantially
646 underestimated absolute levels of this key protein (Fig. 9). When estimating
647 Rubisco abundance from $A \leftrightarrow C_i$ curves, Rubisco is assumed to be fully activated –
648 however, there is growing evidence that Rubisco often operates at less than
649 maximum activity or is in excess of CO_2 fixation requirements (Stitt & Schulze,
650 1994; Warren *et al.*, 2000). Partial activation could be linked to limitations in sink
651 demand for carbohydrates and/or co-limitation by other rock-derived nutrients
652 such as calcium [e.g. Asner *et al.* (2014b)]. Inactive Rubisco might serve as a
653 temporary N store - as such, Rubisco can act as both a metabolic and non-
654 metabolic protein (Stitt & Schulze, 1994; Warren *et al.*, 2000). Viewed from this
655 perspective, *in vivo* estimates of V_{cmax} provide insights into N investment into the
656 *metabolically active* Rubisco, relevant when modelling gross primary productivity

657 of TMF ecosystems. However, if the objective is to assess how plants differ in N
658 investment in both active and inactive forms of Rubisco, then n_R estimated from
659 other approaches, such as Western blots (or similar quantitative techniques)
660 might be required.

661 As noted earlier, the observed values of $V_{\text{cmax},N}^{25}$ were lower than that of
662 trees growing in temperate environments (Kattge *et al.*, 2009). Similarly, when
663 compared at any given M_a , *in vivo* estimates of n_R (i.e. fraction of leaf N allocated
664 to Rubisco estimated from gas exchange) were, on average, lower in our TMF
665 trees compared to the global average (Hikosaka, 2004; Wright *et al.*, 2004) (Fig.
666 S3). By contrast, *in vitro* estimates of n_R (i.e. n_R estimated from Western blots) were
667 often higher than the global average (Fig. S3). This finding raises the possibility
668 that the efficiency of N investment in Rubisco may not necessarily be lower in
669 TMFs; rather, it may be that the activation state is lower in tropical forests
670 compared with their temperate counterparts. Further work is needed to explore
671 this question; additional work is also needed to determine what role, if any,
672 limitations in mesophyll conductance (g_m) have on estimates of V_{cmax} and the
673 associated values of n_R .

674

675 *Additional factors influencing V_{cmax} estimates*

676 In our study, we have so far estimated *in vivo* rates of $V_{\text{cmax},a}^{25}$ assuming a
677 common, single set of kinetic constants (K_c and K_o) for Rubisco (von Caemmerer
678 *et al.*, 1994) and associated activation energies (E_a) (Farquhar *et al.*, 1980), as well
679 as infinite g_m . Such assumptions were made necessary in the absence of K_c , K_o , E_a
680 and g_m values for tropical species. Application of different K_c and K_o values, such
681 as those reported by Bernacchi *et al.* (2002), would alter estimates of $V_{\text{cmax},a}^{25}$ for
682 all trees but would not alter relative differences among sites or elevational classes.
683 By contrast, application of Bernacchi *et al.* (2002) E_a values for K_c and K_o (80.99
684 and 23.72 kJ mol⁻¹, respectively), and V_{cmax} (65.3 kJ mol⁻¹) could potentially relative
685 differences in $V_{\text{cmax},a}^{25}$ between upland and lowland trees, depending on the
686 extent to which leaf temperatures differed among the sites. Similarly, replacement

687 of the Farquhar *et al.* (1980) E_a values of V_{cmax} and J_{max} (of 64.8 and 37.0 kJ mol⁻¹,
 688 respectively) with those of Bernacchi *et al.* (2002) (65.3 and 43.9 kJ mol⁻¹,
 689 respectively) could alter the relative differences in $V_{\text{cmax},a}^{25}$ and $J_{\text{max},a}^{25}$ between
 690 upland and lowland sites. To check whether application of alternative E_a values
 691 change our conclusions regarding site-to-site differences, we calculated $V_{\text{cmax},a}^{25}$
 692 and $J_{\text{max},a}^{25}$ using the respective activation energies of Farquhar *et al.* (1980) and
 693 Bernacchi *et al.* (2002). Use of the Bernacchi *et al.* (2002) E_a values resulted in an
 694 average 10.6% increase in estimates of $V_{\text{cmax}25}$ for lowland trees (Table S7),
 695 reflecting the fact that lowland leaf temperatures were near 30°C (Table S4).
 696 Upland estimates were less affected (3.5% increase; Table S7) as the average leaf
 697 temperature of upland group was 25.7°C (Table S4). Despite the increased
 698 estimates of $V_{\text{cmax}25}$ for lowland trees when using E_a values from Bernacchi *et al.*
 699 (2002), there remained a significant difference between lowland and upland mean
 700 $V_{\text{cmax}25}$ values (Table S7); the same was true for $J_{\text{max},a}^{25}$ (Table S7). As a result,
 701 relationships between photosynthetic properties and site MAT and soil P were
 702 similar when using Farquhar *et al.* (1980) and Bernacchi *et al.* (2002) E_a values (Fig.
 703 S1). Thus, irrespective of which E_a values are used [see Medlyn *et al.* (2002) for
 704 further discussion the temperature dependence of these constants], we are
 705 confident that that mean values of $V_{\text{cmax}25}$ and $J_{\text{max},a}^{25}$ are indeed higher in the
 706 upland plants growing in the Peruvian Andes.

707 What impact might systematic differences in g_m between upland and
 708 lowland TMFs have on our results? If g_m was finite, but similar in upland and
 709 lowland TMF environments, then our conclusion that $V_{\text{cmax},a}^{25}$ is higher in upland
 710 species would hold (albeit with modified values). However, if g_m was more limiting
 711 in lowland TMF trees than their upland counterparts, then calculation of V_{cmax}
 712 using A-C_c curves might fail to differentiate between the upland and lowland
 713 groups. A definitive assessment of this issue will require further work assessing
 714 g_m in tropical trees (e.g. using concurrent measurements of leaf as exchange and
 715 carbon isotope discrimination or chlorophyll fluorescence). Although g_m tends to
 716 decrease with increasing M_a (Flexas *et al.*, 2008), the M_a difference between

lowland and upland groups was small (Table 1). Given the potential for large variations in g_m among species (at a given M_a), it is unlikely that g_m would have been higher in the selected lowland TMF trees. Irrespective of the effect of elevation on g_m , rates of $A_{40,a}$ and $A_{200,a}$ (measured at prevailing leaf T_s) were surprisingly high in plants at the cooler, high elevation sites (Table S4). Given this and our extensive sample size, we feel confident that photosynthetic capacity at a standardised T is likely larger in trees growing at high elevations in the Andes compared to those in the lowland regions of Amazonia, as proposed by van de Weg *et al.* (2012; 2014). Enhanced photosynthetic capacity at high altitude could help negate the inhibitory effects of low T on leaf-level CO_2 uptake, with the result that gross primary productivity (GPP) would not decline with increasing elevation as much as expected.

Recent modelling of C-exchange processes at a high elevation TMF site (3025 m a.s.l.) in Peru suggested that gross primary productivity (GPP) may be 20-40% lower compared to lowland TMFs (Girardin *et al.*, 2014a; van de Weg *et al.*, 2014); low T appeared to be most important factor limiting GPP at high elevations (van de Weg *et al.*, 2014). Our results suggest that the inhibitory effect of low T on GPP of upland TMFs would be greater if photosynthetic capacity remained constant across the elevation gradient. Thus, the greater photosynthetic capacity of upland TMFs might contribute to GPP being relatively homeostatic across the Peruvian Amazon-Andes elevation gradient. Further work is needed to explore how elevation-dependent variations in photosynthetic capacity impact on current and future net primary productivity (NPP) of TMFs, when taking into account other NPP components (e.g. leaf area index, biomass allocation, litter fall, autotrophic respiration).

Concluding statements

Our findings reveal greater photosynthetic capacity in Andean forest leaves compared to lowland western Amazonian leaves, underpinned by greater concentrations of leaf N and N-use efficiency per unit leaf area (Table 2, Fig. 8).

747 Our data also support the hypothesis that variations in leaf and soil P play key
748 role in modulating photosynthetic capacity of TMFs (Fig. 5, Table 3 and S2), with
749 the mixed-effects models (Table 3) providing the modelling community with
750 predictive equations that will enable model parameterization based arguably the
751 largest single tropical V_{cmax} datasets available. Finally, our analyses indicate that
752 a substantial fraction of Rubisco is inactive in trees growing in the Peruvian
753 Amazon and suggest that a greater fraction of leaf N may well be invested in
754 photosynthetic machinery than indicated by leaf gas exchange measurements.

755

756 **Acknowledgements**

757 We thank R. Tupayachi, N. Jaramillo, F. Sinca, L. Carranza-Jimenez and the
758 Spectranomics team for field and laboratory assistance. Measurements were
759 made in plots inventoried and maintained by RAINFOR (www.rainfor.org)
760 investigators from Peru. Access to the field sites was also facilitated by Gordon
761 and Betty Moore Foundation grants (to O.P., Y.M., J.L., and G.A.). Foliar sampling,
762 taxonomic determinations, and chemical analyses were supported by a grant
763 from the Gordon and Betty Moore Foundation to the Carnegie Institution for
764 Science. This work was also funded by grants/fellowships from the Australian
765 Research Council (DP0986823, DP130101252, CE140100008 and FT0991448 to
766 O.K.A.; and, FT110100457 to P.M.), and NERC grants (NE/C51621X/1 and
767 NE/F002149/1 to P.M.). R.G. was supported by a Newton International Fellowship
768 (funded by the Royal Society, the British Academy and the Royal Academy of
769 Engineering). NHAB is funded by Malaysian government postgraduate
770 scholarship.

771

772 **Author Contributions**

773 O.K.A., J.L., P.M., Y.M., O.L.P., G.P.A., R.E.M., F.Y.I., L.K.W., R.G., O.S.O., N.H.A.B., J.R.E. and
 774 B.M.L. planned and designed the research. N.H.A.B., F.Y.I., L.K.W., R.G., O.S.O., K.J.B.,
 775 G.P.A., R.E.M., J.L., Y.M., N.S., E.G.C., T.D., C.A.Q., F.S., A.E.V., P.P.Z.C., J. dA.-P., K.Q.H.,
 776 I.C.T., R.B.L., Y.P.T., J.H.O. and O.K.A conducted fieldwork and/or analysed field-based
 777 data. N.H.A.B., F.Y.I., G.P.A., R.E.M., B.M.L. and J.R.E. performed laboratory experiments
 778 and analysed chemical/biochemical data. N.H.A.B., O.K.A., K.J.B., J.L., O.L.P., P.M., G.P.A.,
 779 J.M., O.S.O., R.G., L.K.W., J.R.E. and B.M.L. wrote the manuscript.

781 **References**

- 782 **Aerts R, Chapin FSI. 2000.** The mineral nutrition of wild plants revisited : a re-evaluation of
 783 processes and patterns. *Advances in Ecological Research* **30**: 1-67.
- 784 **Almeida JP, Montúfar R, Anthelme F. 2012.** Patterns and origin of intraspecific functional
 785 variability in a tropical alpine species along an altitudinal gradient. *Plant Ecology &*
 786 *Diversity* **6**: 423-433.
- 787 **Asner GP, Martin RE. 2011.** Canopy phylogenetic, chemical and spectral assembly in a lowland
 788 Amazonian forest. *New Phytologist* **189**: 999-1012.
- 789 **Asner GP, Anderson CB, Martin RE, Knapp DE, Tupayachi R, Sinca F, Malhi Y. 2014a.**
 790 Landscape-scale changes in forest structure and functional traits along an Andes-to-
 791 Amazon elevation gradient. *Biogeosciences* **11**: 843-856.
- 792 **Asner GP, Martin RE, Tupayachi R, Anderson CB, Sinca F, Carranza-Jiménez L, Martinez P.**
 793 **2014b.** Amazonian functional diversity from forest canopy chemical assembly.
 794 *Proceedings of the National Academy of Sciences, USA* **111**: 5604-5609.
- 795 **Ayub G, Smith RA, Tissue DT, Atkin OK. 2011.** Impacts of drought on leaf respiration in
 796 darkness and light in *Eucalyptus saligna* exposed to industrial-age atmospheric CO₂
 797 and growth temperature. *New Phytologist* **190**: 1003-1018.
- 798 **Beer C, Reichstein M, Tomelleri E, Ciais P, Jung M, Carvalhais N, Rödenbeck C, Arain MA,**
 799 **Baldocchi D, Bonan GB, et al. 2010.** Terrestrial gross carbon dioxide uptake: global
 800 distribution and covariation with climate. *Science* **329**: 834-838.
- 801 **Bernacchi CJ, Portis AR, Nakano H, von Caemmerer S, Long SP. 2002.** Temperature response
 802 of mesophyll conductance. Implications for the determination of Rubisco enzyme
 803 kinetics and for limitations to photosynthesis *in vivo*. *Plant Physiology* **130**: 1992-1998.
- 804 **Bloomfield KJ, Domingues TF, Saiz G, Bird MI, Crayn DM, Ford A, Metcalfe D, Farquhar GD,**
 805 **Lloyd J. 2014a.** Contrasting photosynthetic characteristics of forest vs. savanna species
 806 (far North Queensland, Australia). *Biogeosciences* **11**: 7331-7347.
- 807 **Bloomfield KJ, Farquhar GD, Lloyd J. 2014b.** Photosynthesis–nitrogen relationships in tropical
 808 forest tree species as affected by soil phosphorus availability: a controlled
 809 environment study. *Functional Plant Biology* **41**: 820-832.
- 810 **Brooks A. 1986.** Effects of phosphorus nutrition on ribulose-1,5-bisphosphate carboxylase
 811 activation, photosynthetic quantum yield and amounts of some Calvin-cycle
 812 metabolites in spinach leaves. *Australian Journal of Plant Physiology* **13**: 221-237.
- 813 **Bruhn D, Mikkelsen TN, Atkin OK. 2002.** Does the direct effect of atmospheric CO₂
 814 concentration on leaf respiration vary with temperature? Responses in two species of
 815 *Plantago* that differ in relative growth rate. *Physiologia Plantarum* **114**: 57-64.
- 816 **Bruijnzeel LA, Scatena FN, Hamilton LS. 2011.** *Tropical Montane Cloud Forests: Science for*
 817 *Conservation and Management*: Cambridge University Press.
- 818 **Bruijnzeel LA, Veneklaas EJ. 1998.** Climatic conditions and tropical montane forest
 819 productivity: the fog has not lifted yet. *Ecology* **79**: 3-9.

820 **Carswell FE, Meir P, Wandelli EV, Bonates LCM, Kruijt B, Barbosa EM, Nobre AD, Grace J,**
821 **Jarvis PG. 2000.** Photosynthetic capacity in a central Amazonian rain forest. *Tree*
822 *Physiology* **20**: 179-186.

823 **Cordell S, Goldstein G, Meinzer FC, Handley LL. 1999.** Allocation of nitrogen and carbon in
824 leaves of *Metrosideros polymorpha* regulates carboxylation capacity and $\delta^{13}\text{C}$ along an
825 altitudinal gradient. *Functional Ecology* **13**: 811-818.

826 **Coste S, Roggy J-C, Imbert P, Born C, Bonal D, Dreyer E. 2005.** Leaf photosynthetic traits of 14
827 tropical rain forest species in relation to leaf nitrogen concentration and shade
828 tolerance. *Tree Physiology* **25**: 1127-1137.

829 **Domingues TF, Berry JA, Martinelli LA, Ometto JPHB, Ehleringer JR. 2005.** Parameterization of
830 canopy structure and leaf-level gas exchange for an eastern Amazonian tropical rain
831 forest (Tapajós National Forest, Pará, Brazil). *Earth Interactions* **9**: 1-23.

832 **Domingues TF, Ishida FY, Feldpausch T, Grace J, Meir P, Saiz G, Sene O, Schrodte F, Sonké B,**
833 **Taédoumg H, et al. 2015.** Biome-specific effects of nitrogen and phosphorus on the
834 photosynthetic characteristics of trees at a forest-savanna boundary in Cameroon.
835 *Oecologia* **178**: 659-672.

836 **Domingues TF, Martinelli LA, Ehleringer JR. 2007.** Ecophysiological traits of plant functional
837 groups in forest and pasture ecosystems from eastern Amazônia, Brazil. *Plant Ecology*
838 **193**: 101-112.

839 **Domingues TF, Meir P, Feldpausch TR, Saiz G, Veenendaal EM, Schrodte F, Bird M, Djagbletey**
840 **G, Hien F, Compaore H, et al. 2010.** Co-limitation of photosynthetic capacity by
841 nitrogen and phosphorus in West Africa woodlands. *Plant, Cell & Environment* **33**: 959-
842 980.

843 **Dusenge M, Wallin G, Gårdesten J, Niyonzima F, Adolfsson L, Nsabimana D, Uddling J. 2015.**
844 Photosynthetic capacity of tropical montane tree species in relation to leaf nutrients,
845 successional strategy and growth temperature. *Oecologia* **177**: 1183-1194.

846 **Evans JR. 1989.** Photosynthesis and nitrogen relationships in leaves of C_3 plants. *Oecologia* **78**:
847 9-19.

848 **Evans JR, Seemann JR. 1989.** *The allocation of protein nitrogen in the photosynthetic*
849 *apparatus: costs, consequences, and control.* New York, USA: Alan R. Liss, Inc.

850 **Falster DS, Warton DI, Wright IJ. 2006.** SMATR: Standardised major axis tests and routines,
851 version 2.0.

852 **Farquhar GD, von Caemmerer S, Berry JA. 1980.** A biochemical model of photosynthetic CO_2
853 assimilation in leaves of C_3 species. *Planta* **149**: 78-90.

854 **Flexas J, Ribas-Carbó M, Diaz-Espejo A, Galmés J, Medrano H. 2008.** Mesophyll conductance
855 to CO_2 : current knowledge and future prospects. *Plant, Cell & Environment* **31**: 602-
856 621.

857 **Fredeen AL, Rao IM, Terry N. 1989.** Influence of phosphorus nutrition on growth and carbon
858 partitioning in *Glycine max*. *Plant Physiology* **89**: 225-230.

859 **Fyllas NM, Patiño S, Baker TR, Bielefeld Nardoto G, Martinelli LA, Quesada CA, Paiva R,**
860 **Schwarz M, Horna V, Mercado LM, et al. 2009.** Basin-wide variations in foliar
861 properties of Amazonian forest: phylogeny, soils and climate. *Biogeosciences* **6**: 2677-
862 2708.

863 **Gaspar MM, Ferreira RB, Chaves MM, Teixeira AR. 1997.** Improved method for the extraction
864 of proteins from *Eucalyptus* leaves. Application in leaf response to temperature.
865 *Phytochemical Analysis* **8**: 279-285.

866 **Gentry AH. 1988.** Changes in plant community diversity and floristic composition on
867 environmental and geographical gradients. *Annals of the Missouri Botanical Garden*
868 **75**: 1-34.

869 **Girardin CAJ, Espejo JES, Doughty CE, Huasco WH, Metcalfe DB, Durand-Baca L, Marthews**
870 **TR, Aragao LE, Farfán-Rios W, García-Cabrera K. 2014a.** Productivity and carbon
871 allocation in a tropical montane cloud forest in the Peruvian Andes. *Plant Ecology &*
872 *Diversity* **7**: 107-123.

873 **Girardin CAJ, Farfan-Rios W, Garcia K, Feeley KJ, Jørgensen PM, Murakami AA, Cayola Pérez**
874 **L, Seidel R, Paniagua N, Fuentes Claros AF, et al. 2014b.** Spatial patterns of above-
875 ground structure, biomass and composition in a network of six Andean elevation
876 transects. *Plant Ecology & Diversity* **7**: 161-171.

877 **Girardin CAJ, Malhi Y, Aragao LE, Mamani M, Huaraca Huasco W, Durand L, Feeley KJ, Rapp J,**
878 **Silva-Espejo JE, Silman M, et al. 2010.** Net primary productivity allocation and cycling
879 of carbon along a tropical forest elevational transect in the Peruvian Andes. *Global*
880 *Change Biology* **16**(12): 3176-3192.

881 **Grubb PJ. 1977.** Control of forest growth and distribution on wet tropical mountains: with
882 special reference to mineral nutrition. *Annual Review of Ecology and Systematics* **8**: 83-
883 107.

884 **Güsewell S. 2004.** N : P ratios in terrestrial plants: variation and functional significance. *New*
885 *Phytologist* **164**: 243-266.

886 **Harrison MT, Edwards EJ, Farquhar GD, Nicotra AB, Evans JR. 2009.** Nitrogen in cell walls of
887 sclerophyllous leaves accounts for little of the variation in photosynthetic nitrogen-use
888 efficiency. *Plant, Cell & Environment* **32**: 259-270.

889 **Hikosaka K. 2004.** Interspecific difference in the photosynthesis–nitrogen relationship:
890 patterns, physiological causes, and ecological importance. *Journal of Plant Research*
891 **117**: 481-494.

892 **Hikosaka K, Ishikawa K, Borjigidai A, Muller O, Onoda Y. 2006.** Temperature acclimation of
893 photosynthesis: mechanisms involved in the changes in temperature dependence of
894 photosynthetic rate. *Journal of Experimental Botany* **57**: 291-302.

895 **Hikosaka K, Nagamatsu D, Ishii HS, Hirose T. 2002.** Photosynthesis–nitrogen relationships in
896 species at different altitudes on Mount Kinabalu, Malaysia. *Ecological Research* **17**:
897 305-313.

898 **Hikosaka K, Shigeno A. 2009.** The role of Rubisco and cell walls in the interspecific variation in
899 photosynthetic capacity. *Oecologia* **160**: 443-451.

900 **Jacob J, Lawlor DW. 1992.** Dependence of photosynthesis of sunflower and maize leaves on
901 phosphate supply, ribulose-1,5-bisphosphate carboxylase oxygenase activity, and
902 ribulose-1,5-bisphosphate pool size. *Plant Physiology* **98**: 801-807.

903 **Jacob J, Lawlor DW. 1993.** Extreme phosphate deficiency decreases the *in vivo* CO₂/O₂
904 specificity factor of Ribulose 1,5-Bisphosphate Carboxylase-Oxygenase in intact leaves
905 of sunflower. *Journal of Experimental Botany* **44**: 1635-1641.

906 **Kattge J, Knorr W, Raddatz T, Wirth C. 2009.** Quantifying photosynthetic capacity and its
907 relationship to leaf nitrogen content for global-scale terrestrial biosphere models.
908 *Global Change Biology* **15**: 976-991.

909 **Kraft NJB, Valencia R, Ackerly DD. 2008.** Functional traits and niche-based tree community
910 assembly in an Amazonian forest. *Science* **322**: 580-582.

911 **Kumagai To, Ichie T, Yoshimura M, Yamashita M, Kenzo T, Saitoh TM, Ohashi M, Suzuki M,**
912 **Koike T, Komatsu H. 2006.** Modeling CO₂ exchange over a Bornean tropical rain forest
913 using measured vertical and horizontal variations in leaf-level physiological parameters
914 and leaf area densities. *Journal of Geophysical Research: Atmospheres* **111**: D10107.

915 **Lauer MJ, Pallardy SG, Blevins DG, Randall DD. 1989.** Whole leaf carbon exchange
916 characteristics of phosphate deficient soybeans (*Glycine max* L.). *Plant Physiology* **91**:
917 848-854.

918 **Letts MG, Mulligan M. 2005.** The impact of light quality and leaf wetness on photosynthesis in
919 north-west Andean tropical montane cloud forest. *Journal of Tropical Ecology* **21**: 549-
920 557.

921 **Lloyd J, Bloomfield K, Domingues TF, Farquhar GD. 2013.** Photosynthetically relevant foliar
922 traits correlating better on a mass vs an area basis: of ecophysiological relevance or
923 just a case of mathematical imperatives and statistical quicksand? *New Phytologist*
924 **199**: 311-321.

925 **Loustau D, Brahim MB, Gaudillère J-P, Dreyer E. 1999.** Photosynthetic responses to
 926 phosphorus nutrition in two-year-old maritime pine seedlings. *Tree Physiology* **19**: 707-
 927 715.

928 **Malhi Y. 2010.** The carbon balance of tropical forest regions, 1990–2005. *Current Opinion in*
 929 *Environmental Sustainability* **2**: 237-244.

930 **Medlyn BE, Dreyer E, Ellsworth D, Forstreuter M, Harley PC, Kirschbaum MUF, Le Roux X,**
 931 **Montpied P, Strassmeyer J, Walcroft A, Wang K, Loustau D. 2002.** Temperature
 932 response of parameters of a biochemically based model of photosynthesis. II. A review
 933 of experimental data. *Plant, Cell & Environment* **25**: 1167-1179.

934 **Meir P, Kruijt B, Broadmeadow M, Barbosa E, Kull O, Carswell F, Nobre A, Jarvis PG. 2002.**
 935 Acclimation of photosynthetic capacity to irradiance in tree canopies in relation to leaf
 936 nitrogen concentration and leaf mass per unit area. *Plant, Cell & Environment* **25**: 343-
 937 357.

938 **Meir P, Levy P, Grace J, Jarvis P. 2007.** Photosynthetic parameters from two contrasting
 939 woody vegetation types in West Africa. *Plant Ecology* **192**: 277-287.

940 **Mercado LM, Patiño S, Domingues TF, Fyllas NM, Weedon GP, Sitch S, Quesada CA, Phillips**
 941 **OL, Aragao LE, Malhi Y, et al. 2011.** Variations in Amazon forest productivity
 942 correlated with foliar nutrients and modelled rates of photosynthetic carbon supply.
 943 *Philosophical Transactions of the Royal Society B: Biological Sciences* **366**: 3316-3329.

944 **Niinemets Ü, Tenhunen JD. 1997.** A model separating leaf structural and physiological effects
 945 on carbon gain along light gradients for the shade-tolerant species *Acer saccharum*.
 946 *Plant, Cell & Environment* **20**: 845-866.

947 **Pinheiro J, Bates D. 2000.** *Mixed-Effects Models in S and S-PLUS*: Springer New York.

948 **Pons TL, van der Werf A, Lambers H. 1994.** *Photosynthetic nitrogen use efficiency of inherently*
 949 *low- and fast-growing species: possible explanations for observed differences*. The
 950 Hague, Netherlands: SPB Academic Publishing.

951 **Poorter H, Evans JR. 1998.** Photosynthetic nitrogen-use efficiency of species that differ
 952 inherently in specific leaf area. *Oecologia* **116**: 26-37.

953 **Quesada CA, Lloyd J, Schwarz M, Patiño S, Baker TR, Czimczik C, Fyllas NM, Martinelli L,**
 954 **Nardoto GB, Schmerler J, et al. 2010.** Variations in chemical and physical properties of
 955 Amazon forest soils in relation to their genesis. *Biogeosciences* **7**: 1515-1541.

956 **Quesada CA, Phillips OL, Schwarz M, Czimczik CI, Baker TR, Patiño S, Fyllas NM, Hodnett MG,**
 957 **Herrera R, Almeida S, et al. 2012.** Basin-wide variations in Amazon forest structure
 958 and function are mediated by both soils and climate. *Biogeosciences* **9**: 2203-2246.

959 **Quilici A, Medina E. 1998.** Photosynthesis-nitrogen relationships in pioneer plants of disturbed
 960 tropical montane forest sites. *Photosynthetica* **35**: 525-534.

961 **Raaimakers D, Boot RGA, Dijkstra P, Pot S. 1995.** Photosynthetic rates in relation to leaf
 962 phosphorus content in pioneer versus climax tropical rainforest trees. *Oecologia* **102**:
 963 120-125.

964 **Rada F, García-Núñez C, Ataroff M. 2009.** Leaf gas exchange in canopy species of a Venezuelan
 965 cloud forest. *Biotropica* **41**: 659-664.

966 **Reich P, Oleksyn J, Wright I. 2009.** Leaf phosphorus influences the photosynthesis–nitrogen
 967 relation: a cross-biome analysis of 314 species. *Oecologia* **160**: 207-212.

968 **Reich PB, Walters MB. 1994.** Photosynthesis-nitrogen relations in Amazonian tree species.
 969 *Oecologia* **97**: 73-81.

970 **Sage RF, Kubien DS. 2007.** The temperature response of C₃ and C₄ photosynthesis. *Plant, Cell &*
 971 *Environment* **30**: 1086-1106.

972 **Santiago LS, Mulkey SS. 2003.** A test of gas exchange measurements on excised canopy
 973 branches of ten tropical tree species. *Photosynthetica* **41**: 343-347.

974 **Silman MR. 2014.** Functional megadiversity. *Proceedings of the National Academy of Sciences,*
 975 *USA* **111**: 5763-5764.

976 **Stitt M, Schulze D. 1994.** Does Rubisco control the rate of photosynthesis and plant growth?
 977 An exercise in molecular ecophysiology. *Plant, Cell & Environment* **17**: 465-487.

978 **Takashima T, Hikosaka K, Hirose T. 2004.** Photosynthesis or persistence: nitrogen allocation in
 979 leaves of evergreen and deciduous *Quercus* species. *Plant, Cell & Environment* **27**:
 980 1047-1054.

981 **Tanner E, Vitousek PM, Cuevas E. 1998.** Experimental investigation of nutrient limitation of
 982 forest growth on wet tropical mountains. *Ecology* **79**: 10-22.

983 **Terashima I, Masuzawa T, Ohba H, Yokoi Y. 1995.** Is photosynthesis suppressed at higher
 984 elevations due to low CO₂ pressure? *Ecology* **76**: 2663-2668.

985 **Townsend AR, Cleveland CC, Asner GP, Bustamante MMC. 2007.** Controls over foliar N:P
 986 ratios in tropical rain forests. *Ecology* **88**: 107-118.

987 **van de Weg M, Meir P, Grace J, Atkin OK. 2009.** Altitudinal variation in leaf mass per unit area,
 988 leaf tissue density and foliar nitrogen and phosphorus content along an Amazon-Andes
 989 gradient in Peru. *Plant Ecology & Diversity* **2**: 243-254.

990 **van de Weg M, Meir P, Grace J, Ramos G. 2012.** Photosynthetic parameters, dark respiration
 991 and leaf traits in the canopy of a Peruvian tropical montane cloud forest. *Oecologia*
 992 **168**: 23-34.

993 **van de Weg M, Meir P, Williams M, Girardin C, Malhi Y, Silva-Espejo J, Grace J. 2014.** Gross
 994 primary productivity of a high elevation tropical montane cloud forest. *Ecosystems* **17**:
 995 751-764.

996 **Vårhammar A, Wallin G, McLean CM, Dusenge ME, Medlyn BE, Hasper TB, Nsabimana D,**
 997 **Uddling J. 2015.** Photosynthetic temperature responses of tree species in Rwanda:
 998 evidence of pronounced negative effects of high temperature in montane rainforest
 999 climax species. *New Phytologist* **206**: 1000-1012.

1000 **Vitousek PM. 1984.** Litterfall, nutrient cycling, and nutrient limitation in tropical forests
 1001 *Ecology* **65**: 285-298.

1002 **von Caemmerer S, Evans JR, Hudson GS, Andrews TJ. 1994.** The kinetics of ribulose-1, 5-
 1003 bisphosphate carboxylase/oxygenase *in vivo* inferred from measurements of
 1004 photosynthesis in leaves of transgenic tobacco. *Planta* **195**: 88-97.

1005 **Walker AP, Beckerman AP, Gu LH, Kattge J, Cernusak LA, Domingues TF, Scales JC, Wohlfahrt**
 1006 **G, Wullschleger SD, Woodward FI. 2014.** The relationship of leaf photosynthetic traits
 1007 - V_{cmax} and J_{max} - to leaf nitrogen, leaf phosphorus, and specific leaf area: a meta-
 1008 analysis and modeling study. *Ecology and Evolution* **4**: 3218-3235.

1009 **Warren CR, Adams MA. 2001.** Distribution of N, Rubisco and photosynthesis in *Pinus pinaster*
 1010 and acclimation to light. *Plant, Cell & Environment* **24**: 597-609.

1011 **Warren CR, Adams MA. 2002.** Phosphorus affects growth and partitioning of nitrogen to
 1012 Rubisco in *Pinus pinaster*. *Tree Physiology* **22**: 11-19.

1013 **Warren CR, Adams MA, Chen Z. 2000.** Is photosynthesis related to concentrations of nitrogen
 1014 and Rubisco in leaves of Australian native plants? *Functional Plant Biology* **27**: 407-416.

1015 **Warton DI, Wright IJ, Falster DS, Westoby M. 2006.** Bivariate line-fitting methods for
 1016 allometry. *Biological Reviews* **81**: 259-291.

1017 **Westbeek MHM, Pons TL, Cambridge ML, Atkin OK. 1999.** Analysis of differences in
 1018 photosynthetic nitrogen use efficiency of alpine and lowland *Poa* species. *Oecologia*
 1019 **120**: 19-26.

1020 **Wittich B, Horna V, Homeier J, Leuschner C. 2012.** Altitudinal change in the photosynthetic
 1021 capacity of tropical trees: A case study from Ecuador and a pantropical literature
 1022 analysis. *Ecosystems* **15**: 958-973.

1023 **Wright IJ, Reich PB, Westoby M, Ackerly DD, Baruch Z, Bongers F, Cavender-Bares J, Chapin**
 1024 **T, Cornelissen JHC, Diemer M, et al. 2004.** The worldwide leaf economics spectrum.
 1025 *Nature* **428**: 821-827

1026 **Wullschleger SD. 1993.** Biochemical limitations to carbon assimilation in C₃ plants - a
 1027 retrospective analysis of the A/C_i curves from 109 species. *Journal of Experimental*
 1028 *Botany* **44**: 907-920.

1029 **Zuur A, Ieno EN, Walker N, Saveliev AA, Smith GM. 2009.** *Mixed effects models and extensions*
 1030 *in ecology with R*: Springer.

1032 **Supporting Information**

1033 Additional supporting information may be found in the online version of this article.

1034

1035 SM1: Additional study site details

1036 SM2: Identification of outliers and $A \leftrightarrow C_i$ curve methodological details

1037 SM3: Optimization of protocols for protein extraction from the leaves of recalcitrant tree
1038 species

1039

1040 Table S1. Summary of species sampled at each site and their parameters

1041 Table S2. Pearson correlations for bivariate relationships among leaf traits and
1042 environmental parameters

1043 Table S3. Standardized major axis regression slopes for relationships in Figs 2, 4, 5 & 6

1044 Table S4. Means \pm standard deviation of leaf physiology and chemistry, expressed on
1045 area basis for each site

1046 Table S5. Standardized major axis regression slopes for relationships in Figs 8 & S2

1047 Table S6: Stepwise selection process for the fixed component of the linear mixed effect
1048 model to determine the best predictive model given in Table 3

1049

1050 Figure S1. Plots of photosynthetic parameters against mean annual temperature and
1051 soil [P] for each site

1052 Figure S2. Plots of % n_P , % n_R , and % n_E , in relation to M_a , N_a , and P_a

1053 Figure S3. Plots of fraction of leaf N allocated in Rubisco, n_R in relation to leaf mass per
1054 unit leaf area, M_a

1055 Figure S4. Stacked graph show n_E , n_P and n_R (*in vivo* and *in vitro*) for individual leaves

1056 Figure S5. Plots for linear mixed-effects model goodness of fits, including fixed and
1057 random terms for $V_{\text{cmax},a}^{25}$ and $J_{\text{max},a}^{25}$

1058 Figure S6: Comparison of $V_{\text{cmax},a}^{25}$ in upland and lowland plants calculated using
1059 different activation energies

Table 1: Description of the sampled Peruvian field sites.

Category	Site Code	Latitude	Longitude	Elevation (m a.s.l.)	No. of species	MAT (°C)	MAP (m)	Atm. Pressure (kPa)	Soil classification	Total soil		Leaf chemistry			
										[N] (g kg ⁻¹)	[P] (mg kg ⁻¹)	Leaf N _a (g m ⁻²)	Leaf P _a (g m ⁻²)	Leaf N:P	M _a (g m ⁻²)
Lowland	SUC-05	-3.2558	-72.8942	132	20	26.2	2.75	100	Alisols	1.9	276	1.94 ± 0.61	0.06 ± 0.04	30.1 ± 7.03	129 ± 31
	TAM-05	-12.8309	-69.2705	223	8	24.4	1.90	99	Cambisols	1.6	256	2.14 ± 0.27	0.08 ± 0.02	28.6 ± 9.49	119 ± 27
	JEN-11	-4.8781	-73.6295	131	18	26.6	2.70	100	Acrisols	1.8	141	2.12 ± 0.52	0.06 ± 0.02	27.9 ± 10.4	144 ± 37
	ALP-01	-3.9500	-73.4333	120	18	25.2	2.69	100	Gleysols	0.6	110	1.90 ± 0.40	0.08 ± 0.03	26.2 ± 8.62	119 ± 24
	SUC-01	-3.2519	-72.9078	117	17	26.2	2.75	100	Plinthosols	1.7	305	1.81 ± 0.63	0.09 ± 0.03	22.1 ± 4.99	123 ± 27
	JEN-12	-4.8990	-73.6276	135	19	26.6	2.70	100	Podzols	6.9	133	1.97 ± 0.52	0.09 ± 0.05	21.9 ± 10.42	156 ± 31
	ALP-30	-3.9543	-73.4267	150	21	25.2	2.69	100	Arenosols	0.8	38	1.67 ± 0.47	0.09 ± 0.04	20.8 ± 6.85	145 ± 46
	CUZ-03	-12.5344	-69.0539	205	12	24.4	1.90	99	Cambisols	2.4	727	1.88 ± 0.47	0.10 ± 0.04	17.2 ± 5.97	109 ± 18
	ALP-40	-3.9410	-73.4400	142	12	26.3	2.76	100	Podzols	2.1	59	1.84 ± 0.36	0.10 ± 0.02	16.8 ± 5.00	171 ± 50
	TAM-09	-12.8309	-69.2843	219	13	24.4	1.90	99	Alisols	1.1	326	2.19 ± 0.45	0.14 ± 0.03	16.4 ± 3.77	105 ± 21
	TAM-06	-12.8385	-69.2960	215	13	24.4	1.90	99	Alisols	1.7	529	2.56 ± 0.34	0.17 ± 0.04	15.3 ± 2.84	126 ± 26
Upland	SPD-02	-13.0491	-71.5365	1527	19	18.8	5.30	83	Cambisols	8.8	1631	2.23 ± 0.45	0.16 ± 0.05	15.4 ± 4.05	126 ± 36
	SPD-01	-13.0475	-71.5423	1776	21	17.4	5.30	85	Cambisols	11.9	1071	2.25 ± 0.35	0.16 ± 0.04	14.3 ± 3.34	124 ± 29
	TRU-08	-13.0702	-71.5559	1885	20	18.0	2.47	82	Cambisols	8.1	496	1.99 ± 0.36	0.12 ± 0.05	16.9 ± 3.54	165 ± 38
	ESP-01	-13.1751	-71.5948	2863	17	13.1	1.56	72	Umbrisols	14.8	981	2.39 ± 0.50	0.19 ± 0.05	12.7 ± 1.78	140 ± 32
	TRU-03	-13.1097	-71.5995	3044	13	11.8	1.78	71	Umbrisols	15.5	787	2.24 ± 0.44	0.21 ± 0.04	10.5 ± 2.35	164 ± 40
	WAQ-01	-13.1908	-71.5874	3045	13	11.8	1.56	72	Umbrisols	8.8	1414	2.68 ± 0.42	0.24 ± 0.05	11.5 ± 2.16	149 ± 46
	TRU-01	-13.1136	-71.6069	3379	16	8.0	1.98	67	Umbrisols	15.0	856	2.53 ± 0.31	0.21 ± 0.04	11.2 ± 3.10	151 ± 49

Lowland sites are listed in order of decreasing leaf N:P ratios, while upland sites are listed in order of increasing elevation. Extremely low soil P did not necessarily produce low leaf P as in the case of ALP-03 and ALP-04, therefore lowland sites were ranked according to leaf N to P ratio which provides better indication of nutrient limitation (Aerts & Chapin, 2000). Atmospheric pressure was obtained from a Licor 6400 gas exchange system. For each site name, a site code is shown as designated by the JACARE (the Joint Amazon Carnegie RAINFOR Expedition); values of total soil nitrogen and phosphorus are shown (expressed per unit soil dry mass). Also shown are average leaf area-based concentrations of total nitrogen (N_a) and phosphorus (P_a), as well as the ratio of leaf N:P and leaf mass per unit area, M_a, all shown with SD. Soil classification follows World Reference Base (WRB). Abbreviations: MAP = mean annual precipitation, MAT = mean annual temperature. Source Asner *et al.* (2014a), Quesada (*et al.* 2010; pers. comm. 2014) and Malhi *et al.* (in preparation)

Table 2: Mean values and standard deviation of leaf traits for upland and lowland species.

Leaf Traits	Leaf N _a (g m ⁻²)	Leaf P _a (g m ⁻²)	Leaf N:P	M _a (g m ⁻²)	A _{400,a} (μmol m ⁻² s ⁻¹)	A _{400,N} (μmol gN ⁻¹ s ⁻¹)	V _{cmax,a} ²⁵ (μmol m ⁻² s ⁻¹)	J _{max,a} ²⁵ (μmol m ⁻² s ⁻¹)	J _{max,a} ²⁵ :V _{cmax,a} ²⁵	V _{cmax,N} ²⁵ (μmol gN ⁻¹ s ⁻¹)	n _A	n _P	n _R	n _E
Lowland species	1.96 ± 0.52 ^a	0.09 ± 0.05 ^a	22.2 ± 8.6 ^a	132 ± 35 ^a	8.2 ± 3.9 ^a	4.3 ± 2.2 ^a	35.9 ± 14.6 ^a	66.7 ± 18.6 ^a	1.86 ± 0.40 ^a	18.9 ± 8.1 ^a	37 ± 1 ^a	24 ± 1 ^a	9.0 ± 4.0 ^a	2.8 ± 1.0 ^a
Upland species	2.31 ± 0.44 ^b	0.18 ± 0.06 ^b	13.5 ± 3.6 ^b	143 ± 39 ^b	7.6 ± 3.6 ^a	3.4 ± 1.7 ^b	48.8 ± 20.0 ^b	96.9 ± 36.9 ^b	1.92 ± 0.36 ^a	22.5 ± 9.4 ^b	38 ± 1 ^a	22 ± 1 ^a	10.5 ± 4.3 ^b	3.4 ± 1.4 ^b

Values expressed on area basis. Abbreviation: leaf N_a = leaf nitrogen, leaf P_a = leaf phosphorus, leaf N:P = leaf nitrogen to phosphorus ratio, M_a = leaf mass per unit leaf area, A_{400,a} = area-based light-saturated net photosynthesis measured at 400 μmol mol⁻¹ atmospheric [CO₂], A_{400,N} = area-based light-saturated net photosynthesis measured at 400 μmol mol⁻¹ atmospheric [CO₂] per unit leaf nitrogen, V_{cmax,a}²⁵ = maximum carboxylation velocity of Rubisco normalised to 25°C, J_{max,a}²⁵ = maximum rate of electron transport normalised to 25°C, J_{max,a}²⁵:V_{cmax,a}²⁵ = ratio of maximum Rubisco carboxylation velocity over maximum rate of electron transport, both normalised to 25°C, V_{cmax,N}²⁵ = ratio of maximum carboxylation velocity of Rubisco normalised to 25°C per unit leaf nitrogen, n_A = total fraction of leaf N allocated in photosynthetic metabolism, n_P = fraction of leaf N in pigment-protein complexes, n_R = fraction of leaf N in Rubisco, and n_E = fraction of leaf N in electron transport.

Values are overall mean ± SD of leaf traits for lowland and upland sites. Significantly different means are indicated by different letters (*p* < 0.05).

Table 3: Output from linear mixed-effects models, with $V_{\text{cmax},a}^{25}$ and $J_{\text{max},a}^{25}$ as the response variables, each showing fixed and random effects.

Final model ($V_{\text{cmax},a}^{25}$)				Final model ($J_{\text{max},a}^{25}$)			
Fixed effect	Estimate	S.E	t value	Fixed effect	Estimate	S.E	t value
Intercept	41.470	1.578	26.288	Intercept	77.217	2.712	28.477
log10 (Soil P)	7.909	2.466	3.207	log10 (Soil P)	16.866	4.327	3.898
P_a	68.148	22.558	3.021	P_a	94.483	40.245	2.348
Random effect		Variance	% of total	Random effect		Variance	% of total
Intercept variance: family		45.568	2.49%	Intercept variance: family		121.3	2.79%
Residual error (within family)		1783.626	97.51%	Residual error (within family)		4232.9	97.21%
			100.00%				100.00%
AIC	1645.6			AIC	1342.4		
BIC	1662.0			BIC	1357.3		
-2LL	-817.8			-2LL	-666.2		

$V_{\text{cmax},a}^{25} = 41.47 + (7.91 * \log_{10}[\text{SoilP}]) + (68.15 * P_a)$			
$J_{\text{max},a}^{25} = 77.22 + (16.87 * \log_{10}[\text{SoilP}]) + (94.48 * P_a)$			

Predictive equations for $V_{\text{cmax},a}^{25}$ and $J_{\text{max},a}^{25}$ based on final preferred models are shown at the bottom. For the $V_{\text{cmax},a}^{25}$ and $J_{\text{max},a}^{25}$ model, the fixed component explanatory variables were soil P and leaf P. Parameter estimate, standard error (S.E.) and t-values are given for the explanatory variables. The best predictive models were selected based on a stepwise selection process outlined in Table S6. Prior to inclusion in the models, continuous explanatory variables were centred on the population mean.

Figure Legends

Figure 1: Fitted curves of the response of CO₂ assimilation rate, A (area-based) to intercellular CO₂ (C_i) at saturating light for (A) a lowland species *Glycydendron amazonicum* (TAM-09) and an upland species *Cecropia angustifolia* (SPD-01) and (B) two upland species *Citronella incarum* (TRU-03) and *Schefflera* sp. (WAQ-01). Closed circles are the measured rates of assimilation, A . Solid lines correspond to fitted response and dashed lines correspond to estimated response at high C_i . V_{cmax} (maximum Rubisco carboxylation capacity) was calculated from the curvature of dashed line and J_{max} (maximum electron transport rate) were calculated from the points where A saturated. Individual leaf was measured at varying temperature close to growth temperature, therefore V_{cmax} and J_{max} were then normalised to 25°C. CO₂ was not always saturating for most upland measurement due to low partial pressure and/or phosphate limitation.

Figure 2: Log-log plots of (A) leaf N-area, N_a and (B) leaf P-area, P_a in relation to leaf mass per unit leaf area, M_a . Data points represent individual leaf values (149 lowland species and 97 upland species). Standardized major axis (SMA) tests for common slopes revealed significant differences when comparing $N_a \leftrightarrow M_a$ and $P_a \leftrightarrow M_a$ relationship between lowland and upland species. Symbols: closed symbols, lowland species; open symbols, upland species. SMA regressions: solid line, lowland species; dashed line, upland species. SMA regressions are given only when the relationships are significant ($p < 0.05$), refer to Table S3.

Figure 3: Box and whisker plots of (A) maximum carboxylation velocity of Rubisco normalised to 25°C, $V_{\text{cmax},a}^{25}$, (B) maximum rate of electron transport normalised to 25°C, $J_{\text{max},a}^{25}$, (C) $J_{\text{max},25}:V_{\text{cmax},25}$ ratio, and (D) ratio of $V_{\text{cmax},a}^{25}$ over leaf N, $V_{\text{cmax},a}^{25}:N$ for each site. Values expressed on area basis. Sites are arranged according to decreasing leaf N:P for lowland and increasing elevation for upland sites. The upper and the lower edges of each box indicate the 75th and 25th percentiles, respectively. The horizontal line within each box is the median and the vertical bars indicate the 10th to the 90th percentile ranges.

Figure 4: Plot of maximum carboxylation velocity of Rubisco normalised to 25°C ($V_{\text{cmax},a}^{25}$) against maximum rate of electron transport normalised to 25°C ($J_{\text{max},a}^{25}$). Data points represent individual leaf values (138 lowland species and 69 upland species). Arrows correspond to the four species depicted in the $A \leftrightarrow C_i$ curves. Symbols: closed symbols, lowland species; open symbols, upland species.

Figure 5: Top panel shows log-log plots of maximum carboxylation velocity of Rubisco normalised to 25°C ($V_{\text{cmax},a}^{25}$) in relation to (A) leaf mass per unit leaf area, M_a , (B) leaf N-area, N_a , (C) leaf P-area, P_a and (D) leaf N:P. Data points represent individual leaf values (150 lowland species and 95 upland species). SMA tests for common slopes revealed significant difference when comparing $V_{\text{cmax},a}^{25} \leftrightarrow N_a$,

$V_{\text{cmax},a}^{25} \leftrightarrow P_a$ and $V_{\text{cmax},a}^{25} \leftrightarrow \text{leaf N:P}$ relationships between lowland and upland species, but no significant difference when comparing slopes of $V_{\text{cmax},a}^{25} \leftrightarrow M_a$ relationships between lowland and upland species. Bottom panel shows log-log plots of maximum rate of electron transport normalised to 25°C ($J_{\text{max},a}^{25}$) in relation to (E) leaf mass per unit leaf area, M_a , (F) leaf N-area, N_a , (G) leaf P-area, P_a and (H) leaf N:P. Data points represent individual leaf values (127 lowland species and 58 upland species). SMA tests for common slopes revealed significant difference when comparing $J_{\text{max},a}^{25}$ and leaf traits relationships between lowland and upland species. Symbols: closed symbols, lowland species; open symbols, upland species. SMA regressions are given only when the relationships are significant ($p < 0.05$), refer to Table S3.

Figure 6: Log-log plots of ratio of $V_{\text{cmax},a}^{25}$ to leaf N ($V_{\text{cmax},a}^{25}/N$) in relation to (A) leaf mass per unit leaf area, M_a , (B) leaf P-area, P_a and (C) leaf N:P. Data points represent individual leaf values (150 lowland species and 95 upland species). SMA tests for common slopes revealed significant difference only when comparing $V_{\text{cmax},a}^{25}/N \leftrightarrow P_a$ between lowland and upland species. Symbols: closed symbols, lowland species; open symbols, upland species. SMA regressions are given only when the relationships are significant ($p < 0.05$), refer to Table S3.

Figure 7: Stacked graph show fraction of leaf N in pigment-protein complexes, n_P ; fraction of leaf N in electron transport, n_E ; fraction of leaf N in Rubisco; n_R , for each sites. n_R was estimated from maximum carboxylation velocity of Rubisco (normalised to 25°C), $V_{\text{cmax},a}^{25}$, n_E estimated from maximum electron transport rate (normalised to 25°C), $J_{\text{max},a}^{25}$, and n_P estimated from chlorophyll concentration. n_P were unavailable for five sites due to thawing of leaf samples. Sites are arranged according to decreasing leaf N:P for lowland and increasing elevation for upland sites. Error bar represent standard error of mean.

Figure 8: Log-log plots of the total fraction of leaf N allocated in photosynthetic metabolism, n_A in relation to (A) leaf mass per unit leaf area, M_a , (B) leaf N-area, N_a , and (C) leaf P-area, P_a . Data points represent individual leaf values (126 lowland species and 40 upland species). SMA tests for common slopes revealed no significant difference when comparing relationships between lowland and upland species, but with the elevation (i.e. y-axis intercept) of the bivariate relationship being higher in upland species than in lowland species. Symbols: closed symbols, lowland species; open symbols, upland species. SMA regressions: solid line, lowland species; dashed line, upland species. SMA regressions are given only when the relationships are significant ($p < 0.05$), refer to Table S5.

Figure 9 (A): SDS-PAGE profile of native Rubisco extracted from frozen fresh leaf discs. Individual bands show large subunits of Rubisco. The last five bands on the right side (A-E) correspond to 0.47, 0.54, 0.57, 0.78 and 1.21 g m⁻² of Rubisco of lowland species (*Licania unguiculata* from *Chrysobalanaceae* family), which then translate to n_R

of 0.03, 0.04, 0.04, 0.06, 0.09. In this case, the final value of *in vitro* n_R for *L. unguiculata* was 0.04, as calculated from A - C, since these values fall within the tobacco standard curve. Standard curve was made of a dilution series of tobacco Rubisco. Figure 8 (B): *in vitro* n_R estimated from Rubisco western blot assay plotted against *in vivo* n_R derived from maximum carboxylation velocity of Rubisco (normalised to 25°C), $V_{\text{cmax}_a}^{25}$. n=16

Figure 1:

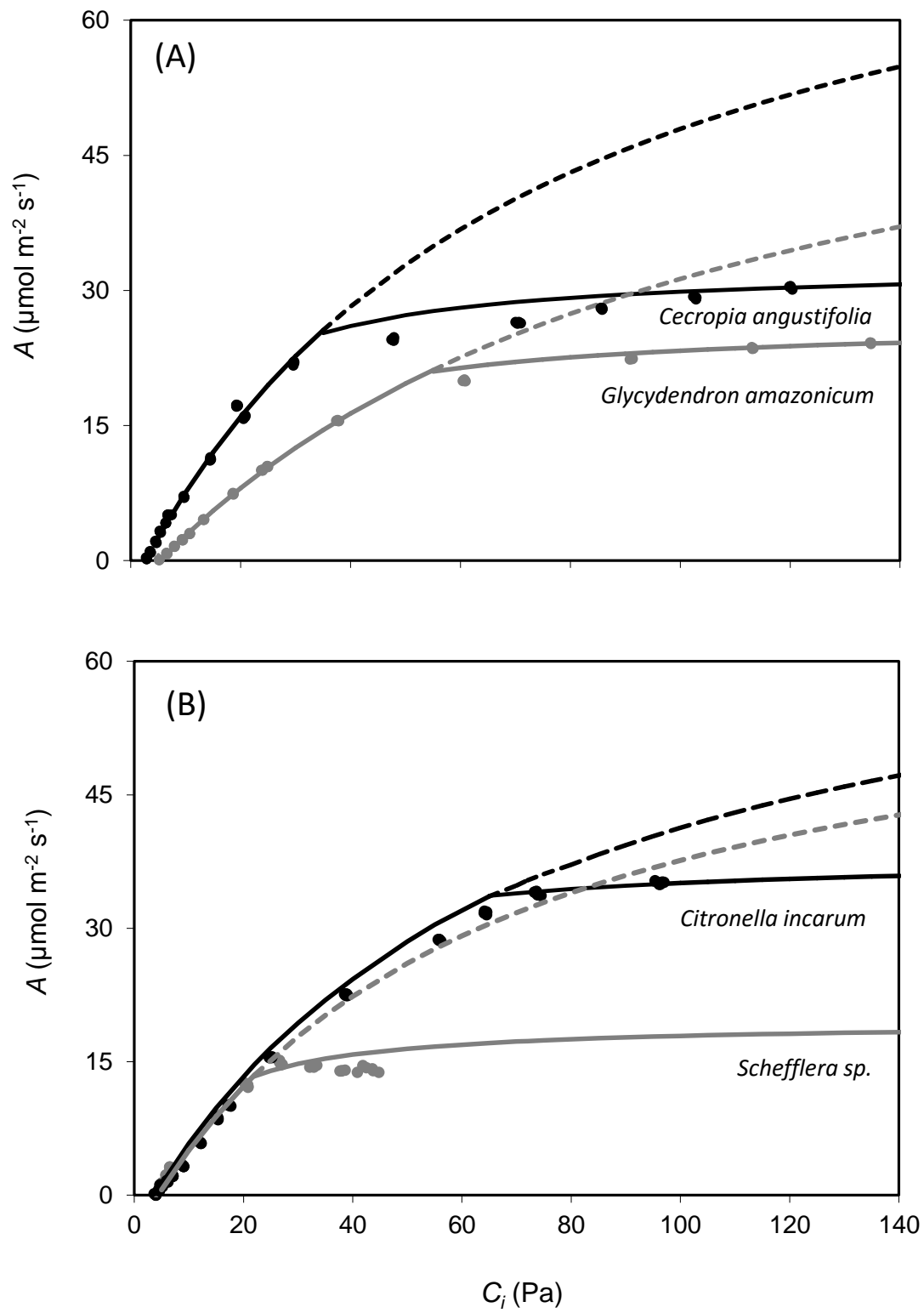


Figure 2:

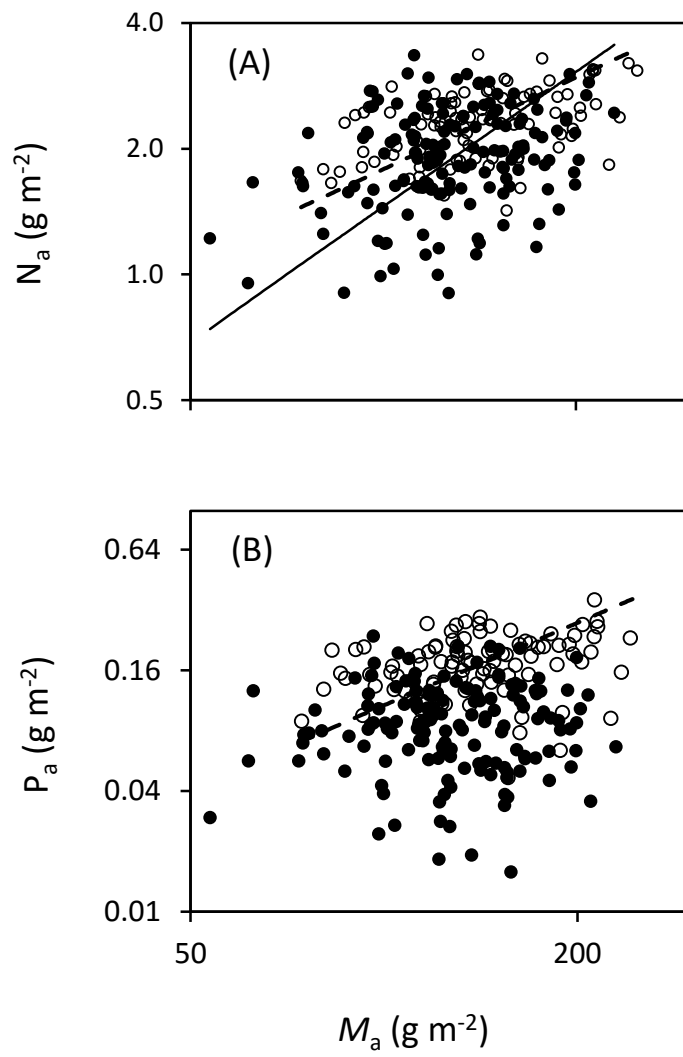


Figure 3:

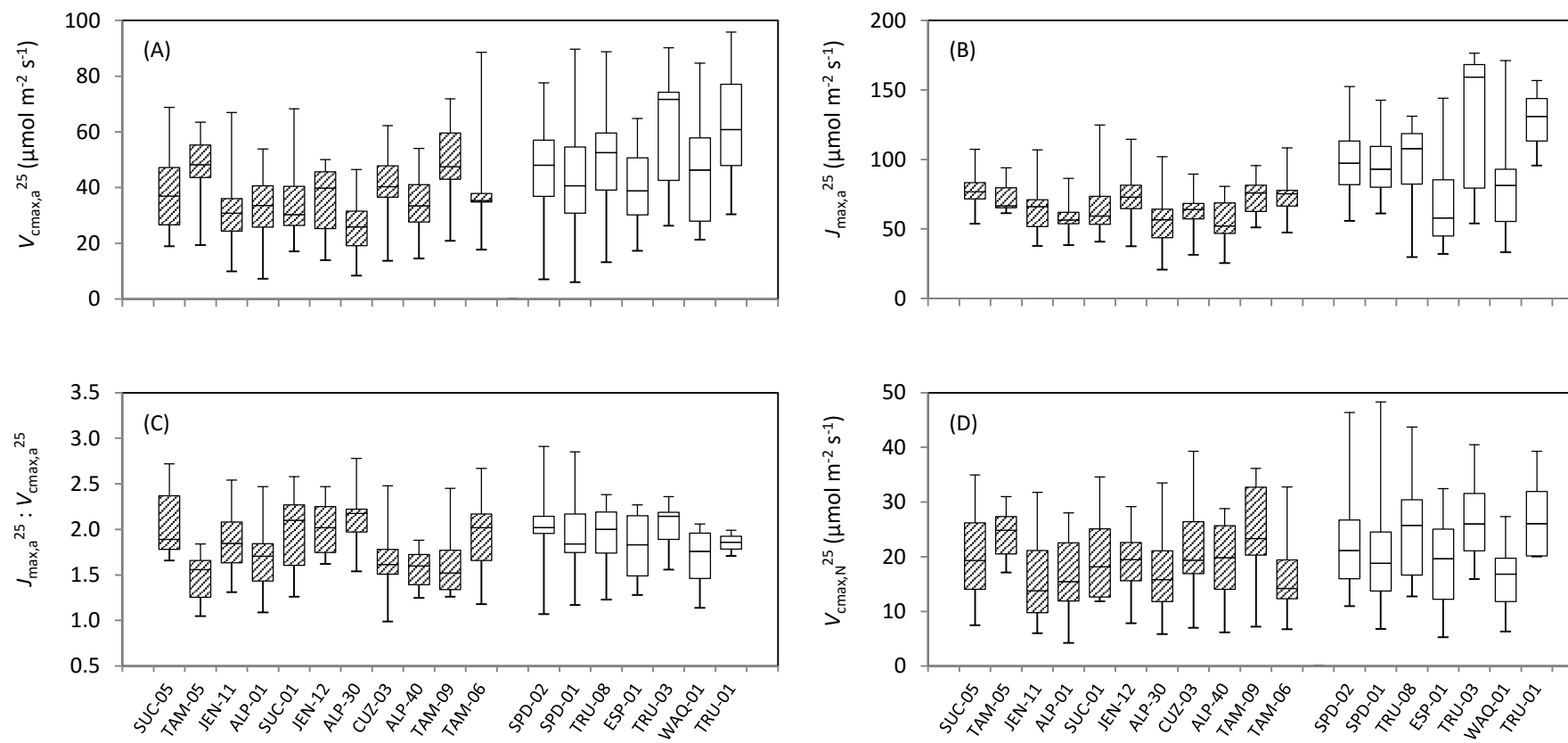


Figure 4:

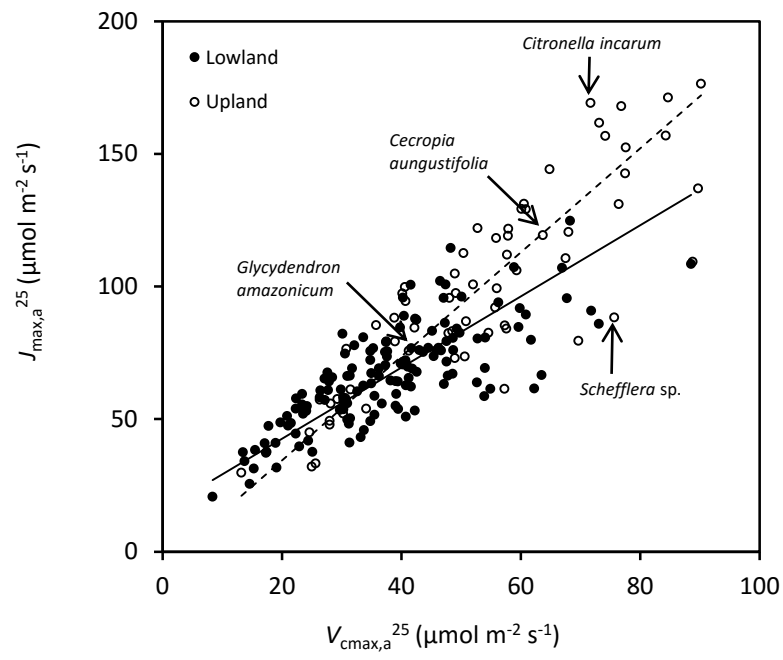


Figure 5:

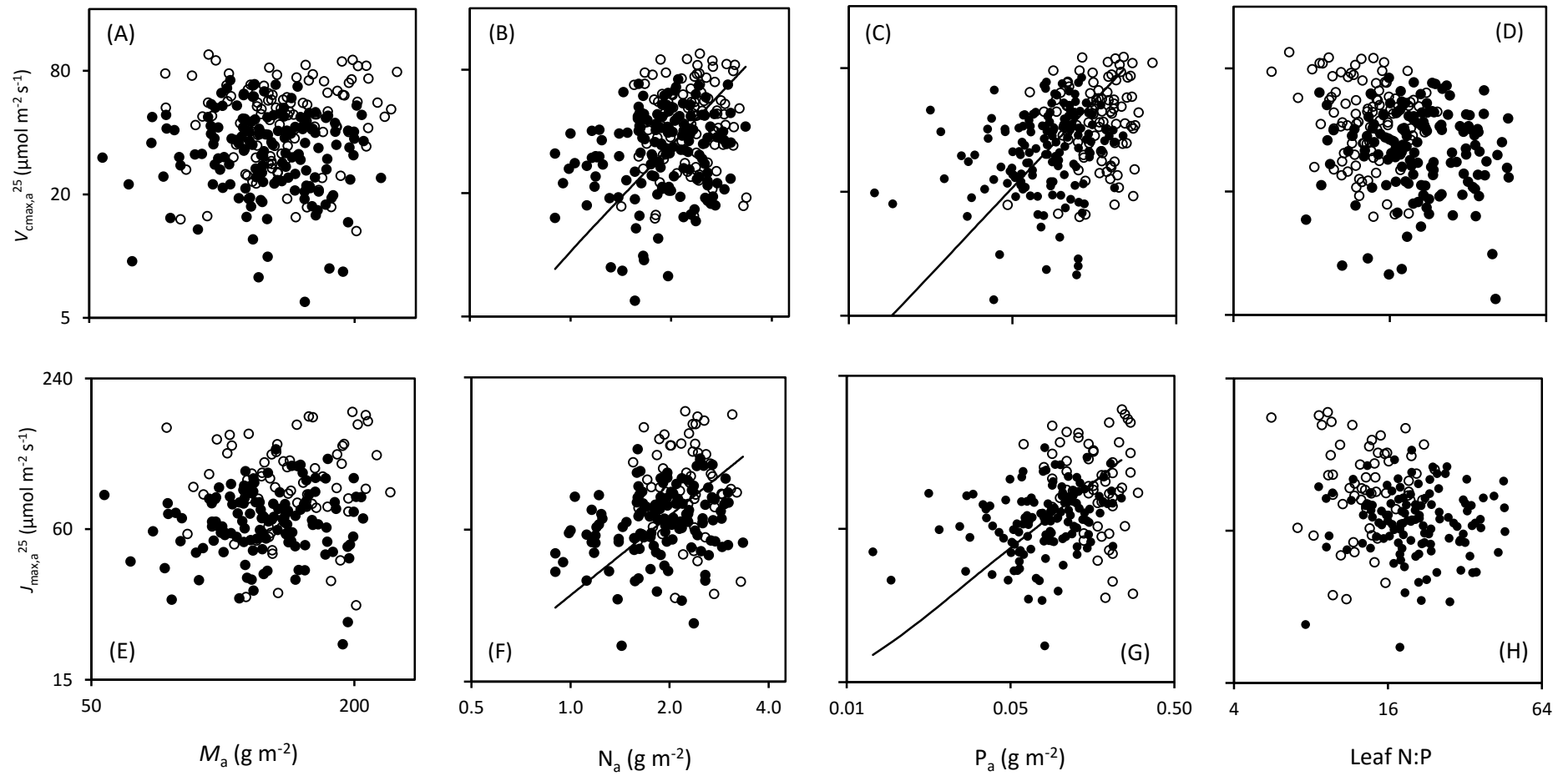


Figure 6:

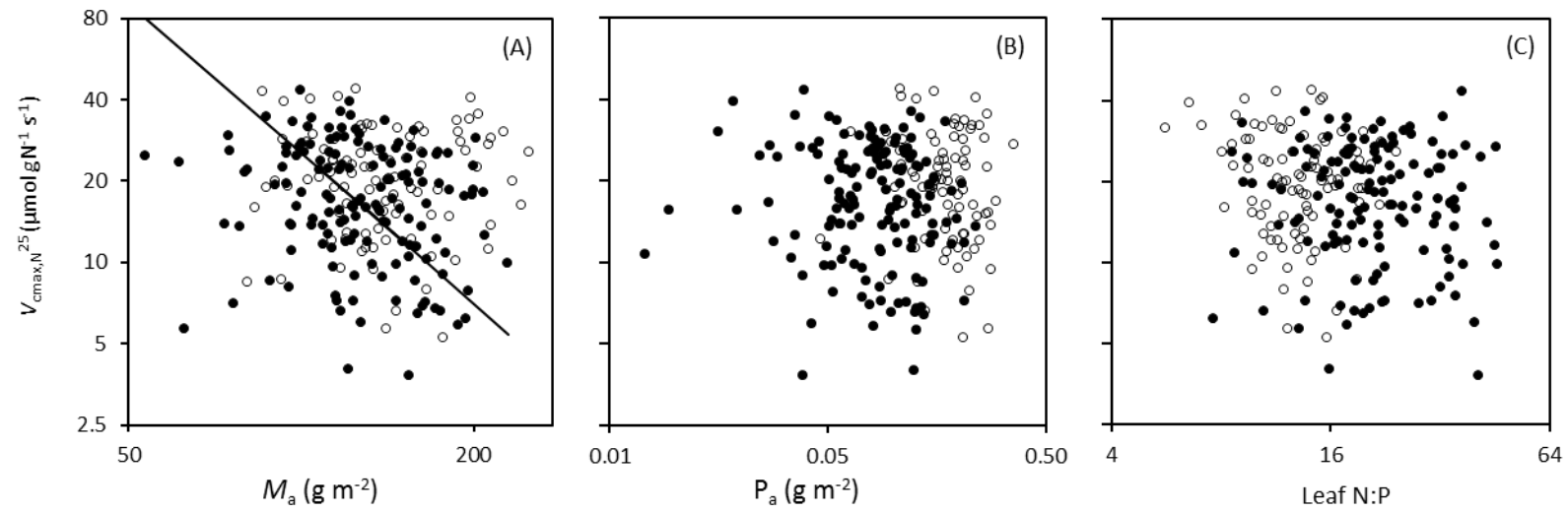


Figure 7:

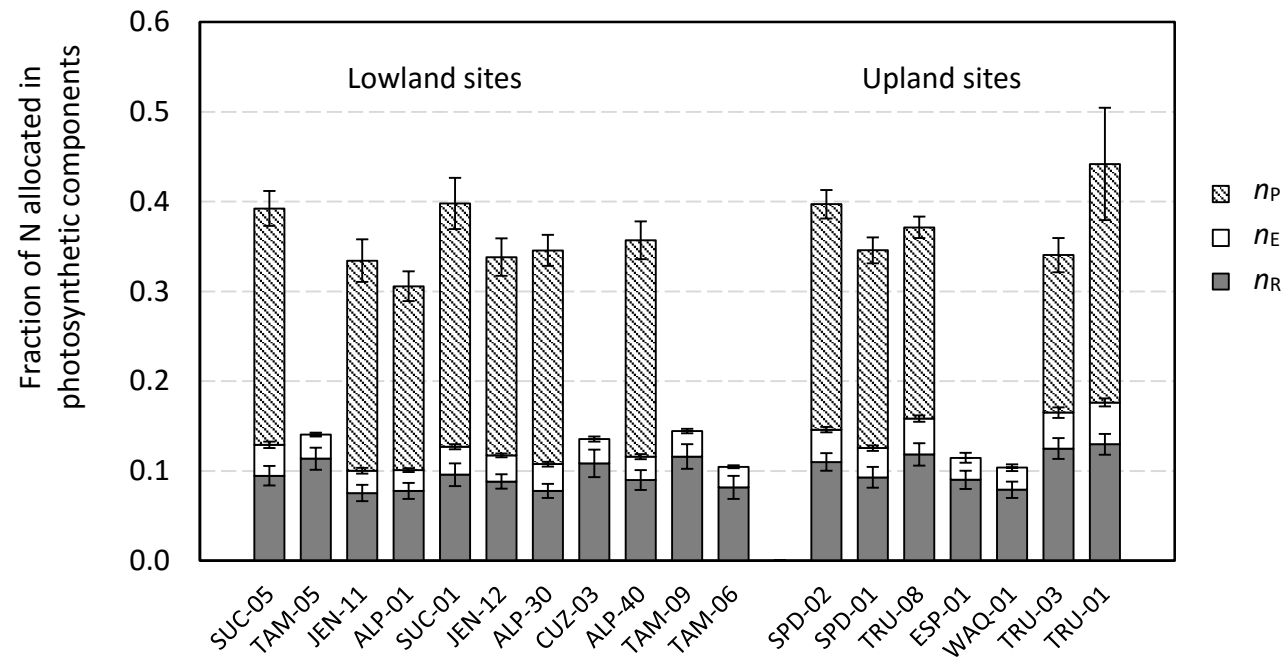


Figure 8:

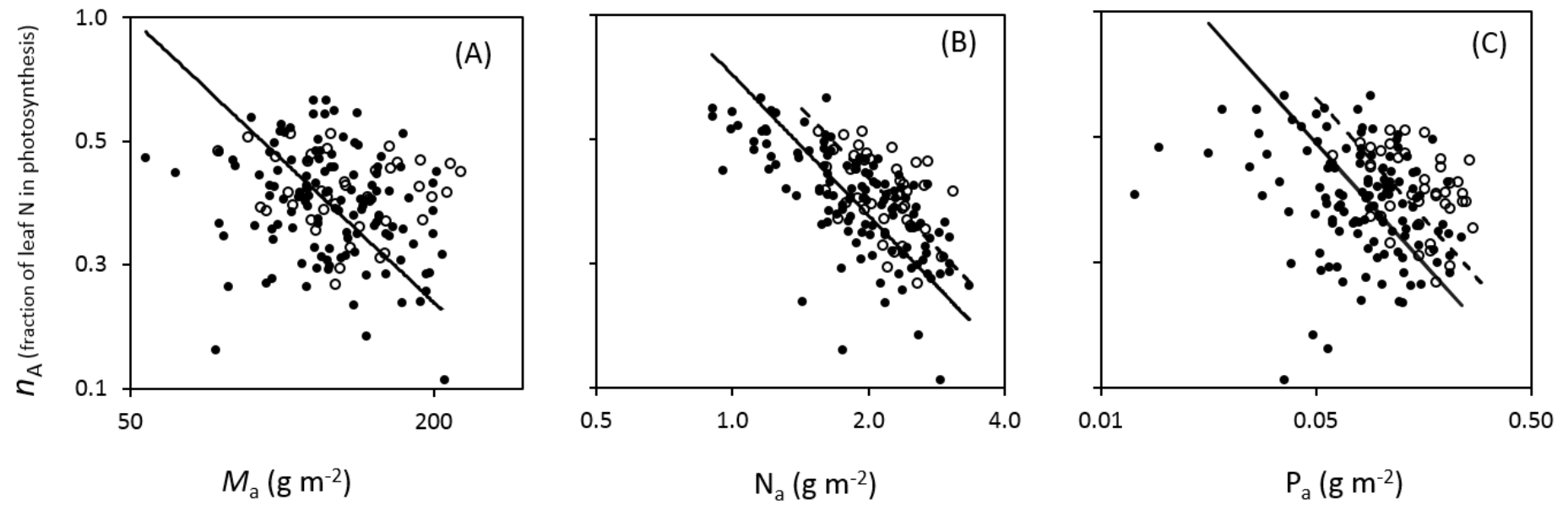
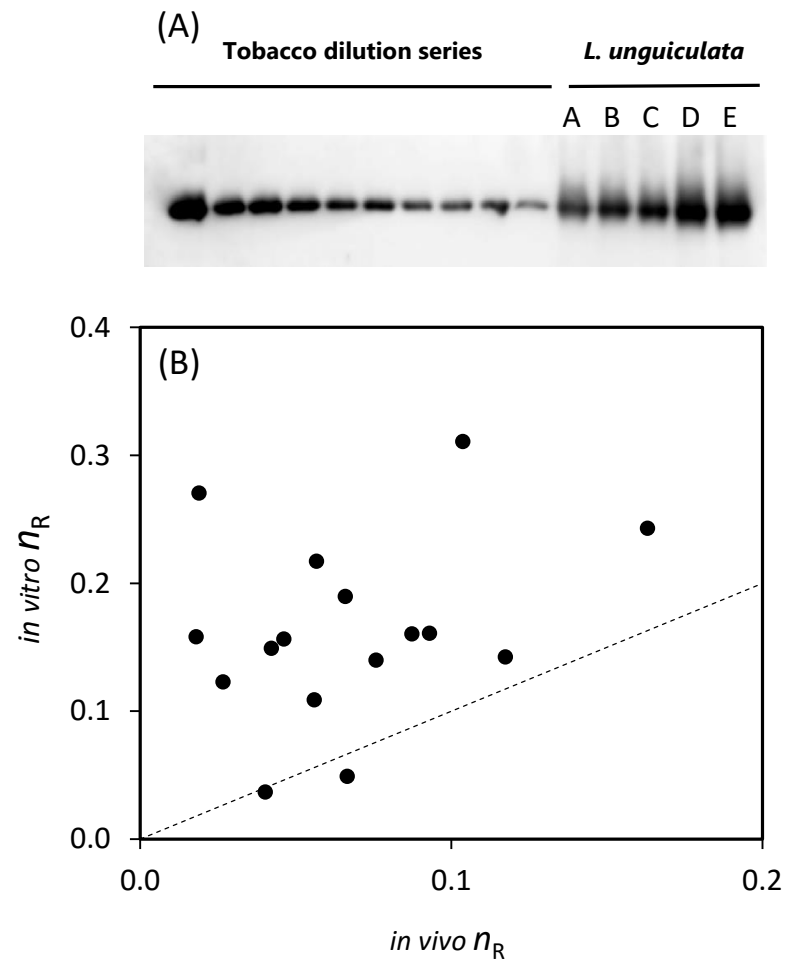


Figure 9:



Supporting Information

Authors: Bahar, Ishida, Weerasinghe *et al.*

Title: Leaf-level photosynthetic capacity in lowland Amazonian and high-elevation, Andean tropical moist forests of Peru

SM1: Additional study site details

Four of the lowland sites (TAM-09, TAM-06, TAM-05 and CUZ-03) were located in the Tambopata watersheds of SE Peru, while seven additional lowland sites (ALP-01, ALP-30, ALP-40, JEN-11, JEN-12, SUC-01, and SUC-05) were located in the Ucayali watershed in NE Peru. Seven upland sites (SPD-01, SPD-02, ESP-01, WAQ-01, TRU-01, TRU-03, and TRU-08) were distributed along SE slopes of the Andes in the Kosñipata valley. The 18 plots used in this study are part of the ABERG Kosñipata study transect (www.andesconservation.org/), Amazon Forest Inventory Network (RAINFOR; <http://www.rainfor.org/>) and the Carnegie Spectranomics Project (<http://spectranomics.ciw.edu/>). The lowland sites lie on a mosaic of young to old soil substrates, whereas upland forests exist primarily on young geologic substrates (van de Weg *et al.*, 2009; Quesada *et al.*, 2010; Fisher *et al.*, 2013). Data on soil type, as well as total N and P concentrations in soils, were obtained from Dr Carlos Alberto Quesada (Instituto Nacional de Pesquisas da Amazônia), using a combination of unpublished and published (Quesada *et al.*, 2010) data. For each tree, voucher specimens were collected and matched to herbarium collections at the National Agrarian University La Molina Herbarium in Peru and the Missouri Botanical Garden for full taxonomic verification by Carnegie Institution taxonomists.

SM2: Identification of outliers and $A \leftrightarrow C_i$ curve methodological details

CO₂ response curves of light-saturated photosynthesis (i.e. $A \leftrightarrow C_i$ curves) were quantified within 30–60 minutes after branch detachment, with CO₂ concentrations inside the reference chamber ranging from 3.5 to 2000 $\mu\text{mol mol}^{-1}$; initial measurements were made at 400 $\mu\text{mol mol}^{-1}$, followed by decreases in CO₂ to 300, 200, 150, 125, 100, 75, 50 and 35 $\mu\text{mol mol}^{-1}$; thereafter, CO₂ concentrations were increased back to 400 $\mu\text{mol mol}^{-1}$, and then to 600, 900, 1250, 1500, 1750 and finally 2000 $\mu\text{mol mol}^{-1}$. Block temperatures within the chamber were set to that of the prevailing day-time air temperature at each site (ranging from 25–28 °C depending on the site). A photosynthetic active radiation (PAR) flux density of 1800 $\mu\text{mol m}^{-2} \text{s}^{-1}$, generated from an artificial light source (6400-02B Red/Blue LED Light Source, Li-Cor, Inc.), was used for all measurements. The resultant $A \leftrightarrow C_i$ curves (examples shown in Figure 1 – main text) were fitted following the model described by the Farquhar, von Caemmerer and Berry (1980) in order to calculate V_{cmax} and maximum rate of electron transport (J_{max}) on a leaf area basis. V_{cmax} and J_{max} values at the prevailing leaf temperature were determined via minimizing the sum of squares of modelled vs observed estimates of net CO₂ exchange at given C_i values. This was done for both the CO₂-limited and CO₂-saturated regions of $A \leftrightarrow C_i$ curves (using C_i values expressed on a partial pressure basis, corrected for altitudinal changes in air pressure), with these regions being defined individually for each replicate. V_{cmax} at the prevailing leaf temperature was calculated under the assumption that at C_i values below 15–20 Pa (depending on site altitude) photosynthesis was limited by Rubisco only. Rates of A at these low CO₂ values were fitted to the Rubisco-limited equation of photosynthesis:

$$A = \left[\frac{V_{\text{cmax}}(C_i - \Gamma^*)}{(C_i + K_c(1 + O/K_o))} \right] - R_{\text{light}} \quad (\text{Eqn 1})$$

where R_{light} is respiration in the light, Γ^* is the CO₂ compensation point in the absence of photorespiration (3.69 Pa at 25°C; von Caemmerer *et al.* (1994)), K_c and K_o are the effective Michaelis-Menten constants for CO₂ and O₂ at 25°C [40.4 Pa and 24.8 kPa,

respectively, von Caemmerer *et al.* (1994)] and O is partial pressure of O_2 , corrected for atmospheric pressure at each altitude, according to:

$$O_2 \text{ partial pressure at site} = O_2 \text{ partial pressure at sea level} \times \frac{\text{air pressure at site}}{\text{air pressure at sea level}}$$

The resultant O_2 partial pressures at each site were then used to modify estimates of Γ^* and K' . C_i values were corrected for air pressure in the same manner. We assumed that K_c and K_o at the measurement temperature could be calculated assuming activation energies (E_a) of K_c and K_o of 59.4 and 36 kJ mol⁻¹, respectively (Farquhar *et al.*, 1980). These enzymatic kinetic constants were taken from von Caemmerer *et al.* (1994), assuming an infinite internal conductance. Γ^* at each leaf temperature was assumed to follow the temperature dependency reported by Brooks and Farquhar (1985). Rates of J_{\max} were calculated using the electron-transport-limited equation of CO_2 assimilation:

$$A = \left[\frac{J_{\max}(C_i - \Gamma^*)}{(4C_i + 8\Gamma^*)} \right] - R_{\text{light}} \quad (\text{Eqn 2})$$

assuming that A is limited by RuBP regeneration at higher concentrations of atmospheric CO_2 (Fig. 1). As atmospheric CO_2 was not always saturating for measurements of upland species (due to low atmospheric partial pressure), J_{\max} may have been underestimated in some cases and we excluded these J_{\max} values from the Andean data set. Rates of CO_2 exchange were corrected for diffusion through the gasket of the LI-6400 leaf chamber (Bruhn *et al.*, 2002) prior to calculation of V_{\max} and J_{\max} . Fitted parameters were scaled to a reference temperature of 25°C using activation energies of 64.8 and 37.0 kJ mol⁻¹ for V_{\max} and J_{\max} , respectively (Farquhar *et al.*, 1980).

Alterations in stomatal conductance (g_s) resulting from branch cutting were assumed to not affect the maximum carboxylation velocity of Rubisco (V_{\max}) (Miyazawa *et al.*, 2011), except where g_s declined to very low levels (Santiago & Mulkey, 2003); in instances where g_s values fell below 0.04 mol m⁻² s⁻¹, data were discarded from the analyses. We also applied a further check on data quality as used elsewhere (Kattge *et al.*, 2009; Domingues *et al.*, 2010; van de Weg *et al.*, 2012) where rates of A_N less than 2 μmol CO_2 g N⁻¹ s⁻¹ were excluded from analysis (52 out of a total of 353 measurements).

SM3: Optimization of protocols for protein extraction from the leaves of recalcitrant tree species

Trouble-shooting using temperate and tropical evergreen species

The analysis of protein recalcitrant to extraction from some tree species is complicated by the abundance of lipids, tannins, phenols, waxes, oils and other secondary compounds (Ekramoddoullah, 1993; Gaspar *et al.*, 1997). The leaves of many of the species analysed in this study are characteristically aromatic and tough in nature and initial attempts to extract protein resulted in smeared bands on SDS-PAGE gels and highly oxidized extracts in most cases. Invariably, the extraction of proteins in their native confirmation (for example for the analysis of Rubisco active site concentration) was impossible. Moreover, previous attempts to isolate protein and Rubisco from hard-leaved species had been unsuccessful (Harrison *et al.*, 2009, Bloomfield, Long, Evans, unpublished). Using a combination of protein extraction from recalcitrant species (Gaspar *et al.*, 1997) and detergent based-extraction buffer (Brown *et al.*, 2008), we successfully extracted protein from Peruvian tropical leaves and Australian tropical and temperate leaves (Long, Atkin, Xiang, Bahar, unpublished).

The process of extracting protein from the leaves was modified from that described by Gaspar *et al.* (1997) in order to allow the extraction and measurement of chlorophyll prior to protein analysis. Leaves were initially pulverised using a Tissue-Lyser (Qiagen) and were treated with one of the following extraction solvents:

- 1) Acetic acid, methanol and water (1:10:9) (as per Gaspar *et al.* (1997))
- 2) 80% (v/v) acetone
- 3) 100% (v/v) methanol

After initial extraction in these solvents, precipitated protein was further washed in hexane and acetone as described by Gaspar *et al.* (1997) to remove lipids and remaining pigments, leaving a protein pellet. Proteins were dissolved in protein extraction buffer [PEB, (Brown *et al.*, 2008)] containing 140 mM Tris base, 105 mM Tris-HCl, 0.5 mM

ethylenediaminetetraacetic acid (EDTA), 2% lithium dodecyl sulfate (LDS), 10% glycerol, 0.1 mg/mL Pefabloc SC (AEBSF) protease inhibitor (Roche) and 5 mM dithiothreitol (DTT) for analysis by SDS-PAGE and Western blotting for Rubisco proteins.

Analysis by SDS-PAGE and Western blotting was performed according to protocols described in *Materials and Methods: Chlorophyll and Rubisco measurements* in the main text. Based on this analysis, extraction with 100% methanol consistently provided the cleanest protein extracts as assessed by SDS-PAGE (lanes 11-15; Fig. SM3.1). The smearing of protein on SDS-PAGE gels may reflect either interference by unwanted compounds in the extract (e.g. lipids) or the degradation of Rubisco. Thus, the clean-up and extraction of protein in a way which prevents this interference/degradation is vital for accurate Rubisco estimation. When applied to protein extraction from the leaves of different tree species, each solvent provided similar estimations of leaf Rubisco content (Fig. SM3.2).

We estimated Rubisco content using an antibody raised against tobacco Rubisco. An alternative approach using Coomassie staining is a common practice, where the relatively high concentration of Rubisco large and small subunits in the total protein extract makes estimation of their concentration possible. Rubisco concentrations determined from Western blotting were compared with those estimated from Coomassie staining (Fig. SM3.3); the Rubisco estimates suggest that estimation of Rubisco from the Western blot were in a similar range to the estimates made by Coomassie staining of gels. Despite the samples being treated differently, both approaches yielded similar estimations of leaf Rubisco content, consistent with the result obtained in Fig SM3.2. Additional tests to check that the primary antibody recognized Rubisco of the study species were performed by spiking temperate evergreen species with Rubisco from tobacco prior to SDS-PAGE analysis. Figure SM3.4 shows a comparison of Rubisco concentration of tree species alone versus that spiked with known concentration of tobacco Rubisco ($0.5 \mu\text{g } \mu\text{L}^{-1}$). The western blot assay estimated $0.31 \mu\text{g } \mu\text{L}^{-1}$ Rubisco in the sample and $0.78 \mu\text{g } \mu\text{L}^{-1}$ in the spiked

sample; a difference closely equivalent to the spike. This suggests that the Western blot antibody assay, typically designed for crop species, is compatible with temperate and tropical evergreen species and that the antibody used can successfully be applied to a variety of land plants (Kellogg & Juliano, 1997). Moreover, this result suggests that possible interference by compounds found in tropical leaves did not affect Rubisco quantification after sample clean-up.

Trouble-shooting using Peruvian tropical species

Leaf protein of lowland Peruvian tree species was extracted using a modified protocol as described above. After initial extraction of chlorophyll using 100% methanol, precipitated protein was further washed in hexane and acetone as described by Gaspar *et al.* (1997) and dissolved in PEB containing 5 mM DTT (Brown *et al.*, 2008). This method was compatible with Peruvian tropical species, as protein bands were observed on Western blot (Fig. SM3.5). However, some of the leaf discs were degraded due to thawing during shipment from Peru, which resulted in no visible bands on the gel. Approximately less than 1.6 µg sample was required per lane to yield clear, unsaturated band with low background intensity (Fig. SM3.5).

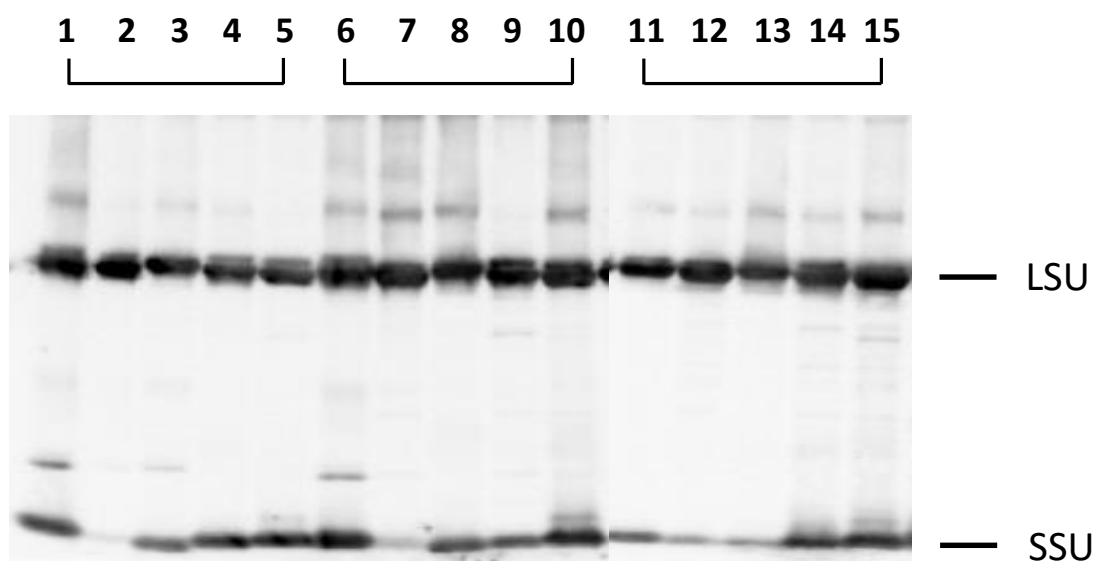


Figure SM3.1: The effect of leaf extraction solvents on Rubisco western blot quality. Typical western blot profile of Rubisco extracted from five temperate evergreen species after acetic acid, methanol and water (1:10:9) (1-5), 80% (v/v) acetone (6-10) and 100% methanol (11-15) clean-up, prior to washing with hexane and acetone (Gaspar *et al.*, 1997) and dissolution in PEB containing 5 mM DTT (Brown *et al.*, 2008). Individual bands represent Rubisco large subunits (LSU, ~55 kDa) and small subunits (SSU, 15 kDa). Greatest quality blots were consistently observed from 100% methanol-treated leaf samples.

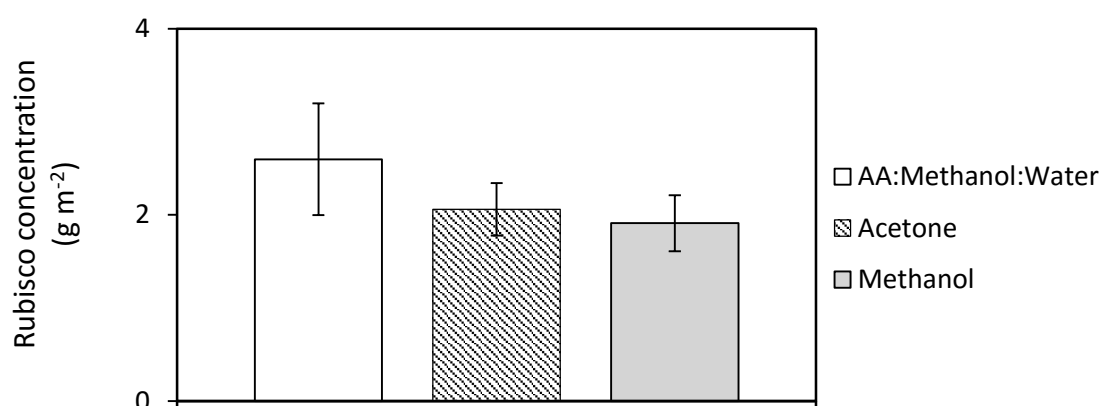


Figure SM3.2: The effect of leaf extraction solvents on estimated Rubisco in protein extracts. The graph shows estimated Rubisco concentration in leaves of five temperate evergreen species (\pm S.E.) after acetic acid (AA), methanol and water (1:10:9), 80% acetone and 100% methanol clean-up, prior to washing with hexane and acetone (Gaspar *et al.*, 1997) and dissolution in PEB containing 5 mM DTT (Brown *et al.*, 2008).

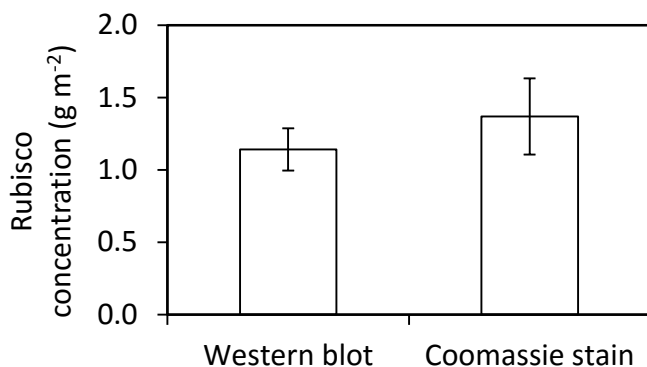


Figure SM3.3: Comparison of western blotting and Coomassie staining for estimation of Rubisco quantities in leaf extracts. Shown are estimated Rubisco concentrations (\pm S.E.) of *Atherosperma moschatum* leaves ($n=3$), determined from Western blot antibody and Coomassie staining. Rubisco estimated from Western blotting was washed with 100% methanol, hexane and acetone, while Rubisco estimated from Coomassie staining was washed with acetic acid, methanol and water (1:10:9), prior to washing with hexane and acetone according to Gaspar *et al.* (1997). Protein was dissolved in PEB containing 5 mM DTT (Brown *et al.*, 2008).

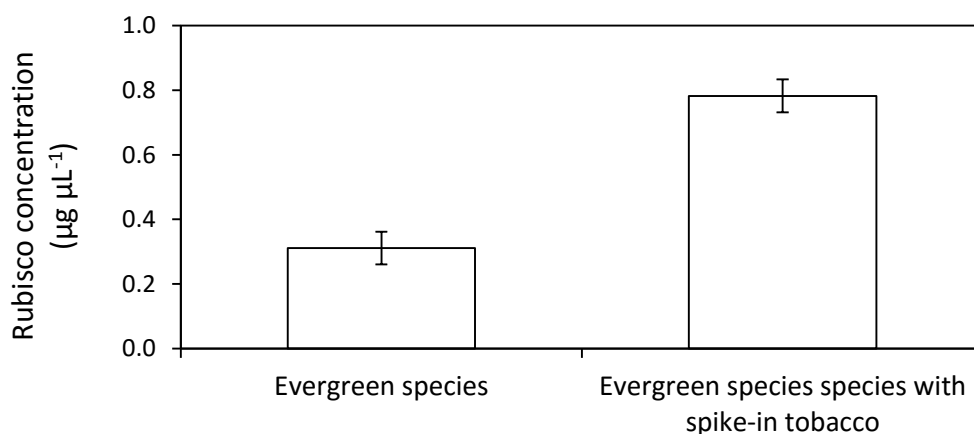


Figure SM3.4: Measurement of Rubisco by western blotting with and without additional Rubisco spike. Estimated Rubisco concentration of *Atherosperma moschatum* (temperate evergreen) and *Micrandra spruceana* (tropical evergreen) determined from protein extract alone and extract with Rubisco from tobacco spiked into the samples ($0.5 \mu\text{g } \mu\text{L}^{-1}$). Rubisco from evergreen species was prepared from 100% methanol clean-up, prior to washing with hexane and acetone (Gaspar *et al.*, 1997) and dissolution in PEB containing 5 mM DTT (Brown *et al.*, 2008). Rubisco from tobacco was extracted using extraction buffer (50mM EPPS [4-(2-hydroxyethyl)-1-piperazinepropanesulfonic acid]-NaOH, 1mM EDTA, 1% Polyvinylpolypyrrolidone (PVPP), 10mM DTT, 0.01% Triton, pH 7.8).

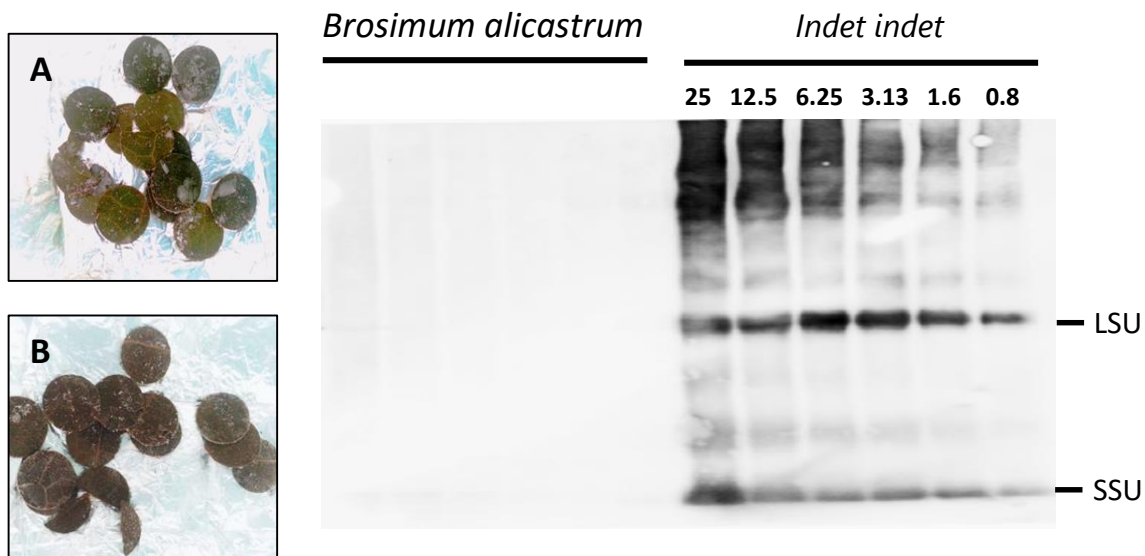


Figure SM3.5: Isolation of Rubisco from tropical leaf samples. Western blot profile of Rubisco extracted from two lowland species (A) *Indet indet* and (B) *Brosimum alicastrum*. Samples were loaded in a dilution series (25 to 0.8 µg) to estimate the amount of protein to load per lane that yields clear and unsaturated band. No visible bands were seen for *B. alicastrum*, which were consistent with brownish appearance of the leaf discs (A) resulting from thawing during transport. Individual bands represent Rubisco large subunits (LSU, ~55 kDa) and small subunits (SSU, 15 kDa).

Table S1: Summary of species sampled at each site and their parameters. Sites are sorted according to decreasing leaf N:P for lowland sites and increasing elevation for upland sites. * marked species site average where $n=2$.

Abbreviations: M_a = leaf mass per unit leaf area, leaf N_a = leaf nitrogen, leaf P_a = leaf phosphorus, $A_{400,a}$ = light-saturated net photosynthesis measured under 400 $\mu\text{mol mol}^{-1}$ atmospheric $[\text{CO}_2]$, $A_{2000,a}$ = light-saturated net photosynthesis measured under 2000 $\mu\text{mol mol}^{-1}$ atmospheric $[\text{CO}_2]$, $V_{\text{cmax},a}^{25}$ = maximum carboxylation velocity of Rubisco normalised to 25°C, $J_{\text{max},a}^{25}$ = maximum rate of electron transport normalised to 25°C, R_{light} = leaf respiration measured in the light at 400 $\mu\text{mol mol}^{-1}$ atmospheric $[\text{CO}_2]$, Leaf T = leaf temperature inside gas exchange cuvette, Chl = chlorophyll a and b content, n_E = fraction of leaf N in electron transport, n_R = fraction of leaf N in Rubisco, n_P = fraction of leaf N in pigment-protein complexes.

Site	Family	Genus	Species	M_a (g m ⁻²)	Leaf N_a (g m ⁻²)	Leaf P_a (g m ⁻²)	$A_{400,a}$ ($\mu\text{mol m}^{-2} \text{s}^{-1}$)	$A_{2000,a}$ ($\mu\text{mol m}^{-2} \text{s}^{-1}$)	$V_{\text{cmax},a}^{25}$ ($\mu\text{mol m}^{-2} \text{s}^{-1}$)	$J_{\text{max},a}^{25}$ ($\mu\text{mol m}^{-2} \text{s}^{-1}$)	R_{light} ($\mu\text{mol m}^{-2} \text{s}^{-1}$)	Leaf T (°C)	Chl (g m ⁻²)	n_E	n_R	n_P
SUC-05	Urticaceae	Pourouma	bicolor	144	2.54	0.09	15.8	30.8	58.9	107.3	1.3	28.8	0.74	0.03	0.11	0.20
SUC-05	Chrysobalanaceae	Couepia	bracteosa	172	1.88	0.06	13.7	26.2	47.1	95.7	0.9	28.0	0.76	0.04	0.12	0.28
SUC-05	Burseraceae	Protium	paniculatum	123	1.56	0.03	2.7	15.3	23.4	55.5	1.3	29.2	0.63	0.03	0.07	0.28
SUC-05	Sapotaceae	Micropholis	guyanensis	163	2.29	0.13	3.5	14.8	19.8	.	1.2	29.2	0.40	.	0.04	0.12
SUC-05	Myristicaceae	Osteophloeum	platyspermum	122	1.87	0.06	13.8	24.6	41.7	76.7	-0.4	29.5	0.78	0.03	0.11	0.29
SUC-05	Sapotaceae	Pouteria	caimito	158	1.62	0.02	13.9	23.8	49.8	82.5	0.7	28.5	0.65	0.04	0.15	0.27
SUC-05	Apocynaceae	Rhigospira	quadrangularis	54	1.22	0.03	6.2	22.5	30.2	82.1	1.4	28.5	0.51	0.05	0.12	0.29
SUC-05	Rubiaceae	Chimarrhis	gentryana	96	2.52	0.09	5.4	18.4	27.9	64.2	1.5	29.4	1.17	0.02	0.05	0.32
SUC-05	Sapotaceae	Pouteria	filipes	95	2.75	0.09	5.8	15.6	22.3	53.9	1.2	29.4	0.71	0.02	0.04	0.18
SUC-05	Chrysobalanaceae	Licania	latifolia	104	1.03	0.03	6.8	22.4	33.6	80.8	1.3	28.1	0.49	0.06	0.15	0.32
SUC-05	Moraceae	Naucleopsis	mello-barretoii	115	2.53	0.07	4.1	14.5	19.0	.	1.2	29.6	1.09	.	0.04	0.30
SUC-05	Rubiaceae	Ladenbergia	magnifolia	127	1.59	0.06	10.0	29.1	47.4	100.7	2.3	29.4	0.57	0.05	0.14	0.24
SUC-05	Myristicaceae	Virola	calophylla	.	.	.	7.2	12.0	27.7	.	1.4	28.5	.	.	.	0.11
SUC-05	unidentified	unidentified	unidentified	119	.	.	14.3	35.7	68.8	.	0.7	28.8
SUC-05	Anacardiaceae	Tapirira	obtusa	.	.	.	10.9	20.7	40.4	71.5	1.4	29.2	.	.	.	0.22
SUC-05	Moraceae	Pseudolmedia	rigida	122	1.16	0.04	7.8	18.6	40.4	71.7	1.9	28.5	0.70	0.05	0.17	0.42
SUC-05	Apocynaceae	Parahancornia	peruviana	137	1.47	0.02	5.4	16.7	23.2	.	1.2	28.4	0.87	.	0.07	0.41
SUC-05	Humiriaceae	Humiriastrum	excelsum	154	1.97	0.03	2.3	20.0	30.6	74.6	1.9	28.7	0.90	0.03	0.07	0.31
SUC-05	Moraceae	Helicostylis	scabra	135	3.01	0.13	15.1	16.7	49.3	84.0	1.0	28.0	0.84	0.02	0.08	0.19
SUC-05	Lauraceae	Licaria	cannella	181	.	0.06	11.7	20.6	44.5	76.8	1.2	28.0	.	0.02	.	.
TAM-05	Ulmaceae	Ampelocera	edentula	.	.	.	6.0	17.2	19.4	.	0.5	30.0
TAM-05	Bixaceae	Bixa	arborea	75	1.65	0.07	13.0	22.6	48.7	76.0	0.1	28.8	.	0.04	0.14	.
TAM-05	Lauraceae	Ocotea	bofo	127	2.28	0.06	9.5	20.6	39.0	64.3	0.3	29.8	.	0.02	0.08	.
TAM-05	unidentified	unidentified	unidentified	138	2.52	0.07	6.6	21.2	47.8	66.4	0.5	30.3	.	0.02	0.09	.
TAM-05	Sapotaceae	Pouteria	torta subsp. tuberculata	117	2.05	0.10	6.8	25.9	45.2	83.3	1.3	30.4	.	0.03	0.10	.

TAM-05	Malvaceae	Huberodendron	switenioides	95	2.17	0.12	10.6	20.5	54.9	61.4	0.4	30.4	.	0.02	0.12	.
TAM-05	Melastomataceae	Miconia	pyrifolia	155	2.27	0.05	11.9	28.7	56.3	94.0	1.6	30.6	.	0.03	0.12	.
TAM-05	Elaeocarpaceae	Sloanea	brevipes	125	2.05	0.08	11.5	20.7	63.5	66.6	1.3	31.0	.	0.03	0.15	.
JEN-11	Sapotaceae	Micropholis	guyanensis	156	.	0.05	2.5	22.1	32.1	77.8	2.2	29.5	.	0.02	.	.
JEN-11	Olacaceae	Aptandra	liriosmoides	165	2.35	0.11	5.3	15.7	18.2	.	1.0	29.5	0.98	.	0.04	0.29
JEN-11	Lauraceae	Mezilaureus	synandra	230	2.43	0.07	3.9	21.0	29.2	.	1.6	29.5	.	.	0.06	0.43
JEN-11	Lecythidaceae	Eschweilera	coriacea	124	1.74	0.06	5.3	18.8	27.7	67.6	1.3	28.8	0.35	0.03	0.08	0.14
JEN-11	Vochysiaceae	Qualea	paraensis	154	1.79	.	11.2	14.6	35.5	51.7	0.4	28.4	0.83	0.02	0.09	0.32
JEN-11	Melastomataceae	Mouriri	nigra	124	2.57	0.04	4.5	10.3	22.9	39.6	1.1	28.7	0.73	0.01	0.04	0.19
JEN-11	Sapotaceae	Pouteria	guianensis	163	1.78	0.05	4.9	16.1	24.2	.	1.1	28.9	0.71	.	0.06	0.27
JEN-11	Goupiaceae	Goupia	glabra	103	2.07	0.08	15.5	37.4	65.8	.	1.6	28.9	0.52	0.05	0.15	0.17
JEN-11	Myristicaceae	Osteophloeum	platyspermum	141	2.86	0.11	11.6	17.5	39.9	70.9	1.0	28.5	0.88	0.02	0.07	0.21
JEN-11	Sapotaceae	Pouteria	platyphylla	149	1.98	0.06	9.5	10.8	31.4	41.1	0.2	28.6	0.77	0.02	0.08	0.27
JEN-11	unidentified	unidentified	unidentified	.	.	.	7.7	20.2	37.6	73.5	2.3	29.2
JEN-11	Myrtaceae	Myrciaria	floribunda	127	1.65	0.04	3.2	5.5	9.9	.	0.5	28.4	0.62	.	0.03	0.26
JEN-11	Urticaceae	Pourouma	bicolor	149	2.42	0.10	.	31.1	66.9	107.0	0.6	28.7	0.69	0.03	0.13	0.20
JEN-11	Chrysobalanaceae	Licania	indet	147	2.57	0.05	9.0	10.5	25.1	37.7	0.6	28.4	0.41	0.01	0.05	0.11
JEN-11	Lecythidaceae	Eschweilera	tessmannii	134	2.39	0.05	7.5	16.0	23.4	59.4	1.3	28.5	0.69	0.02	0.05	0.20
JEN-11	Apocynaceae	Couma	macrocarpa	81	1.25	0.06	2.8	12.7	31.4	66.3	1.5	29.0	0.51	0.04	0.12	0.28
JEN-11	Sapotaceae	Micropholis	guyanensis	210	2.88	0.04	10.3	18.2	36.3	66.2	1.0	29.0	0.23	0.02	0.06	0.05
JEN-11	Elaeocarpaceae	Sloanea	brevipes	101	1.19	0.08	9.4	15.1	30.3	56.8	1.2	28.2	0.64	0.04	0.12	0.37
ALP-01	Fabaceae	Dipteryx	micrantha	143	1.96	0.09	11.4	16.6	39.5	53.7	0.0	29.1	0.70	0.02	0.10	0.24
ALP-01	Sapotaceae	Pouteria	subrotata	.	.	.	11.6	26.7	47.3	86.3	0.9	29.4
ALP-01	Chrysobalanaceae	Licania	arachnoidea	98	1.20	0.02	6.9	7.5	29.9	61.2	0.8	30.1	0.47	0.04	0.12	0.27
ALP-01	Annonaceae	Guatteria	schomburgkiana	125	2.20	0.07	2.9	22.1	32.4	.	2.0	29.7	0.47	.	0.07	0.15
ALP-01	Olacaceae	Minquartia	guianensis	126	1.40	0.05	9.7	19.3	39.1	55.0	0.4	30.6	0.61	0.03	0.13	0.30
ALP-01	Myristicaceae	Iryanthera	lancifolia	154	1.81	0.08	12.7	21.9	43.7	75.2	0.3	28.8	0.45	0.03	0.11	0.17
ALP-01	Euphorbiaceae	Hevea	pauciflora	121	1.96	0.12	0.9	4.5	8.3	.	1.2	30.5	0.52	.	0.02	0.18
ALP-01	Olacaceae	Chaunochiton	kappleri	124	2.43	0.15	7.5	17.7	30.8	57.0	1.3	30.2	0.70	0.02	0.06	0.20
ALP-01	Ochnaceae	Cespedesia	spathulata	119	1.86	0.10	4.2	22.5	30.0	.	1.2	30.0	0.58	.	0.08	0.21
ALP-01	Fabaceae	Taralea	oppositifolia	154	1.56	0.04	1.9	7.0	7.2	.	0.5	30.6	0.78	.	0.02	0.34
ALP-01	Moraceae	Brosimum	rubescens	114	1.61	0.07	2.9	12.0	15.5	38.3	0.9	30.2	.	0.02	0.05	.
ALP-01	Fabaceae	Swartzia	polyphylla	117	2.49	0.06	7.4	17.9	34.8	49.2	0.9	30.4	0.60	0.02	0.07	0.16
ALP-01	Lepidobotryaceae	Ruptiliocarpon	caracolito	74	1.75	0.06	5.5	15.6	24.4	41.8	0.6	30.3	0.18	0.02	0.07	0.07

ALP-01	Clusiaceae	Caraipa	punctulata	161	1.94	0.06	9.5	23.1	41.6	62.3	0.9	30.6	0.49	0.03	0.10	0.17
ALP-01	Euphorbiaceae	Senefeldera	inclinata	116	2.67	0.09	2.3	18.6	23.3	54.2	1.2	29.3	0.86	0.02	0.04	0.22
ALP-01	Urticaceae	Pourouma	guianensis subsp. guianensi	100	1.95	0.09	15.9	19.3	53.9	58.6	-0.3	29.6	0.59	0.02	0.13	0.21
ALP-01	Euphorbiaceae	Hevea	pauciflora	108	1.67	0.11	10.2	19.0	36.8	55.8	0.3	29.2	0.57	0.03	0.10	0.24
ALP-01	Fabaceae	Inga	striata	78	.	0.10	11.9	21.6	41.1	69.7	0.1	29.0	0.62	0.02	0.06	0.14
SUC-01	Myristicaceae	Virola	sebifera	124	2.57	0.11	1.4	25.2	32.2	.	3.2	30.6	0.63	.	0.06	0.17
SUC-01	Myristicaceae	Otoba	glycyarpa	132	.	.	6.0	16.2	27.1	.	1.3	29.8	0.34	.	.	.
SUC-01	Elaeocarpaceae	Sloanea	gladysiae	127	0.90	0.03	1.7	12.2	17.1	40.8	0.8	29.6	0.62	0.04	0.09	0.47
SUC-01	Sapotaceae	Pouteria	filipes	113	1.89	0.09	3.3	18.0	26.5	.	1.7	27.8	0.46	.	0.07	0.16
SUC-01	Urticaceae	Pourouma	bicolor	118	1.91	0.09	16.9	24.7	59.8	91.8	1.2	27.9	0.75	0.04	0.15	0.27
SUC-01	Lepidobotryaceae	Ruptiliocarpon	caracolito	101	1.18	0.06	5.9	13.9	21.5	48.5	0.8	28.6	0.71	0.03	0.09	0.41
SUC-01	Myristicaceae	Iryanthera	lancifolia	131	1.82	0.09	11.3	24.3	48.6	67.1	-0.5	31.0	0.54	0.03	0.13	0.20
SUC-01	Lecythidaceae	Gustavia	hexapetala	112	3.35	0.15	9.2	20.8	42.3	53.2	0.5	31.1	0.73	0.01	0.06	0.15
SUC-01	Chrysobalanaceae	Licania	heteromorpha	.	.	.	3.6	17.7	27.8	60.9	1.6	29.7	.	.	.	0.42
SUC-01	Humiriaceae	Schistostemon	reticulatum subsp. reticula	187	2.20	0.09	4.9	14.0	.	.	.	31.3	0.80	.	.	0.25
SUC-01	Moraceae	Helicostylis	scabra	80	1.40	0.08	8.3	15.7	30.3	53.6	1.7	29.9	0.65	0.03	0.10	0.32
SUC-01	Sapindaceae	Talisia	sylvatica	173	2.18	0.12	7.0	17.7	26.4	60.8	0.8	29.1	0.39	0.02	0.06	0.12
SUC-01	Fabaceae	Inga	capitata	139	.	0.13	10.2	21.7	37.7	75.5	1.0	28.8	0.91	0.01	0.04	0.14
SUC-01	Lecythidaceae	Eschweilera	itayensis	87	0.90	0.05	10.2	14.2	31.2	48.3	0.5	29.0	0.48	0.04	0.16	0.37
SUC-01	Hypericaceae	Vismia	amazonica	132	1.61	0.08	18.8	37.5	68.3	124.8	0.6	29.2	0.59	0.06	0.20	0.25
SUC-01	Euphorbiaceae	Nealchornea	yapurensis	115	1.61	0.09	10.0	25.7	40.5	88.9	1.3	29.1	1.10	0.04	0.12	0.47
SUC-01	Olacaceae	Minquartia	guianensis	105	1.63	0.09	4.6	16.5	22.4	57.8	1.1	29.1	0.58	0.03	0.07	0.24
SUC-01	Combretaceae	Buchenavia	tomentosa	120	2.04	0.10	7.2	16.3	24.2	54.8	0.8	29.4	0.55	0.02	0.06	0.19
JEN-12	Apocynaceae	Macoubea	sprucei	116	1.24	0.08	9.4	18.7	36.3	69.1	0.8	28.0	0.73	0.04	0.14	0.40
JEN-12	Sapotaceae	Pouteria	lucumifolia	175	1.32	0.13	1.0	9.1	13.9	.	1.5	28.8	0.61	.	0.05	0.32
JEN-12	Clusiaceae	Caraipa	tereticaulis	181	1.60	0.05	9.5	16.3	40.3	.	1.5	28.8	0.44	.	0.12	0.19
JEN-12	Icacinaceae	Emmotum	floribundum	.	.	.	9.2	26.6	45.8	75.9	-1.7	29.0
JEN-12	Linaceae	Roucheria	columbiana	.	.	.	5.2	13.2	17.1	.	0.7	28.8	.	.	.	0.36
JEN-12	Euphorbiaceae	Micrandra	spruceana	123	1.93	0.10	6.6	16.8	31.0	66.2	1.8	28.4	0.44	0.03	0.08	0.15
JEN-12	Melastomataceae	Mouriri	nigra	196	3.01	0.05	7.8	14.1	23.6	52.0	0.7	28.3	0.83	0.01	0.04	0.19
JEN-12	Moraceae	Brosimum	utile subsp. ovatifolium	134	1.80	0.13	12.3	20.4	40.7	72.2	0.9	28.5	0.43	0.03	0.11	0.16
JEN-12	Clusiaceae	Tovomitia	calophyllophylla	179	1.83	0.01	4.6	13.5	19.7	48.7	0.8	28.5	0.78	0.02	0.05	0.29
JEN-12	Apocynaceae	Aspidosperma	desmanthum	163	2.02	0.21	5.0	23.6	39.8	84.5	1.8	29.1	0.50	0.03	0.09	0.17

JEN-12	Lauraceae	Licaria	cannella	166	2.04	0.06	7.3	18.1	33.6	62.6	1.3	29.1	0.62	0.02	0.08	0.21
JEN-12	Malvaceae	Lueheopsis	althaeiflora	208	2.69	0.12	15.4	23.6	48.6	80.6	0.6	28.9	0.61	0.02	0.09	0.16
JEN-12	Burseraceae	Protium	polybotryum	152	1.97	0.08	8.3	29.2	41.6	100.6	1.9	29.4	0.50	0.04	0.10	0.17
JEN-12	Moraceae	Brosimum	rubescens	156	1.70	0.04	13.6	21.6	45.4	73.7	1.0	29.0	0.42	0.03	0.13	0.17
JEN-12	Moraceae	Pseudolmedia	rigida	160	2.71	0.14	1.5	17.8	27.1	65.2	1.7	29.1	0.68	0.02	0.05	0.17
JEN-12	Sapotaceae	Chrysophyllum	sanguinolentum	163	1.97	0.11	14.6	23.7	50.1	96.1	1.0	28.3	0.63	0.04	0.12	0.22
JEN-12	Euphorbiaceae	Alchornea	triplinervia	93	2.12	0.07	13.7	23.5	47.6	79.4	0.8	29.1	0.28	0.03	0.11	0.09
JEN-12	Apocynaceae	Parahancornia	peruviana	117	1.11	0.01	4.1	10.6	17.4	37.6	1.3	29.1	0.61	0.03	0.07	0.37
JEN-12	Sapotaceae	Micropholis	guyanensis subsp. guyanensi	174	2.48	0.15	13.4	37.2	48.3	114.4	1.3	28.9	0.65	0.04	0.09	0.18
ALP-30	Fabaceae	Tachigali	bracteosa	151	2.48	0.15	4.4	22.9	31.5	.	1.9	29.6	0.84	.	0.06	0.23
ALP-30	Moraceae	Brosimum	potabile	158	2.57	0.14	5.6	16.5	21.9	.	1.5	29.4	0.44	.	0.04	0.12
ALP-30	Elaeocarpaceae	Sloanea	floribunda	.	.	0.06	5.6	13.6	21.0	47.5	1.1	29.2		0.02	0.05	0.24
ALP-30	Euphorbiaceae	Micrandra	spruceana	63	1.66	0.13	2.0	7.1	10.3	.	0.5	29.3	0.29	.	0.03	0.12
ALP-30	Simaroubaceae	Simarouba	amara	182	1.88	0.09	8.4	20.5	34.8	72.3	1.5	29.5	0.45	0.03	0.09	0.16
ALP-30	Humiriaceae	Humiria	balsamifera	140	1.12	0.12	7.6	15.7	27.2	57.2	0.8	28.5	0.56	0.04	0.12	0.34
ALP-30	Lauraceae	Ocotea	aciphylla	199	1.75	0.06	8.2	16.2	31.0	56.0	0.6	28.8	0.59	0.03	0.08	0.23
ALP-30	Apocynaceae	Aspidosperma	desmanthum	199	2.18	0.19	10.0	27.4	40.3	95.8	1.4	28.8	0.56	0.03	0.09	0.18
ALP-30	Fabaceae	Diploctropis	sp	113	1.63	0.08	13.6	31.0	46.5	102.1	0.6	29.2	0.44	0.05	0.14	0.18
ALP-30	Annonaceae	Guatteria	decurrens	142	1.19	0.05	5.7	14.7	24.1	53.1	1.0	28.5	0.62	0.04	0.10	0.36
ALP-30	Euphorbiaceae	Micrandra	elata	88	1.57	0.07	2.5	11.0	13.5	37.5	0.8	29.4	0.58	0.02	0.04	0.25
ALP-30	Lauraceae	Ocotea	myriantha	166	2.00	0.06	4.6	14.3	18.0	.	0.5	30.5	0.46	.	0.04	0.16
ALP-30	Apocynaceae	Aspidosperma	excelsum	159	1.88	0.12	3.9	21.4	25.9	.	1.4	29.5	0.69	.	0.07	0.25
ALP-30	Myrtaceae	Calyptanthus	bipennis	154	1.31	0.05	3.9	12.8	18.9	41.0	0.8	30.1	0.55	0.02	0.07	0.29
ALP-30	Lauraceae	Aniba	perutilis	144	1.75	0.06	8.2	15.3	30.3	58.1	1.2	28.1	0.61	0.03	0.08	0.24
ALP-30	Fabaceae	Macrolobium	microcalyx	109	1.39	0.06	7.7	8.5	19.1	31.7	0.6	28.7	0.58	0.02	0.07	0.28
ALP-30	Myristicaceae	Virola	pavonis	141	1.22	0.05	12.7	16.6	40.8	62.7	0.9	29.0	0.69	0.04	0.16	0.39
ALP-30	Chrysobalanaceae	Licania	unguiculata	140	2.25	0.18	11.1	18.5	31.8	69.1	1.4	28.2	0.59	0.02	0.07	0.18
ALP-30	Anacardiaceae	Tapirira	guianensis	62	0.95	0.06	6.5	12.2	22.3	44.6	0.8	28.3	0.38	0.04	0.11	0.27
ALP-30	Linaceae	Roucheria	schomburgkii	99	0.99	0.04	6.1	15.6	26.3	58.1	1.3	28.8	0.52	0.05	0.13	0.36
ALP-30	Icacinaeae	Emmotum	floribundum	188	1.43	0.08	2.9	5.6	8.4	20.8	0.8	29.3	0.34	0.01	0.03	0.16
CUZ-03	Moraceae	Pseudolmedia	laevis	95	1.48	0.08	10.0	19.9	39.4	64.2	0.6	29.9	.	0.03	0.13	.
CUZ-03	Sapotaceae	Pouteria	torta subsp. glabra	138	2.01	0.11	10.0	19.8	52.7	63.8	1.2	30.4	.	0.03	0.12	.
CUZ-03	Moraceae	Poulsenia	armata	119	1.59	0.12	6.8	23.5	46.3	76.8	1.4	29.9	.	0.04	0.14	.
CUZ-03	Combretaceae	Terminalia	oblonga	130	2.26	0.14	5.5	20.0	41.3	65.5	1.4	30.0	.	0.02	0.09	.

CUZ-03	Malvaceae	Guazuma	crinita	112	2.37	.	16.2	28.0	60.9	89.5	-0.1	29.2	.	0.03	0.12	.
CUZ-03	Sapotaceae	Pouteria	franciscana	111	2.16	0.15	8.2	19.5	38.2	64.5	1.0	30.0	.	0.02	0.08	.
CUZ-03	Phytolaccaceae	Gallsia	integrifolia	98	2.62	0.10	8.2	27.0	42.3	87.8	1.0	29.8	.	0.03	0.08	.
CUZ-03	Dichapetalaceae	Tapura	sp.	122	1.00	0.02	8.3	17.8	39.2	59.5	1.2	29.9	.	0.05	0.19	.
CUZ-03	Meliaceae	Trichilia	sp.	90	1.63	0.15	7.7	14.5	31.5	50.3	0.8	30.0	.	0.02	0.09	.
CUZ-03	Meliaceae	Trichilia	sp.	118	1.83	0.10	3.3	10.4	13.7	34.1	1.0	30.4	.	0.01	0.04	.
CUZ-03	Malvaceae	Apeiba	aspera	100	1.44	0.04	11.0	20.7	62.3	61.5	1.1	30.8	.	0.03	0.20	.
CUZ-03	Fabaceae	Swartzia	sp.	76	2.18	0.08	4.3	9.2	15.3	31.3	0.3	28.9	.	0.01	0.03	.
ALP-40	Fabaceae	Dicymbe	uaiparuensis	113	1.93	0.10	5.8	15.8	33.2	43.2	2.3	31.7	0.81	0.02	0.08	0.29
ALP-40	Sapotaceae	Chrysophyllum	sanguinolentum	202	1.88	0.10	15.9	25.1	54.0	80.7	-0.3	29.5	0.70	0.03	0.14	0.25
ALP-40	Myristicaceae	Virola	pavonis	193	2.33	0.13	8.3	18.7	40.8	51.0	1.8	31.4	0.47	0.02	0.08	0.14
ALP-40	unidentified	unidentified	unidentified	195	.	0.08	8.4	15.7	33.8	45.8	1.1	30.6	.	0.02	.	.
ALP-40	Icacinaeae	Emmotum	floribundum	.	1.97	.	4.8	18.4	21.4	.	2.0	31.3	.	.	0.05	0.25
ALP-40	Fabaceae	Jacqueshuberia	loretensis	75	1.63	0.08	10.5	21.8	41.8	69.0	0.8	29.5	0.38	0.03	0.12	0.16
ALP-40	Elaeocarpaceae	Sloanea	robusta	174	1.16	0.09	6.7	19.5	29.7	53.4	1.1	30.8	0.62	0.04	0.12	0.37
ALP-40	Myrsinaceae	Cybianthus	nestorii	200	1.64	0.09	9.4	21.7	37.3	70.3	0.3	30.4	0.61	0.03	0.11	0.25
ALP-40	Icacinaeae	Emmotum	floribundum	123	1.56	0.07	2.6	15.8	30.9	49.8	1.4	31.1	0.59	0.03	0.09	0.26
ALP-40	unidentified	unidentified	unidentified	193	2.37	.	3.5	8.9	14.6	25.5	0.9	32.4	0.62	0.01	0.03	0.18
ALP-40	Apocynaceae	Indet	indet	147	1.61	0.12	6.5	23.8	42.6	67.7	2.6	31.2	.	0.03	0.13	.
ALP-40	Araliaceae	Dendropanax	resinosus	177	2.13	0.10	3.6	14.3	19.2	.	1.0	31.1	0.82	.	0.04	0.26
TAM-09	Lauraceae	Ocotea	sp	112	2.09	0.11	11.3	25.2	46.7	75.9	0.8	30.7	.	0.03	0.11	.
TAM-09	Urticaceae	Pourouma	minor	108	2.28	0.14	14.2	17.5	54.0	69.2	0.9	30.7	.	0.02	0.11	.
TAM-09	Annonaceae	.	.	69	.	.	11.2	19.0	35.5	58.8	0.3	30.2
TAM-09	Urticaceae	Pourouma	sp.	.	.	.	10.7	9.8	47.2	63.2	0.7	30.1
TAM-09	Burseraceae	Trattinnickia	glaziovii	97	1.60	0.17	12.3	19.8	52.8	80.4	0.6	29.5	.	0.04	0.16	.
TAM-09	Euphorbiaceae	Glycydendron	amazonicum	94	2.19	0.11	10.0	24.4	43.0	76.0	0.6	30.1	.	0.03	0.09	.
TAM-09	Boraginaceae	Cordia	.	118	2.95	0.13	11.1	29.6	67.8	95.5	0.4	29.9	.	0.03	0.11	.
TAM-09	Fabaceae	Hymenaea	longifolia	112	1.96	0.11	14.5	21.6	61.7	79.8	0.6	27.7	.	0.03	0.15	.
TAM-09	Anacardiaceae	Thyrsodium	sp	118	1.65	0.12	11.2	22.7	59.6	84.6	0.8	28.0	.	0.04	0.17	.
TAM-09	Moraceae	Pseudolmedia	macrophylla	112	2.14	0.13	6.2	16.5	32.6	60.4	0.5	28.1	.	0.02	0.07	.
TAM-09	Meliaceae	Cabrlea	canjerana	70	.	.	9.3	26.2	47.5	.	1.2	28.5	.	0.03	.	.
TAM-09	Lauraceae	Nectandra	purpurea	105	2.10	0.13	14.1	24.1	71.8	90.9	0.5	27.5	.	0.03	0.16	.
TAM-09	Moraceae	Castilla	sp.	147	2.89	0.21	8.9	14.7	20.9	51.2	-0.5	27.8	.	0.01	0.03	.
TAM-06	Euphorbiaceae	Sapium	marmieri	.	.	.	7.6	28.0	37.9	.	1.3	30.6

TAM-06	<i>Fabaceae</i>	<i>Inga</i>	<i>alba</i>	.	.	.	7.3	22.0	35.0	67.3	0.7	30.3
TAM-06	<i>Moraceae</i>	<i>Ficus</i>	<i>schultesii</i>	151	2.30	0.15	13.2	23.0	47.6	71.6	0.9	30.8	.	0.02	0.10	.
TAM-06	<i>Fabaceae</i>	<i>Pterocarpus</i>	<i>rohrii</i>	.	.	.	7.1	24.8	28.7	.	1.0	30.2
TAM-06	<i>Moraceae</i>	<i>Pseudolmedia</i>	<i>laevis</i>	137	1.83	0.10	7.4	19.7	28.4	65.8	0.4	29.2	.	0.03	0.07	.
TAM-06	unidentified	unidentified	unidentified	96	2.74	0.24	7.2	24.4	37.5	79.0	1.4	30.2	.	0.02	0.07	.
TAM-06	<i>Moraceae</i>	<i>Sorocea</i>	<i>pileata</i>	109	3.02	0.18	9.1	22.7	35.3	76.7	0.6	29.3	.	0.02	0.06	.
TAM-06	<i>Fabaceae</i>	<i>Dipteryx</i>	<i>alata</i>	112	2.34	0.14	16.4	26.4	73.1	86.0	1.2	29.9	.	0.03	0.15	.
TAM-06	<i>Moraceae</i>	<i>Sorocea</i>	<i>trophoides</i>	96	2.52	0.15	9.9	20.4	35.0	63.5	0.2	29.9	.	0.02	0.07	.
TAM-06	<i>Lecythidaceae</i>	<i>Bertolletia</i>	<i>excelsa</i>	151	2.70	0.20	14.8	.	88.6	108.4	-2.7	28.8	.	0.03	0.16	.
TAM-06	<i>Moraceae</i>	<i>Brosimum</i>	<i>sp.</i>	172	2.63	0.13	4.0	14.0	17.8	47.5	1.0	29.4	.	0.01	0.03	.
TAM-06	<i>Cannabaceae</i>	<i>Celtis</i>	<i>schippii</i>	131	2.93	0.21	9.8	23.0	34.8	75.6	0.8	29.5	.	0.02	0.06	.
TAM-06	<i>Moraceae</i>	<i>Clarisia</i>	<i>racemosa</i>	105	2.56	0.20	8.2	22.4	37.3	75.2	1.7	30.0	.	0.02	0.07	.
SPD-02	<i>Burseraceae</i>	<i>Protium</i>	<i>sagotianum</i>	170	2.70	0.19	8.7	25.6	40.2	97.3	0.4	27.3	1.36	0.03	0.07	0.35
SPD-02	<i>Phyllanthaceae</i>	<i>Hieronyma</i>	<i>macrocarpa</i>	105	2.02	0.15	7.7	31.2	60.2	129.2	1.5	26.7	0.48	0.05	0.14	0.16
SPD-02	<i>Sapotaceae</i>	<i>Chrysophyllum</i>	<i>sp.</i>	182	2.91	0.24	4.8	25.1	43.0	.	1.9	27.3	1.19	.	0.07	0.28
SPD-02	<i>Sapindaceae</i>	<i>Matayba</i>	<i>guianensis</i>	210	3.01	0.20	.	.	7.1	.	1.1	25.9	1.17	.	.	0.27
SPD-02	<i>Fabaceae</i>	<i>Inga</i>	<i>killipiana</i>	95	2.51	0.15	8.0	8.2	48.1	.	0.4	27.1	0.71	.	0.09	0.19
SPD-02	<i>Melastomataceae</i>	<i>Miconia</i>	<i>coelestis</i>	74	1.67	0.09	11.8	39.5	77.6	152.4	0.1	26.9	0.45	0.07	0.22	0.18
SPD-02	<i>Ebenaceae</i>	<i>sp1(1046WFR)</i>	<i>sp.</i>	108	1.69	0.13	5.8	19.9	34.9	.	0.6	27.8	0.86	.	0.10	0.35
SPD-02	<i>Burseraceae</i>	<i>Protium</i>	<i>nodulosum</i>	60	.	.	7.1	23.4	32.7	.	0.0	27.7	0.21	.	.	.
SPD-02	<i>Burseraceae</i>	<i>Protium</i>	<i>spruceanum cf</i>	113	1.95	0.12	5.2	21.1	42.2	84.4	0.6	27.5	0.89	0.03	0.10	0.31
SPD-02	<i>Lauraceae</i>	<i>Beilschmiedia</i>	<i>latifolia</i>	123	2.25	0.11	12.7	27.7	52.0	100.7	-0.7	27.6	1.11	0.04	0.11	0.34
SPD-02	<i>Caryocaraceae</i>	<i>Caryocar</i>	<i>sp.</i>	120	1.85	0.14	5.3	16.0	22.6	.	0.2	26.9	0.56	.	0.06	0.21
SPD-02	<i>Araliaceae</i>	<i>Dendropanax</i>	<i>cuneatus</i>	128	2.57	0.18	6.4	11.8	28.2	55.8	1.0	27.4	0.58	0.02	0.05	0.16
SPD-02	<i>Aquifoliaceae</i>	<i>Ilex</i>	<i>sp.</i>	163	1.91	0.08	9.4	26.9	49.0	104.8	0.5	27.2	0.90	0.04	0.12	0.32
SPD-02	<i>Moraceae</i>	<i>Pseudolmedia</i>	<i>laevigata</i>	103	2.82	0.17	8.6	33.4	56.8	.	2.0	27.1	0.65	.	0.10	0.16
SPD-02	<i>Moraceae</i>	<i>*Ficus</i>	<i>americana subsp. guianensis</i>	140	2.04	0.22	11.7	17.5	56.5	76.7	1.7	27.4	0.69	0.03	0.13	0.23
SPD-02	<i>Sapotaceae</i>	<i>Pouteria</i>	<i>torta</i>	121	2.38	0.11	9.7	21.4	38.9	79.3	-0.2	27.3	0.83	0.03	0.08	0.24
SPD-02	<i>Rubiaceae</i>	<i>Elaeagia</i>	<i>mariae</i>	.	.	.	11.4	31.9	58.0	121.7	0.3	27.3	.	.	.	0.27
SPD-02	<i>Cunoniaceae</i>	<i>Weinmannia</i>	<i>lechleriana</i>	116	1.67	0.11	5.6	36.5	68.4	.	6.1	26.7	0.81	.	0.19	0.33
SPD-02	<i>Lauraceae</i>	<i>Nectandra</i>	<i>sp.</i>	134	2.10	0.20	7.9	45.2	.	.	.	27.0	0.64	.	.	0.21
SPD-01	<i>Euphorbiaceae</i>	<i>Alchornea</i>	<i>anamariae</i>	123	2.32	0.18	10.6	27.1	49.1	97.5	-0.3	27.8	0.79	0.03	0.10	0.23
SPD-01	<i>Lauraceae</i>	<i>Ocotea</i>	<i>cernua</i>	114	1.98	0.10	6.4	21.8	37.5	79.3	0.3	27.9	1.00	0.03	0.09	0.34
SPD-01	<i>Lauraceae</i>	<i>Endlicheria</i>	<i>chalsea</i>	156	2.90	0.15	11.5	24.3	54.6	82.5	-0.2	28.6	0.63	0.02	0.09	0.15

SPD-01	Brunelliaceae	Brunellia	stenoptera	97	1.86	0.13	19.0	38.8	89.7	137.0	-1.0	28.0	0.47	0.06	.	0.17
SPD-01	Lauraceae	Endlicheria	macrophylla	90	2.40	0.20	5.6	22.3	47.9	82.4	0.1	28.4	0.79	0.03	0.09	0.23
SPD-01	Lauraceae	Licaria	cannella	81	1.79	0.13	3.1	10.7	17.1	.	1.0	26.0	0.39		0.05	0.15
SPD-01	Urticaceae	Cecropia	angustifolia	103	2.44	0.16	15.9	30.3	68.0	120.6	-1.5	25.6	0.73	0.04	0.13	0.21
SPD-01	Euphorbiaceae	Hyeronima	moritziana	117	2.42	0.20	10.2	21.7	33.4	.	1.4	25.9	1.07	.	0.07	0.30
SPD-01	Meliaceae	Cabralea	canjerana	117	2.67	0.27	9.5	24.4	40.6	99.8	0.1	25.9	0.79	0.03	0.07	0.20
SPD-01	Urticaceae	Pourouma	bicolor subsp. scobina	93	1.96	0.21	10.4	25.5	56.0	99.3	-0.6	26.2	0.47	0.04	0.14	0.16
SPD-01	Flacourtiaceae	sp5(1101KGC)	sp.	93	1.80	0.10	4.5	10.1	15.6	.	0.1	27.5	0.34	.	0.04	0.13
SPD-01	Chrysobalanaceae	Licania	sp.	143	2.48	0.15	5.9	29.9	50.4	112.6	0.6	27.5	0.65	0.04	0.10	0.18
SPD-01	Lauraceae	Endlicheria	sp.	168	.	0.15	1.8	.	9.5	.	0.6	27.7	.	0.01	.	.
SPD-01	Lauraceae	Nectandra	amazonum	147	2.34	0.14	3.4	8.5	15.9	.	0.7	27.9	1.07	.	0.03	0.31
SPD-01	Sapotaceae	Pouteria	sagotiana	137	2.38	0.17	5.3	15.9	31.5	61.2	-0.1	27.1	0.67	0.02	0.06	0.19
SPD-01	Phyllanthaceae	Hieronyma	asperifolia	166	2.66	0.22	3.5	26.1	36.3	.	2.2	28.2	0.70	.	0.06	0.18
SPD-01	Hypericaceae	*Vismia	glaziovii	95	1.85	0.14	15.6	29.7	76.6	115.5	-0.9	27.8	0.74	0.05	0.20	0.27
SPD-01	Anacardiaceae	*Tapirira	obtusa	154	2.09	0.17	7.4	20.1	36.0	76.1	0.4	27.5	0.61	0.03	0.08	0.21
SPD-01	Sapindaceae	Matayba	guianensis	154	2.64	0.13	.	.	6.1	.	0.3	27.2	1.18	.	.	0.31
TRU-08	Aquifoliaceae	Ilex	rimbachii	194	.	.	7.7	12.2	40.3	70.6	1.2	24.2	0.56	.	.	.
TRU-08	Anacardiaceae	Tapirira	obtusa	140	.	.	11.9	22.3	59.3	106.1	1.0	24.0	0.48	.	.	.
TRU-08	Myrtaceae	Siphoneugena	densiflora	202	.	.	4.9	5.9	13.2	29.8	0.2	23.3	0.71	.	.	.
TRU-08	Rubiaceae	Elaeagia	mariae	138	.	.	10.6	24.1	57.7	112.0	0.7	24.3	0.44	.	.	.
TRU-08	Lauraceae	Nectandra	laurel	183	.	.	12.7	26.0	63.7	119.3	0.3	24.0	0.75	.	.	.
TRU-08	Proteaceae	Panopsis	rubescens var. sprucei	182	.	.	9.3	18.9	42.6	87.5	0.5	24.0	0.50	.	.	.
TRU-08	Alzateaceae	Alzatea	verticillata subsp. vertici	120	.	.	6.8	22.0	55.9	.	2.8	24.4	0.33	.	.	.
TRU-08	Clethraceae	Clethra	fagifolia	190	2.17	0.10	10.9	28.7	60.6	131.2	0.9	24.4	0.45	0.05	0.13	0.14
TRU-08	Myrtaceae	Myrcia	fallax	156	1.42	0.05	2.9	12.7	22.0	.	1.3	25.1	0.39	.	0.07	0.19
TRU-08	Araliaceae	Schefflera	patula	130	2.20	0.21	4.0	8.5	28.0	47.8	1.5	24.5	0.54	0.02	0.06	0.17
TRU-08	Proteaceae	Roupala	monosperma	225	1.83	0.09	10.4	25.9	55.9	118.3	1.2	24.7	0.61	0.05	0.14	0.23
TRU-08	Moraceae	Ficus	americana	187	2.66	0.21	13.8	21.7	88.8	109.4	1.9	24.9	0.77	0.03	0.16	0.20
TRU-08	Lauraceae	Nectandra	cuspidata	188	2.01	0.06	12.6	29.8	60.9	129.1	0.3	25.0	0.76	0.05	0.14	0.26
TRU-08	Annonaceae	Guatteria	terminalis	114	1.71	0.09	5.8	20.8	40.7	94.4	1.2	25.1	0.42	0.04	0.11	0.17
TRU-08	Melastomataceae	Miconia	sp.	136	2.03	0.11	7.6	25.1	52.4	.	1.6	24.9	0.80	.	0.12	0.27
TRU-08	Myrtaceae	Myrcia	mollis	.	2.15	0.11	7.4	18.3	35.8	85.4	1.2	24.6	.	0.03	0.08	0.17
TRU-08	Rosaceae	Prunus	pleiantha	164	1.61	0.09	9.8	15.2	49.0	73.0	0.4	25.3	0.59	0.04	0.14	0.25
TRU-08	Hypericaceae	Vismia	schultesii	125	1.55	0.11	16.5	25.5	67.5	110.6	-0.5	24.3	0.59	0.06	0.21	0.26

TRU-08	<i>Euphorbiaceae</i>	<i>Alchornea</i>	<i>anamariae</i>	133	2.35	0.16	11.4	24.9	52.8	121.9	1.9	24.4	0.86	0.04	0.11	0.25
TRU-08	<i>Sapindaceae</i>	<i>Cupania</i>	<i>rubiginosa</i>	134	2.24	0.13	3.5	10.4	29.0	.	2.0	24.3	0.70	.	0.06	0.21
ESP-01	<i>Clethraceae</i>	<i>Clethra</i>	<i>scabra</i>	143	2.35	0.16	6.2	13.3	57.3	85.3	1.0	25.5	.	0.03	0.12	.
ESP-01	<i>Primulaceae</i>	<i>*Myrsine</i>	<i>coriacea</i>	125	2.29	0.20	6.7	20.7	47.7	.	1.2	26.5	.	.	0.11	.
ESP-01	<i>Rosaceae</i>	<i>Prunus</i>	<i>integrifolia</i>	141	2.86	0.25	6.9	12.7	34.4	.	0.8	26.7	.	.	0.06	.
ESP-01	<i>Myricaceae</i>	<i>Morella</i>	<i>pavonis</i>	115	2.29	0.11	8.5	34.9	64.8	144.1	1.8	27.0	.	0.05	0.13	.
ESP-01	<i>Brunelliaceae</i>	<i>Brunellia</i>	<i>cuzcoensis</i>	129	.	.	5.7	13.2	30.6	57.8	1.3	26.4
ESP-01	<i>Melastomataceae</i>	<i>Miconia</i>	<i>livida</i>	106	.	.	2.7	10.8	30.2	52.1	1.1	25.9
ESP-01	<i>Cunoniaceae</i>	<i>Weinmannia</i>	<i>pubescens</i>	132	1.87	0.15	2.8	20.9	38.8	88.1	1.6	26.6	.	0.04	0.10	.
ESP-01	<i>Primulaceae</i>	<i>*Myrsine</i>	<i>youngii</i>	120	2.27	0.18	6.4	15.4	43.6	32.1	1.5	26.8	.	0.01	0.09	.
ESP-01	<i>Lauraceae</i>	<i>Persea</i>	<i>buchtienii</i>	174	2.74	0.21	6.6	10.5	50.6	73.6	2.3	29.9	.	0.02	0.09	.
ESP-01	<i>Melastomataceae</i>	<i>Miconia</i>	<i>sp</i>	114	1.80	0.17	6.0	26.7	43.4	.	1.2	27.8	.	.	0.11	.
ESP-01	<i>Lauraceae</i>	<i>Cinnamomum</i>	<i>floccosum</i>	215	3.08	0.28	1.9	23.9	44.0	.	2.9	29.7	.	.	0.07	.
ESP-01	<i>Clethraceae</i>	<i>Clethra</i>	<i>sp.</i>	186	2.43	0.17	2.2	11.3	24.6	45.0	1.2	29.0	.	0.01	0.05	.
ESP-01	<i>Isocarpaceae</i>	<i>Citronella</i>	<i>sp.</i>	177	3.29	0.21	2.8	8.4	17.3	37.2	0.9	26.6	.	0.01	0.03	.
ESP-01	<i>Melastomataceae</i>	<i>Miconia</i>	<i>theizans</i>	.	.	.	3.0	12.9	22.3	.	0.8	25.6
ESP-01	<i>Lauraceae</i>	<i>Ocotea</i>	<i>cernua</i>	110	1.69	0.12	2.6	19.2	46.3	.	2.1	24.5	.	.	0.13	.
WAQ-01	<i>Lauraceae</i>	<i>Ocotea</i>	<i>sp6(1674KGC)</i>	134	2.73	0.28	6.1	6.2	25.6	33.3	1.3	29.1	.	0.01	0.04	.
WAQ-01	<i>Araliaceae</i>	<i>Schefflera</i>	<i>sp.</i>	194	2.70	0.22	11.3	14.2	69.7	79.5	1.1	25.6	.	0.02	0.12	.
WAQ-01	<i>Myrsinaceae</i>	<i>Myrsine</i>	<i>coriacea</i>	141	3.36	0.27	4.0	17.9	21.3	.	0.3	28.5	.	.	0.03	.
WAQ-01	<i>Chloranthaceae</i>	<i>Hedyosmum</i>	<i>maximum</i>	130	2.37	0.20	5.4	12.1	28.0	49.3	1.2	28.3	.	0.02	0.06	.
WAQ-01	<i>Melastomataceae</i>	<i>Axinaea</i>	<i>sp.</i>	77	.	.	5.4	24.1	62.0	.	2.6	25.4	.	0.03	.	.
WAQ-01	<i>Escalloniaceae</i>	<i>Escallonia</i>	<i>paniculata</i>	130	2.58	0.27	10.4	25.9	57.9	119.1	1.4	24.7	.	0.04	0.11	.
WAQ-01	<i>Chletracae</i>	<i>Chletra</i>	<i>cuneata</i>	213	3.10	.	6.8	42.8	84.7	171.2	2.7	27.0	.	0.04	0.13	.
WAQ-01	<i>Lauraceae</i>	<i>Cinnamomum</i>	<i>floccosum</i>	141	2.88	0.30	6.8	17.6	48.6	83.1	1.9	27.3	.	0.02	0.08	.
WAQ-01	<i>Podocarpaceae</i>	<i>Podocarpus</i>	<i>oleifolius</i>	169	2.29	0.22	3.4	13.9	27.0	.	1.1	24.3	.	.	0.06	.
WAQ-01	<i>Melastomataceae</i>	<i>Miconia</i>	<i>coelestis</i>	139	1.90	0.14	3.1	15.1	29.3	57.5	0.4	27.4	.	0.02	0.07	.
WAQ-01	<i>Rubiaceae</i>	<i>Cinchona</i>	<i>officinalis</i>	87	2.30	0.15	5.3	25.2	43.4	.	-0.1	26.9	.	.	0.09	.
WAQ-01	<i>Styracaceae</i>	<i>Styrax</i>	<i>foveolaria</i>	242	3.20	0.23	5.3	17.1	57.6	84.1	1.1	24.8	.	0.02	0.09	.
WAQ-01	<i>Lauraceae</i>	<i>Persea</i>	<i>sp.</i>	147	2.76	0.27	6.0	18.3	46.3	.	1.3	27.0	.	.	0.08	.
TRU-03	<i>Cunoniaceae</i>	<i>Weinmannia</i>	<i>auriculata</i>	119	1.60	0.14	2.5	10.6	34.1	53.9	0.9	23.8	0.59	0.03	0.10	0.25
TRU-03	<i>Cardiopteridaceae</i>	<i>Citronella</i>	<i>incarnum</i>	157	.	0.25	8.7	35.2	71.7	169.2	1.8	24.0	.	0.03	.	.
TRU-03	<i>Lauraceae</i>	<i>Persea</i>	<i>corymbosa</i>	213	3.07	0.24	6.2	17.8	50.9	86.9	2.6	25.2	1.24	0.02	0.08	0.28
TRU-03	<i>Primulaceae</i>	<i>Myrsine</i>	<i>sp.</i>	128	2.67	0.23	6.4	28.3	84.0	.	1.3	22.3	0.79	.	0.15	0.20

TRU-03	<i>Araliaceae</i>	<i>Schefflera</i>	<i>allicotantha</i>	162	1.87	0.22	13.1	17.8	42.6	.	-0.5	22.7	0.48	.	0.11	0.17
TRU-03	unidentified	unidentified	unidentified	83	1.65	0.20	4.0	10.1	26.3	57.3	1.6	22.5	.	0.03	0.08	.
TRU-03	<i>Aquifoliaceae</i>	<i>Ilex</i>	<i>biserrulata</i>	203	2.51	0.18	4.3	23.9	58.4	.	1.7	23.0	0.35	.	0.11	0.10
TRU-03	<i>Clethraceae</i>	<i>Clethra</i>	<i>cuneata</i>	215	2.55	0.26	8.8	31.8	73.1	161.7	1.3	22.6	0.95	0.05	0.14	0.26
TRU-03	<i>Aquifoliaceae</i>	<i>Ilex</i>	<i>sessiliflora</i>	197	2.15	0.19	9.1	35.6	72.5	.	1.4	22.7	0.36	.	0.16	0.12
TRU-03	<i>Primulaceae</i>	<i>Myrsine</i>	<i>coriacea</i>	148	2.35	0.20	8.1	31.3	74.2	156.7	1.2	23.5	0.57	0.05	0.15	0.17
TRU-03	<i>Clethraceae</i>	<i>Clethra</i>	<i>sp.</i>	198	2.23	0.24	8.8	34.5	90.2	176.4	1.5	22.8	0.37	0.06	0.19	0.11
TRU-03	<i>Pentaphylacaceae</i>	<i>Freziera</i>	<i>karsteniana</i>	161	2.43	.	13.5	33.2	76.9	167.9	0.7	22.4	0.42	0.05	0.15	0.12
TRU-03	<i>Lauraceae</i>	<i>Persea</i>	<i>buchtienii</i>	146	1.82	0.16	9.1	17.4	37.4	.	0.0	22.4	0.43	.	0.10	0.16
TRU-01	<i>Melastomataceae</i>	<i>Miconia</i>	<i>cf. denticulata</i>	135	2.18	0.18	7.2	23.6	43.8	.	0.7	24.8	1.25	.	0.10	0.39
TRU-01	<i>Primulaceae</i>	<i>Myrsine</i>	<i>andina</i>	120	2.27	0.21	.	.	59.1	.	1.4	24.2	.	.	0.12	.
TRU-01	<i>Melastomataceae</i>	<i>Miconia</i>	<i>setulosa</i>	133	2.39	0.23	9.2	24.0	76.4	131.0	1.2	25.4	0.69	0.04	0.15	0.20
TRU-01	<i>Melastomataceae</i>	<i>Miconia</i>	<i>media</i>	145	2.75	0.20	5.9	26.7	55.4	.	1.8	22.8	.	.	0.10	.
TRU-01	<i>Asteraceae</i>	<i>Senecio</i>	<i>sp</i>	93	2.44	.	10.1	40.6	95.8	.	1.9	22.8	.	.	0.19	.
TRU-01	<i>Symplocaceae</i>	<i>Symplocos</i>	<i>psiloclada</i>	234	2.37	0.16	5.9	20.2	47.6	.	0.8	21.8	0.72	.	0.10	0.21
TRU-01	<i>Melastomataceae</i>	<i>Miconia</i>	<i>atrofusca</i>	155	2.93	0.19	10.9	39.9	85.3	.	1.0	22.6	.	.	0.14	.
TRU-01	<i>Clethraceae</i>	<i>*Clethra</i>	<i>cuneata</i>	227	2.74	0.27	10.9	31.0	81.6	156.9	1.1	22.4	.	0.05	0.14	.
TRU-01	<i>Cunoniaceae</i>	<i>Weinmannia</i>	<i>microphylla</i>	75	.	.	4.3	32.0	64.8	.	3.3	23.4
TRU-01	<i>Aquifoliaceae</i>	<i>Ilex</i>	<i>sessiliflora</i>	171	.	.	9.5	30.4	71.1	.	1.1	23.5	0.74	.	.	.
TRU-01	<i>Symplocaceae</i>	<i>Symplocos</i>	<i>quitensis</i>	174	.	.	11.6	33.2	62.5	.	0.5	22.5	0.78	.	.	.
TRU-01	<i>Lauraceae</i>	<i>Persea</i>	<i>ferruginea</i>	.	.	.	7.9	22.0	51.7	.	0.7	23.3
TRU-01	<i>Melastomataceae</i>	<i>Miconia</i>	<i>sp.</i>	128	.	.	3.9	15.0	48.0	95.6	0.9	22.0
TRU-01	<i>Brunelliaceae</i>	<i>*Brunellia</i>	<i>inermis</i>	122	.	.	4.3	14.1	26.8	.	1.1	21.8	0.68	.	.	.

Table S2. Pearson correlations for bivariate relationships among leaf traits and environmental parameters. Number of replicates is given in bracket. Abbreviations: N_a = leaf nitrogen, P_a = leaf phosphorus, leaf N:P = leaf nitrogen to phosphorus ratio, M_a = leaf mass per unit leaf area, Chl = chlorophyll a and b content, $V_{cmax,a}^{25}$ = maximum carboxylation velocity of Rubisco normalised to 25°C, $J_{max,a}^{25}$ = maximum rate of electron transport normalised to 25°C, $V_{N,25}$ = ratio of maximum carboxylation velocity of Rubisco normalised to 25°C over leaf nitrogen, Soil P=soil phosphorus, Soil N=soil nitrogen, MAT = mean annual temperature, MAP = mean annual precipitation. Environmental parameters at each site were obtained using site information from Quesada *et al.* 2010; pers. comm. 2014) and Asner *et al.* (2014a). Note that the coefficient of determination, r^2 , equals the square of the Pearson correlation coefficient.

	N_a	P_a	Leaf N:P	M_a	Chl	$V_{cmax,a}^{25}$	$J_{max,a}^{25}$	$V_{cmax,N}^{25}$	Soil P	Soil N	Elevation	MAT	MAP
N_a (g m ⁻²)	1 (248)	0.613** (240)	-0.208** (232)	0.353** (246)	0.370** (171)	0.226** (246)	0.227** (184)	-0.297** (242)	0.356** (248)	0.319** (248)	0.368** (248)	-0.375** (248)	-0.041 (248)
P_a (g m ⁻²)		1 (248)	-0.769** (227)	0.188** (246)	0.229** (170)	0.331** (241)	0.366** (186)	-0.013 (234)	0.611** (248)	0.623** (248)	0.694** (248)	-0.711** (248)	-0.004 (248)
Leaf N:P			1 (245)	-0.085 (232)	-0.047 (159)	-0.280** (243)	-0.244** (177)	-0.157* (227)	-0.476** (245)	-0.512** (245)	-0.539** (245)	0.551** (245)	-0.020 (245)
M_a (g m ⁻²)				1 (274)	0.157* (185)	0.077 (272)	0.196** (199)	-0.095 (240)	-0.029 (274)	0.195** (274)	0.194** (274)	-0.162** (274)	-0.111 (274)
Chl (g m ⁻²)					1 (185)	-0.001 (183)	0.085 (133)	-0.109 (166)	0.285** (185)	0.153* (185)	0.145* (185)	-0.151* (185)	0.239** (185)
$V_{cmax,a}^{25}$ (μmol m ⁻² s ⁻¹)						1 (283)	0.840** (209)	0.810** (242)	0.287** (290)	0.354** (290)	0.384** (283)	-0.399** (283)	-0.070 (283)
$J_{max,a}^{25}$ (μmol m ⁻² s ⁻¹)							1 (209)	0.629** (182)	0.373** (209)	0.475** (209)	0.461** (209)	-0.462** (209)	0.152* (209)
$V_{cmax,N}^{25}$ (μmol gN ⁻¹ s ⁻¹)								1 (242)	0.143* (242)	0.201** (242)	0.186** (242)	-0.198** (242)	0.028 (242)
Soil P (mg kg ⁻¹)									1 (292)	0.681** (292)	0.716** (292)	-0.720** (292)	0.380** (292)
Soil N (g kg ⁻¹)										1 (292)	0.921** (292)	-0.902** (292)	0.104 (292)
Elevation (m a.s.l.)											1 (292)	-0.992** (292)	-0.068 (292)
MAT (°C)												1 (292)	0.070 (292)
MAP (mm)													1 (292)

** Correlation is significant at $p < 0.01$

* Correlation is significant at $p < 0.05$

Table S3: Standardized major axis regression slopes and their confidence intervals for log-log transformed relationships comparing leaf traits of lowland (~173 species) and upland (~120 species) species, depicted in Figures 2, 4 and 5 in the main text. Analysis undertaken using individual replicates. Coefficients of determination (r^2) and significance values (p) of each bivariate relationship are shown. Significantly different p values are shown in bold. 95% confidence intervals (CI) of SMA slopes and y-axis intercepts are shown in parentheses. Where SMA tests for common slopes revealed no significant differences between the two groups (i.e. $p > 0.05$), common slopes were used (with CI of the common slopes provided). Where there was a significant difference in the elevation (i.e. y-axis intercept) of the common-slope SMA regressions, values for the y-axis intercept are provided. Where appropriate, significant shifts along a common slope are indicated.

Bivariate relationship (y- vs. x-axis)	Group	r^2	p	Slope	Slope CI	Intercept	p	Common slope	Common slope CI	p	Common slope y-axis intercept	Shift along a common slope?
N_a vs. M_a	Lowland	0.069	0.001	1.027	(0.879, 1.199)	-1.889	0.003					
	Upland	0.198	<0.001	0.709	(0.593, 0.848)	-1.165						
P_a vs. M_a	Lowland	<0.001	0.985	-2.096	(-2.463, -1.784)	3.323	0.002					
	Upland	0.038	0.034	1.345	(1.104, 1.639)	-3.661						
$V_{cmax,a}^{25}$ vs. M_a	Lowland	0.003	0.468	-1.753	(-2.054, -1.495)	5.183	0.595	1.705	(1.511, 1.925)	0.010	-2.089	Yes, $p < 0.001$
	Upland	0.014	0.212	1.642	(1.362, 1.981)	-1.863					-1.999	
$V_{cmax,a}^{25}$ vs. N_a	Lowland	0.024	0.050	1.707	(1.454, 2.005)	1.022	0.014					
	Upland	0.003	0.613	2.384	(1.950, 2.914)	0.801						
$V_{cmax,a}^{25}$ vs. P_a	Lowland	0.041	0.013	0.841	(0.717, 0.986)	2.417	0.003					
	Upland	0.005	0.502	1.231	(1.003, 1.511)	2.602						
$V_{cmax,a}^{25}$ vs. leaf N:P	Lowland	0.002	0.563	-1.246	(-1.468, -1.057)	3.136	0.028					
	Upland	0.027	0.113	-1.657	(-2.030, -1.353)	3.494						
$J_{max,a}^{25}$ vs. M_a	Lowland	0.004	0.473	1.136	(0.956, 1.349)	-0.577	0.022					
	Upland	0.005	0.552	1.620	(1.268, 2.069)	-1.533						
$J_{max,a}^{25}$ vs. N_a	Lowland	0.050	0.012	1.046	(0.881, 1.242)	1.518	0.001					
	Upland	0.001	0.794	-2.224	(-2.897, -1.707)	2.736						
$J_{max,a}^{25}$ vs. P_a	Lowland	0.077	0.002	0.5113	(0.432, 0.605)	2.368	0.001					
	Upland	0.029	0.205	-1.101	(-1.432, -0.846)	1.086						
$J_{max,a}^{25}$ vs. leaf N:P	Lowland	<0.001	0.888	-0.813	(-0.974, -0.679)	2.876	0.003					
	Upland	<0.001	0.930	-1.378	(-1.800, -1.055)	3.493						
$V_{cmax,N}^{25}$ vs. M_a	Lowland	0.044	0.010	-1.841	(-2.157, -1.570)	5.092	0.789	-1.866	(-1.647, -2.114)	<0.001	5.146	No, $P = 0.809$
	Upland	0.010	0.327	-1.908	(-2.336, -1.559)	5.385					5.295	
$V_{cmax,N}^{25}$ vs. P_a	Lowland	0.012	0.195	-0.890	(-1.048, -0.756)	0.239	0.004					
	Upland	0.030	0.101	-1.301	(-1.599, -1.059)	0.275						
$V_{cmax,N}^{25}$ vs. leaf N:P	Lowland	0.003	0.536	-1.307	(-1.548, -1.103)	2.945	0.057	-1.455	(-1.455, -1.274)	<0.001	3.141	Yes, $p < 0.001$
	Upland	0.020	0.185	-1.709	(-2.105, -1.388)	3.185					2.903	
$J_{max,a}^{25}$ vs. $V_{cmax,a}^{25}$ (not log-transformed)	Lowland	0.590	<0.001	1.341	(1.204, 1.439)	15.81	0.001					
	Upland	0.748	<0.001	1.962	(1.736, 2.217)	-4.803						

Table S4: Means \pm standard deviation of leaf physiology and chemistry, expressed on area basis for each site. Leaf traits are sorted according to decreasing leaf N:P for lowland sites and increasing elevation for upland sites.

Abbreviations: $A_{400,a}$ light-saturated net photosynthesis measured under 400 $\mu\text{mol mol}^{-1}$ atmospheric $[\text{CO}_2]$; C_{i400} , intercellular CO_2 partial pressure at 400 $\mu\text{mol mol}^{-1}$ atmospheric $[\text{CO}_2]$; C_{a400} , atmospheric CO_2 partial pressure at 400 $\mu\text{mol mol}^{-1}$ atmospheric $[\text{CO}_2]$; $C_{i400}:C_{a400}$, ratio of intercellular to atmospheric CO_2 at 400 $\mu\text{mol mol}^{-1}$ $[\text{CO}_2]$; $A_{400:N}$, ratio of light-saturated net photosynthesis measured under 400 $\mu\text{mol mol}^{-1}$ atmospheric $[\text{CO}_2]$ over leaf N; $A_{2000,a}$, light-saturated net photosynthesis measured under 2000 $\mu\text{mol mol}^{-1}$ atmospheric $[\text{CO}_2]$; C_{i2000} , intercellular CO_2 at 2000 $\mu\text{mol mol}^{-1}$ atmospheric $[\text{CO}_2]$; $A_{2000:N}$, ratio of light-saturated net photosynthesis measured under 2000 $\mu\text{mol mol}^{-1}$ atmospheric $[\text{CO}_2]$ over leaf N; R_d , leaf dark respiration measured at 400 $\mu\text{mol mol}^{-1}$ atmospheric $[\text{CO}_2]$; Leaf T , leaf temperature inside gas exchange cuvette; Chl, chlorophyll a and b content.

	Sites	$A_{400,a}$ ($\mu\text{mol m}^{-2} \text{s}^{-1}$)	C_{i400} (Pa)	C_{a400} (Pa)	$C_{i400}:C_{a400}$	$A_{400:N}$ ($\mu\text{mol gN}^{-1} \text{s}^{-1}$)	$A_{2000,a}$ ($\mu\text{mol m}^{-2} \text{s}^{-1}$)	C_{i2000} (Pa)	$A_{2000:N}$ ($\mu\text{mol gN}^{-1} \text{s}^{-1}$)	R_{light} ($\mu\text{mol m}^{-2} \text{s}^{-1}$)	Leaf T ($^{\circ}\text{C}$)	Chl (g m^{-2})
Lowland	SUC-05	8.8 \pm 4.5	28.9 \pm 2.9	38.5 \pm 0.7	0.75 \pm 0.08	4.6 \pm 2.5	20.9 \pm 6.1	156.5 \pm 21.8	11.9 \pm 5.1	1.2 \pm 0.5	28.8 \pm 0.5	0.73 \pm 0.21
	TAM-05	9.5 \pm 2.7	25.3 \pm 2.6	38.0 \pm 0.5	0.67 \pm 0.06	4.8 \pm 1.7	22.2 \pm 3.6	147.5 \pm 21.1	10.9 \pm 2.1	0.7 \pm 0.6	30.2 \pm 0.7	
	JEN-11	7.3 \pm 3.7	31.4 \pm 2.9	38.9 \pm 0.6	0.81 \pm 0.07	4.1 \pm 2.3	17.4 \pm 7.5	171.7 \pm 14.2	8.3 \pm 3.9	1.1 \pm 0.6	28.8 \pm 0.4	0.69 \pm 0.30
	ALP-01	7.5 \pm 4.4	27.2 \pm 3.4	39.2 \pm 0.4	0.69 \pm 0.09	3.9 \pm 2.4	17.4 \pm 6.1	146.5 \pm 20.4	8.7 \pm 3.0	0.7 \pm 0.6	29.9 \pm 0.6	0.58 \pm 0.15
	SUC-01	7.8 \pm 4.7	29.2 \pm 4.3	38.9 \pm 0.6	0.77 \pm 0.08	3.8 \pm 2.3	19.6 \pm 6.2	157.4 \pm 21.2	10.5 \pm 3.4	1.1 \pm 0.8	29.5 \pm 1.0	0.64 \pm 0.19
	JEN-12	8.5 \pm 4.4	30.5 \pm 2.8	38.9 \pm 0.5	0.78 \pm 0.07	4.5 \pm 2.3	19.9 \pm 6.8	161.5 \pm 24.8	10.3 \pm 3.1	1.0 \pm 0.8	28.8 \pm 0.4	0.57 \pm 0.15
	ALP-03	6.7 \pm 3.2	30.2 \pm 2.5	39.2 \pm 0.4	0.77 \pm 0.07	4.3 \pm 2.4	16.1 \pm 6.2	165.3 \pm 14.0	10.0 \pm 3.8	1.0 \pm 0.4	29.1 \pm 0.6	0.54 \pm 0.13
	CUZ-03	8.3 \pm 3.4	25.5 \pm 3.3	37.8 \pm 0.5	0.67 \pm 0.08	4.7 \pm 2.2	19.2 \pm 5.7	147.6 \pm 24.0	10.8 \pm 3.9	0.9 \pm 0.4	29.9 \pm 0.5	
	ALP-04	7.2 \pm 3.7	25.4 \pm 3.1	39.1 \pm 0.3	0.65 \pm 0.08	4.0 \pm 2.3	18.3 \pm 4.5	129.7 \pm 27.8	10.7 \pm 3.9	1.3 \pm 0.8	30.9 \pm 0.8	0.62 \pm 0.14
	TAM-09	11.2 \pm 2.3	26.5 \pm 2.7	37.2 \pm 0.5	0.71 \pm 0.07	5.5 \pm 1.8	20.9 \pm 5.4	153.6 \pm 18.6	10.2 \pm 2.6	0.6 \pm 0.4	29.1 \pm 1.2	
Lowland mean	TAM-06	9.4 \pm 3.5	26.7 \pm 3.6	38.0 \pm 0.6	0.70 \pm 0.09	4.0 \pm 1.7	22.6 \pm 3.6	150.3 \pm 21.5	9.1 \pm 2.1	0.6 \pm 1.0	29.9 \pm 0.6	
		8.2 \pm 3.9^a	28.4 \pm 3.7^a	38.6 \pm 0.8^a	0.74 \pm 0.09^a	4.3 \pm 2.2^a	19.2 \pm 6.1^a	155.2 \pm 22.7^a	10.1 \pm 3.6^a	1.0 \pm 0.7^a	29.4 \pm 0.9^a	0.62 \pm 0.17^a
Upland	SPD-02	8.4 \pm 2.7	21.0 \pm 1.9	32.2 \pm 0.3	0.65 \pm 0.06	3.9 \pm 1.4	25.3 \pm 9.7	89.3 17.1	11.3 \pm 5.2	1.0 \pm 1.5	27.2 \pm 0.5	0.78 \pm 0.30
	SPD-01	8.6 \pm 5.0	20.4 \pm 2.4	33.2 \pm 0.6	0.61 \pm 0.07	3.8 \pm 2.2	23.0 \pm 8.6	95.2 16.5	10.5 \pm 4.4	0.1 \pm 0.8	27.3 \pm 1.0	0.72 \pm 0.23
	TRU-08	9.0 \pm 3.7	20.4 \pm 3.0	32.0 \pm 0.5	0.64 \pm 0.10	4.1 \pm 1.7	19.9 \pm 7.0	90.4 20.4	10.6 \pm 3.8	1.1 \pm 0.8	24.5 \pm 0.5	0.59 \pm 0.16
	ESP-01	4.9 \pm 2.9	16.7 \pm 2.4	28.5 \pm 0.3	0.58 \pm 0.09	2.3 \pm 1.4	17.1 \pm 7.7	55.1 11.9	8.1 \pm 4.4	1.4 \pm 0.6	26.9 \pm 1.7	
	WAQ-01	6.1 \pm 2.4	16.5 \pm 2.2	27.9 \pm 0.4	0.59 \pm 0.08	2.3 \pm 0.9	19.3 \pm 8.9	58.0 17.9	7.1 \pm 3.1	1.2 \pm 0.8	26.6 \pm 1.6	
	TRU-03	7.9 \pm 3.2	17.6 \pm 2.3	27.7 \pm 0.3	0.63 \pm 0.08	3.6 \pm 1.7	25.2 \pm 9.4	65.3 12.6	10.8 \pm 3.6	1.2 \pm 0.8	23.1 \pm 0.8	0.60 \pm 0.29
	TRU-01	7.8 \pm 3.1	17.1 \pm 2.1	26.3 \pm 0.3	0.65 \pm 0.08	3.5 \pm 1.2	26.5 \pm 8.6	58.8 11.7	11.5 \pm 2.6	1.3 \pm 0.7	23.0 \pm 1.1	0.81 \pm 0.22
Upland mean		7.6 \pm 3.6^a	18.8 \pm 3.0^b	30.1 \pm 2.6^b	0.62 \pm 0.08^b	3.4 \pm 1.7^b	22.3 \pm 8.9^b	75.8 \pm 22.8^b	10.0 \pm 4.3^a	1.0 \pm 1.0^a	25.7 \pm 2.1^b	0.69 \pm 0.25^b

Table S5: Standardized major axis regression slopes and their confidence intervals for relationships comparing leaf traits of lowland (~126 species) and upland (~40 species) species, depicted in Figures 7 and S2 in the main text. Analysis undertaken using individual replicates. Coefficients of determination (r^2) and significance values (p) of each bivariate relationship are shown. Significantly different p values are shown in bold. 95% confidence intervals (CI) of SMA slopes and y-axis intercepts are shown in parentheses. Where SMA tests for common slopes revealed no significant differences between the two groups (i.e. $p > 0.05$), common slopes were used (with CI of the common slopes provided). Where there was a significant difference in the elevation (i.e. y-axis intercept) of the common-slope SMA regressions, values for the y-axis intercept are provided. Where appropriate, significant shifts along a common slope are indicated.

Bivariate relationship (y- vs. x-axis)	Group	r^2	p	Slope	Slope CI	Intercept	p	Common slope	Common slope CI	p	Common slope y-axis intercept	Shift along a common slope?
n_P vs. M_a	Lowland	0.012	0.258	-0.2421	(-0.292, -0.201)	57.02	0.072	-0.2172	(-0.187, -0.253)	0.698	53.600	No, $p = 0.185$
	Upland	0.002	0.719	-0.1797	(-0.231, -0.134)	47.64					52.945	
n_R vs. M_a	Lowland	0.042	0.011	-0.1217	(-0.143, -0.104)	24.841	0.482	-0.1176	(-0.104, -0.133)	<0.001	24.303	No, $p = 0.794$
	Upland	0.001	0.809	0.1110	(0.090, 0.137)	-5.861					27.171	
n_E vs. M_a	Lowland	0.023	0.087	-0.0279	(-0.033, -0.023)	6.362	0.249	-0.0296	(-0.026, -0.034)	<0.001	6.579	No, $p = 0.227$
	Upland	0.001	0.870	-0.0339	(-0.045, -0.026)	8.240					7.605	
n_P vs. N_a	Lowland	0.358	<0.001	-16.52	(-19.23, -14.18)	55.21	0.711	-16.76	(-14.73, -19.08)	0.017	55.676	Yes, $p < 0.001$
	Upland	0.001	0.773	-17.43	(-22.36, -13.59)	60.53					59.063	
n_R vs. N_a	Lowland	0.171	<0.001	-7.876	(-9.127, -6.797)	24.29	0.101	-8.499	(-7.544, -9.564)	<0.001	25.515	No, $p = 0.065$
	Upland	0.094	0.003	-9.725	(-11.842, -7.987)	32.64					29.802	
n_E vs. N_a	Lowland	0.382	<0.001	-1.732	(-1.992, -1.506)	6.156	0.001					
	Upland	0.165	0.002	-3.039	(-3.889, -2.374)	10.278						
n_P vs. P_a	Lowland	0.154	<0.001	-225.4	(-268.6, -189.2)	42.22	0.002					
	Upland	0.028	0.186	-129.5	(-165.9, -101.1)	43.04						
n_R vs. P_a	Lowland	0.013	0.175	-90.48	(-106.4, -76.96)	17.23	0.167	-84.48	(-74.36, -96.08)	<0.001	16.677	Yes, $p < 0.001$
	Upland	0.030	0.106	-75.48	(92.97, -61.28)	23.26					24.851	
n_E vs. P_a	Lowland	0.050	0.013	-19.99	(-23.79, -16.80)	4.635	0.568	-20.60	-17.84 -23.75	<0.001	4.692	Yes, $p = 0.001$
	Upland	0.155	0.003	-21.89	(-28.19, -16.99)	7.047					6.824	
n_A vs. M_a (log-transformed)	Lowland	0.070	0.003	-1.2405	(-1.471, -1.046)	2.143	0.085	-1.152	(-0.992, -1.345)	0.025	1.958	No, $p = 0.742$
	Upland	0.002	0.794	-0.8934	(-1.233, -0.647)	1.475					2.026	
n_A vs. N_a (log-transformed)	Lowland	0.445	<0.001	-1.078	(-1.231, -0.945)	-0.159	0.099	-1.129	(-0.999, -1.273)	<0.001	-0.145	No, $p = 0.189$
	Upland	0.156	0.011	-1.403	(-1.881, -1.046)	0.037					-0.054	
n_A vs. P_a (log-transformed)	Lowland	0.056	0.008	-0.556	(-0.661, -0.468)	-1.065	0.446	-0.576	(-0.495, -0.670)	<0.001	-1.086	Yes, $p < 0.001$
	Upland	0.100	0.047	-0.640	(-0.869, -0.471)	-0.957					-0.904	

Table S6: Stepwise selection process for the fixed component of linear mixed effect models: with $V_{\text{cmax},a}^{25}$ and $J_{\text{max},a}^{25}$ as the response variables. Continuous explanatory variables are N_a , P_a , M_a , total soil P and N, MAT and effective cation exchange capacity of soil. Given the large number of species in our dataset, we treated phylogeny as a random component within the model construct and so focused on phylogenetic variation rather than individual species mean values. Because of low replication at the species level, a simple random term of Family was found to perform just as well as the fully nested Family/Genus/Species. In choosing explanatory terms for the model's fixed component, we began by adopting a beyond-optimal model including those continuous variables suggested by our starting hypotheses, initial data exploration, and with care to avoid problems of collinearity - a limited number of two-way interactions were included (specifically N:P). A backward, stepwise selection process adopted the Maximum Likelihood method; the model's random component was held constant through these iterations. The effect of dropping sequential terms was tested by comparing the nested model variants. The model's random component was identical in all variants. Test parameters and statistics are DF (degrees of freedom), AIC (Akaike Information Criterion), BIC (Bayesian Information Criterion) and -2LL (-2 restricted Log Likelihood). The effect of dropping sequential terms was tested by comparing the nested model variants. The best predictive model, underlined, was selected based on a combination of low criteria score and simplicity, considering two-way interactions only. Because our final preferred model, arrived at by backward selection, was so parsimonious, we then tested the effect of adding selected terms and interactions not previously included - in no case did those additional terms improve model performance. For the J_{max} model, it was not thought necessary to include site average terms for leaf N and P, since those terms had proved so marginal in the equivalent V_{cmax} model selection steps.

Model	Fixed component	DF	AIC	BIC	-2LL
$V_{\text{cmax},a}^{25}$					
1	$\log_{10}(\text{Soil P}) + N_a + \text{Site}.N_a + P_a + \text{Site}.P_a + N_a.P_a$	9	1663.5	1693.1	-822.7
2	$\log_{10}(\text{Soil P}) + N_a + \text{Site}.N_a + P_a + \text{Site}.P_a + \log_{10}(\text{Soil P}).N_a$	9	1664.0	1693.7	-823.0
3	$\log_{10}(\text{Soil P}) + N_a + \text{Site}.N_a + P_a + \text{Site}.P_a$	8	1663.2	1689.6	-823.6
4	$\log_{10}(\text{Soil P}) + N_a + \text{Site}.N_a + P_a$	7	1661.4	1684.4	-823.7
5	$\log_{10}(\text{Soil P}) + N_a + P_a$	6	1661.5	1681.3	-824.7
6	<u>$\log_{10}(\text{Soil P}) + P_a$</u>	<u>5</u>	<u>1659.7</u>	<u>1676.1</u>	<u>-824.8</u>
7	$\log_{10}(\text{Soil P}) + P_a + \text{MAT} + P_a:\text{MAT}$	7	1663.1	1686.1	-824.5
8	$\log_{10}(\text{Soil P}) + P_a + \text{MAT}$	6	1661.1	1680.9	-824.6
9	$\log_{10}(\text{Soil P}) + P_a + \text{Soil N}$	6	1658.9	1678.6	-823.4
10	$\log_{10}(\text{Soil P}) + P_a + \text{ECEC}$	6	1657.5	1677.2	-822.7
11	$\log_{10}(\text{Soil P}) + P_a + M_a$	6	1660.8	1680.5	-824.4
$J_{\text{max},a}^{25}$					
1	$\log_{10}(\text{Soil P}) + P_a + N_a + M_a + \text{MAT} + N_a.P_a$	9	1361.1	1388.0	-671.5
2	$\log_{10}(\text{Soil P}) + P_a + N_a + M_a + \text{MAT} + \log_{10}(\text{Soil P}).N_a$	9	1358.7	1385.7	-670.4
3	$\log_{10}(\text{Soil P}) + P_a + N_a + M_a + \text{MAT}$	8	1360.3	1384.3	-672.2
4	$\log_{10}(\text{Soil P}) + P_a + M_a + \text{MAT}$	7	1358.3	1379.3	-672.2
5	$\log_{10}(\text{Soil P}) + P_a + M_a$	6	1357.3	1375.3	-672.6
6	<u>$\log_{10}(\text{Soil P}) + P_a$</u>	<u>5</u>	<u>1359.9</u>	<u>1374.9</u>	<u>-674.9</u>
7	$\log_{10}(\text{Soil P})$	4	1363.4	1375.4	-677.7

Abbreviations: N_a = leaf nitrogen, P_a = leaf phosphorus, M_a = leaf mass per unit leaf area, Soil P = soil phosphorus, Soil N = soil nitrogen, MAT = mean annual temperature, ECEC = effective cation exchange capacity of soil. Environmental parameters at each site were obtained using site information from Quesada (*et al.* 2010; pers. comm. 2014), Asner *et al.* (2014a) and Malhi *et al.* (in prep.).

Table S7: Comparison of mean values of V_{cmax} and J_{max} at 25°C values ($V_{\text{cmax}25}$ and $J_{\text{max}25}$, respectively) in upland and lowland plants calculated using different activation energies (E_a) for each parameter (i.e. V_{cmax} and J_{max}), and K_c and K_o constants when calculating V_{cmax} . Here, we compare values calculated using E_a values reported by Farquhar *et al.* (1980) and Bernacchi *et al.* (2002). For Farquhar *et al.* (1980), E_a values of K_c and K_o used were 59.4 and 36.0 kJ mol⁻¹, respectively. For Bernacchi *et al.* (2002), the E_a values of K_c and K_o were 80.99 and 23.72 kJ mol⁻¹. For calculations made using Farquhar *et al.* (1980), we used E_a values for V_{cmax} and J_{max} of 64.8 and 37.0 kJ mol⁻¹, respectively; for Bernacchi *et al.* (2002), the E_a values for V_{cmax} and J_{max} were 65.3 and 43.9 kJ mol⁻¹, respectively. Values are overall mean \pm SD of leaf traits for lowland and upland sites. Significantly different means are indicated by different letters ($p < 0.05$).

Source of constants		$V_{\text{cmax},a}^{25}$ ($\mu\text{mol m}^{-2} \text{s}^{-1}$)	$J_{\text{max},a}^{25}$ ($\mu\text{mol m}^{-2} \text{s}^{-1}$)
Farquhar et al. (1980)	Lowland species	35.9 \pm 14.6 ^a	66.7 \pm 18.6 ^a
	Upland species	48.8 \pm 20.0 ^b	96.9 \pm 36.9 ^b
Bernacchi et al. (2002)	Lowland species	39.7 \pm 15.6 ^a	64.7 \pm 18.6 ^a
	Upland species	50.5 \pm 18.5 ^b	96.6 \pm 37.3 ^b

Figure S1: Plots of maximum carboxylation velocity of Rubisco normalised to 25°C, $V_{\text{cmax},a}^{25}$ against (A) mean annual temperature (MAT) and (F) soil P concentration; maximum rate of electron transport normalised to 25°C, $J_{\text{max},a}^{25}$ against (B) MAT and (G) soil P; ratio of $V_{\text{cmax},a}^{25}$ over leaf N, $V_{\text{cmax},a}^{25}/N$ against (C) MAT and (H) soil P; ratio of light-saturated net photosynthesis measured at 400 $\mu\text{mol mol}^{-1}$ atmospheric $[\text{CO}_2]$ over leaf N, A_{400}/N against (D) MAT and (I) soil P; and ratio of light-saturated net photosynthesis measured at 2000 $\mu\text{mol mol}^{-1}$ atmospheric $[\text{CO}_2]$ over leaf N, A_{2000}/N against (E) MAT and (J) soil P for each site. In (A)-(H), black circles (and solid regression lines) represent photosynthetic parameters calculated using constants of Farquhar *et al.* (1980) and grey circles (and dashed regression lines) represent parameters calculated using Bernacchi *et al.* constants (2002). R^2 values shown are for Farquhar *et al.* (1980) only regressions. Environmental parameters at each site were obtained using site information from Quesada (*et al.* 2010; pers. comm. 2014) and Asner *et al.* (2014a).

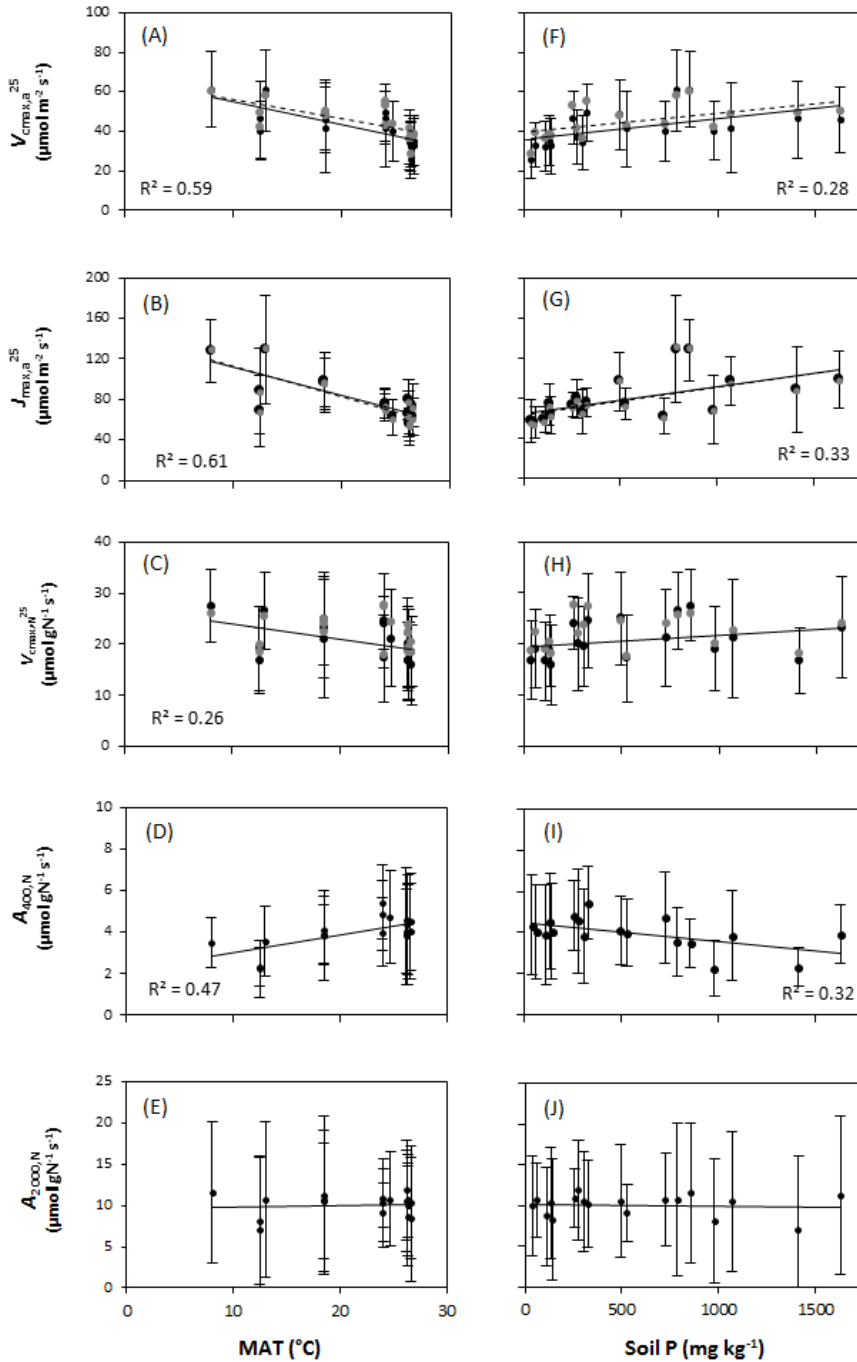


Figure S2: Plots of % of leaf N to pigment-protein complexes, n_P , % of leaf N to Rubisco, n_R , and % of leaf N to electron transport, n_E , in relation to (A) leaf mass per unit leaf area, M_a , (B) leaf N-area, N_a , and (C) leaf P-area, P_a . Data points represent individual leaf values (150 lowland species and 92 upland species).

SMA regressions: solid line, lowland species; dashed line, upland species. SMA regressions are given only when the relationships are significant ($p < 0.05$) and when lowland and upland shared similar slopes, refer to Table S5. Analyses were performed on percentage instead of fraction of N to meet the requirement of SMA analyses.

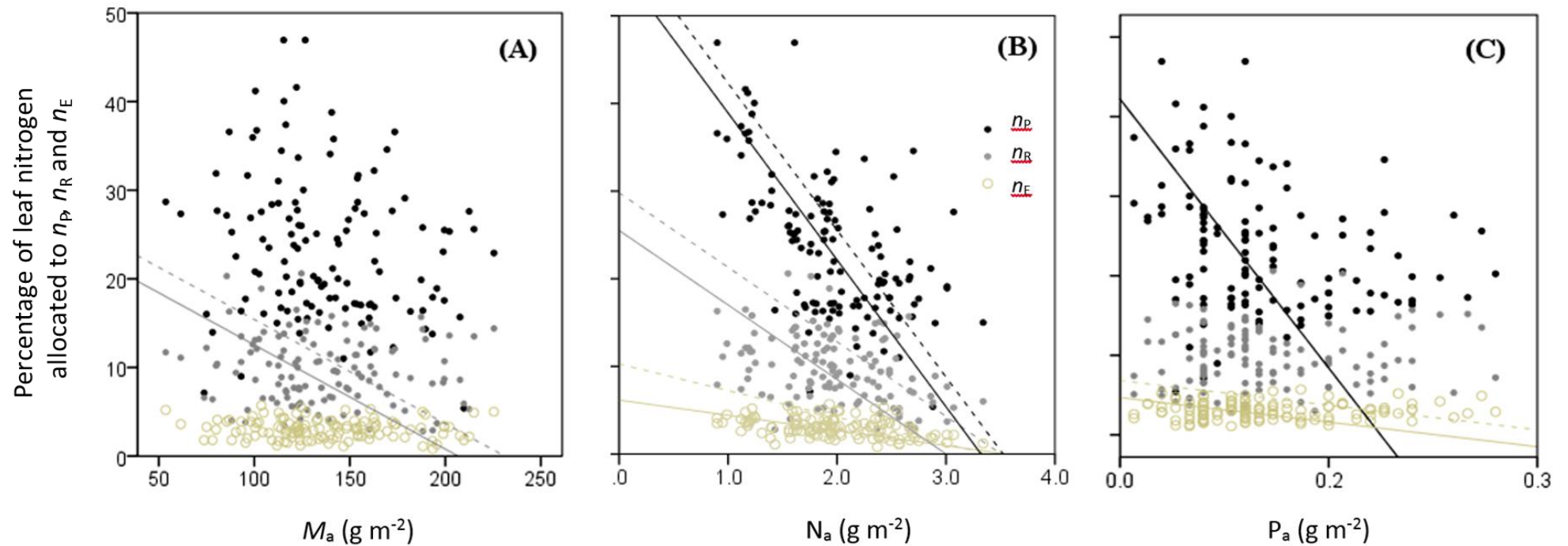


Figure S3: Plots of fraction of leaf N allocated in Rubisco, n_R in relation to leaf mass per unit leaf area, M_a , for (A) 16 lowland species for where both *in vivo* and *in vitro* estimates were available; and (B) 150 lowland and 92 upland species for where *in vivo* data was available. Black circles in Fig S3A are *in vivo* n_R derived from maximum carboxylation velocity of Rubisco (normalised to 25°C) (i.e. a subset of those in Fig S3B). Grey circles in Fig S3A are *in vitro* n_R derived from Rubisco western blot assay. n_R in Fig 3B is derived from maximum carboxylation velocity of Rubisco (normalised to 25°C), $V_{\text{cmax},a}^{25}$. In both figures, the line shown is inferred from the global relationship between photosynthetic rate per unit leaf N and M_a (Hikosaka, 2004; Wright *et al.*, 2004), the equation $n_R = M_a^{-0.435}$ given in Harrison *et al.* (2009)

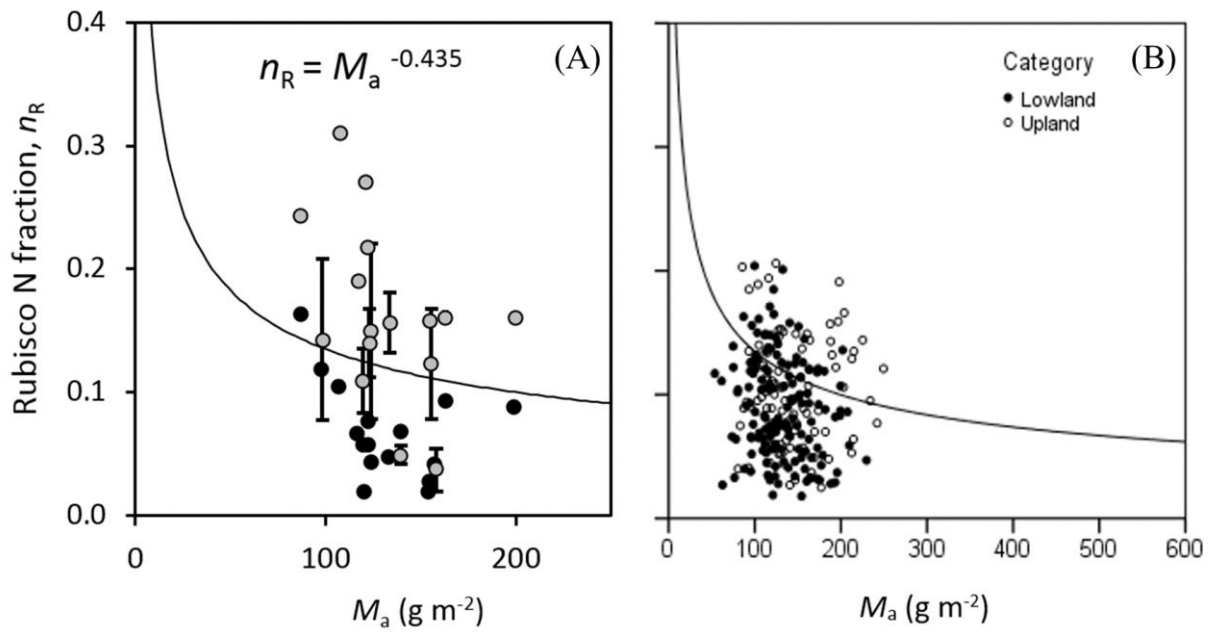


Figure S4: Stacked graph show n_E , n_P and n_R for individual leaves. Individual leaf is arranged first according to sites with increasing soil P (soil P value in mg kg^{-1} depicted underneath site code), then according to decreasing leaf N:P within each site. Leaf N:P for individual leaf is provided on top of the bar. n_E was estimated from maximum electron transport rate (normalised to 25°C), $J_{\text{max,a}}^{25}$ and n_P estimated from chlorophyll concentration. Grey panel depicts *in vitro* n_R estimated from Rubisco western blot assay, where black mark within grey panel indicates *in vivo* n_R derived from maximum carboxylation velocity of Rubisco (normalised to 25°C), $V_{\text{cmax,a}}^{25}$. Horizontal axis shows family of individual leaf.

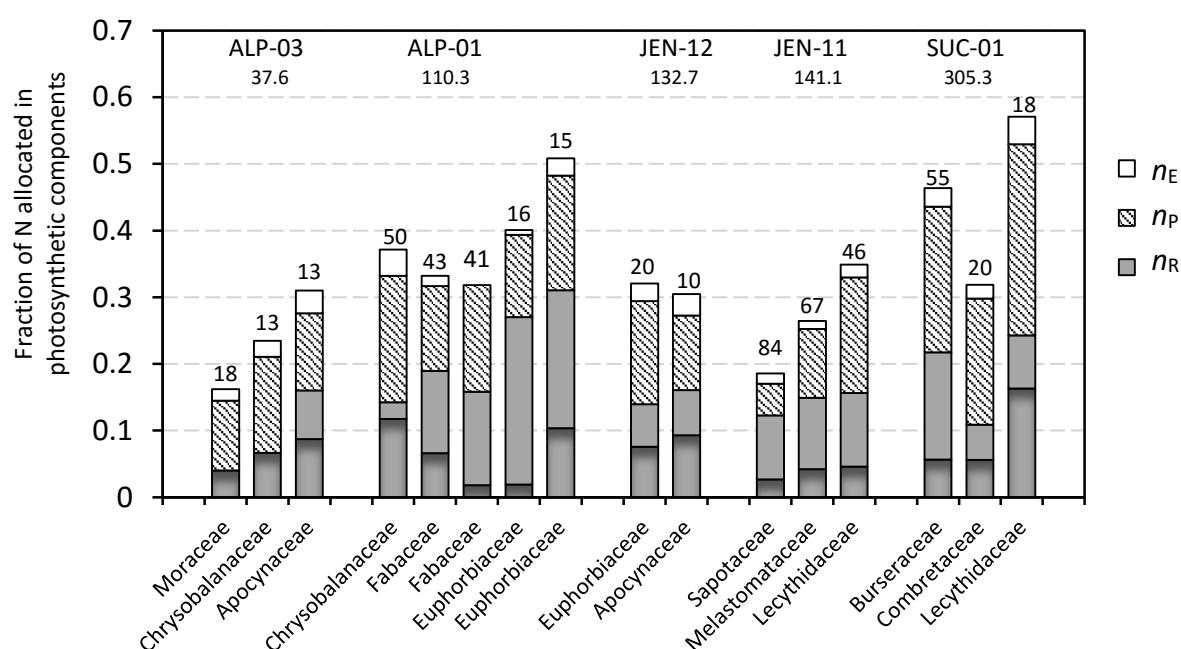
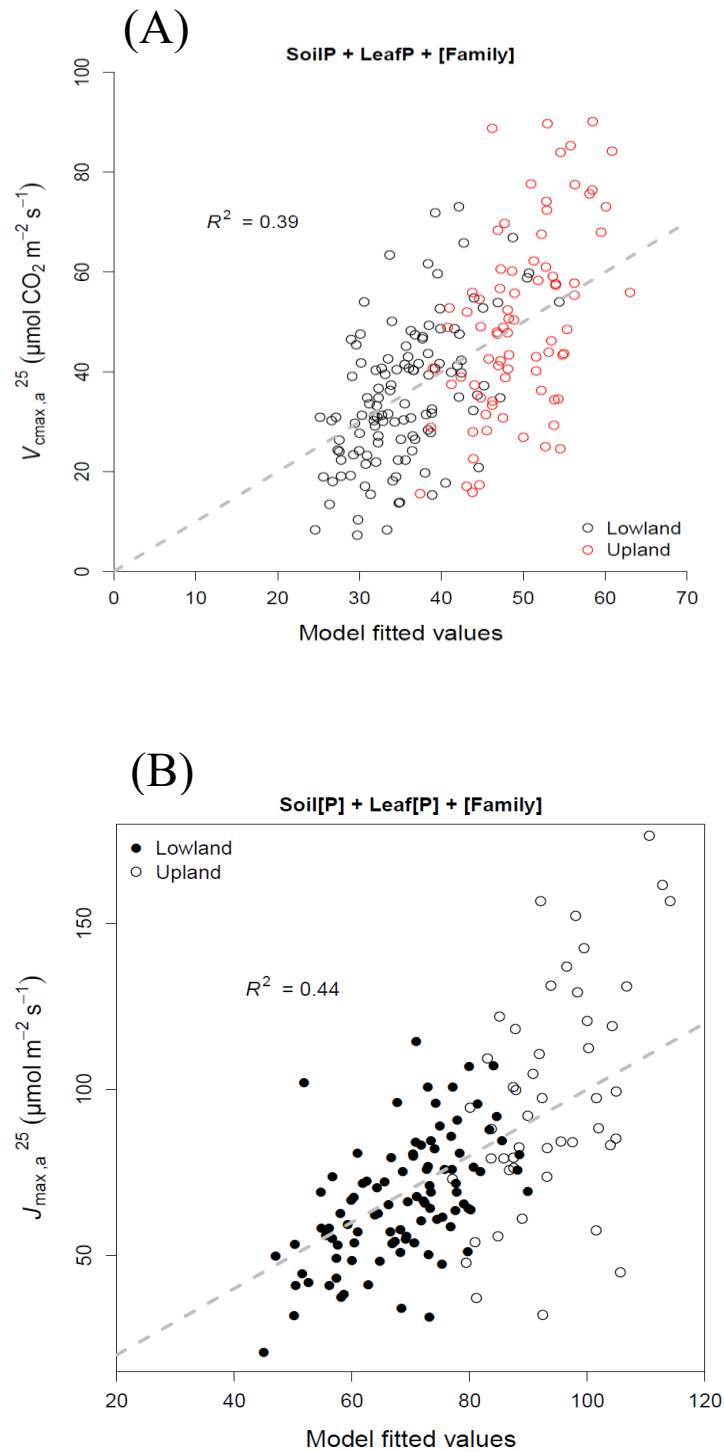


Figure S5: Plots for linear mixed-effects model goodness of fits, including fixed and random terms for (A) $V_{\text{cmax},a}^{25}$; and, (B) $J_{\text{max},a}^{25}$. Measured values of $V_{\text{cmax},a}^{25}$ and $J_{\text{max},a}^{25}$ are plotted against model predictions (using the 'best' predictive models detailed in Table 3). For $V_{\text{cmax},a}^{25}$ and $J_{\text{max},a}^{25}$ model, the fixed component explanatory variables were: soil P and leaf P (P_a).



Supporting information - References

- Brooks A, Farquhar G. 1985.** Effect of temperature on the CO₂/O₂ specificity of ribulose-1, 5-bisphosphate carboxylase/oxygenase and the rate of respiration in the light. *Planta* **165**: 397-406.
- Brown C, MacKinnon J, Cockshutt A, Villareal T, Campbell D. 2008.** Flux capacities and acclimation costs in *Trichodesmium* from the Gulf of Mexico. *Marine Biology* **154**: 413-422.
- Bruhn D, Mikkelsen TN, Atkin OK. 2002.** Does the direct effect of atmospheric CO₂ concentration on leaf respiration vary with temperature? Responses in two species of *Plantago* that differ in relative growth rate. *Physiologia Plantarum* **114**: 57-64.
- Domingues TF, Meir P, Feldpausch TR, Saiz G, Veenendaal EM, Schrodte F, Bird M, Djagbletey G, Hien F, Compaore H, et al. 2010.** Co-limitation of photosynthetic capacity by nitrogen and phosphorus in West Africa woodlands. *Plant, Cell & Environment* **33**: 959-980.
- Ekramoddoullah AKM. 1993.** Analysis of needle proteins and N-terminal amino acid sequences of two photosystem II proteins of western white pine (*Pinus monticola* D. Don). *Tree Physiology* **12**: 101-106.
- Farquhar GD, von Caemmerer S, Berry JA. 1980.** A biochemical model of photosynthetic CO₂ assimilation in leaves of C₃ species. *Planta* **149**: 78-90.
- Fisher J, Malhi Y, Torres I, Metcalfe D, van de Weg M, Meir P, Silva-Espejo J, Huasco W. 2013.** Nutrient limitation in rainforests and cloud forests along a 3,000-m elevation gradient in the Peruvian Andes. *Oecologia* **172**: 889-902.
- Gaspar MM, Ferreira RB, Chaves MM, Teixeira AR. 1997.** Improved method for the extraction of proteins from *Eucalyptus* leaves. Application in leaf response to temperature. *Phytochemical Analysis* **8**: 279-285.
- Harrison MT, Edwards EJ, Farquhar GD, Nicotra AB, Evans JR. 2009.** Nitrogen in cell walls of sclerophyllous leaves accounts for little of the variation in photosynthetic nitrogen-use efficiency. *Plant, Cell & Environment* **32**: 259-270.
- Hikosaka K. 2004.** Interspecific difference in the photosynthesis–nitrogen relationship: patterns, physiological causes, and ecological importance. *Journal of Plant Research* **117**: 481-494.
- Kattge J, Knorr W, Raddatz T, Wirth C. 2009.** Quantifying photosynthetic capacity and its relationship to leaf nitrogen content for global-scale terrestrial biosphere models. *Global Change Biology* **15**: 976-991.
- Kellogg E, Juliano N. 1997.** The structure and function of RuBisCO and their implications for systematic studies. *American Journal of Botany* **84**: 413-413.
- Miyazawa Y, Tateishi M, Komatsu H, Kumagai To, Otsuki K. 2011.** Are measurements from excised leaves suitable for modeling diurnal patterns of gas exchange of intact leaves? *Hydrological Processes* **25**: 2924-2930.
- Quesada CA, Lloyd J, Schwarz M, Patiño S, Baker TR, Czimczik C, Fyllas NM, Martinelli L, Nardoto GB, Schmerler J, et al. 2010.** Variations in chemical and physical properties of Amazon forest soils in relation to their genesis. *Biogeosciences* **7**: 1515-1541.
- Santiago LS, Mulkey SS. 2003.** A test of gas exchange measurements on excised canopy branches of ten tropical tree species. *Photosynthetica* **41**: 343-347.
- Bernacchi CJ, Portis AR, Nakano H, von Caemmerer S, Long SP. 2002.** Temperature response of mesophyll conductance. Implications for the determination of Rubisco enzyme kinetics and for limitations to photosynthesis in vivo. *Plant Physiology* **130**: 1992-1998.
- van de Weg M, Meir P, Grace J, Atkin OK. 2009.** Altitudinal variation in leaf mass per unit area, leaf tissue density and foliar nitrogen and phosphorus content along an Amazon-Andes gradient in Peru. *Plant Ecology & Diversity* **2**: 243-254.
- van de Weg M, Meir P, Grace J, Ramos G. 2012.** Photosynthetic parameters, dark respiration and leaf traits in the canopy of a Peruvian tropical montane cloud forest. *Oecologia* **168**: 23-34.

- 51 **von Caemmerer S, Evans JR, Hudson GS, Andrews TJ. 1994.** The kinetics of ribulose-1, 5-
52 bisphosphate carboxylase/oxygenase *in vivo* inferred from measurements of photosynthesis
53 in leaves of transgenic tobacco. *Planta* **195**: 88-97.
- 54 **Wright IJ, Reich PB, Westoby M, Ackerly DD, Baruch Z, Bongers F, Cavender-Bares J, Chapin T,**
55 **Cornelissen JHC, Diemer M, et al. 2004.** The worldwide leaf economics spectrum. *Nature*
56 **428**: 821-827.